UNIVERSIDADE D
COIMBRA

Catarina Isabel Moreira Leitão

IMPACT OF AN ASTROCYTIC PATHOLOGY ON HIPPOCAMPAL MEMORY

Dissertação no âmbito do Mestrado em Biologia Celular e Molecular orientada pela Professora Doutora Paula Maria Garcia Agostinho e pelo Professor Doutor Ângelo José Ribeiro Tomé e apresentada ao Departamento das Ciências da Vida.

Agosto de 2018

IMPACT OF AN ASTROCYTIC PATHOLOGY ON HIPPOCAMPAL MEMORY

Catarina Isabel Moreira Leitão

Dissertação no âmbito do Mestrado em Biologia Celular e Molecular orientada pela Professora Doutora Paula Maria Garcia Agostinho e pelo Professor Doutor Ângelo José Ribeiro Tomé e apresentada ao Departamento das Ciências da Vida.

Agosto de 2018

UNIVERSIDADE D
COIMBRA

The present work was performed in the Purines group, at the Center of Neuroscience and Cell Biology, University of Coimbra, under scientific guidance of Doctor Paula Agostinho.

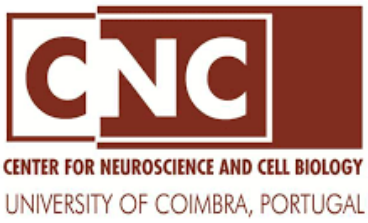

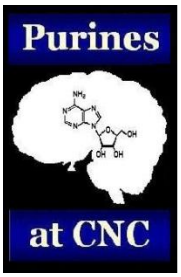

This work is funded by European Regional Development Fund (ERDF) through the COMPETE 2020 programme and Portuguese National Funds via FCT – Fundação para a Ciência e a Tecnologia, I.P., under projects ref POCI-01-0145-FEDER007440 and PTDC/NEU-NMC/4154/2014 -AstroA2AR (POCI-01-0145-FEDER-016684)

Agradecimentos

Com o culminar desta etapa, não poderia deixar de agradecer a um conjunto de pessoas que me apoiaram nesta fase e que, de certa maneira, contribuíram para a realização deste trabalho:

Em primeiro lugar, o meu reconhecido agradecimento à Professora Doutora Paula Agostinho por ter acedido supervisionar o meu trabalho experimental, pela preocupação, confiança, disponibilidade e sinceridade, sempre presentes ao longo deste ano. Durante a realização deste projeto foi permanentemente incansável e, sem ela, a sua execução não teria sido possível.

Ao Professor Doutor Ângelo Tomé, pela contante ajuda e coorientação.

À Doutora Paula Canas, que sempre se revelou disponível para dissipar quaisquer dúvidas.

O meu sincero e profundo agradecimento ao Professor Doutor Rodrigo Cunha, por me ter concedido a oportunidade de realizar trabalho de investigação presente nesta dissertação, no seu laboratório, algo por que sempre ansiei.

Tenho também que agradecer aos meus colegas do grupo "Purines at CNC" que tão bem me acolheram e que sempre se revelaram prestáveis em ajudar-me. Um agradecimento especial à Inês Amaral, que também contribuiu para este trabalho, bem como por todos os conselhos que, altruisticamente, me transmitiu e, à Cátia Lopes, com quem partilhei alegrias e frustrações, inerentes a este tipo de projetos.

A todos os meus bons amigos, Diana, Micaela, Catarina, Cláudia, Andreia, David, Beatriz, Rafael, Cristiana, Ana Gomes, Ana Figueiredo e Joana, por todo o apoio e companheirismo ao longo de todo o meu percurso académico.

Finalmente, um agradecimento muito especial aos meus pais, Isabel e Fernando, à minha irmã Leonor e aos meus avós, por todo o apoio incondicional ao longo dos anos, pois sem eles, esta viagem não teria sido imaginável.

Muito obrigada a todos!

Index

Index of Tables

Index of Figures

List of Abbreviations

α-KG – alpha-ketoglutarate

Aβ – Amyloid-beta peptide

AAT – Aspartate aminotransferase

Acetyl-CoA – acetyl-coenzyme A

AD – Alzheimer's disease

Aldh1L1 – Aldehyde dehydrogenase 1 family member L1

AMPA - α-amino-3-hydroxy-5-methyl-4-isozolepropionic acid

AMPARs – α-amino-3-hydroxy-5-methyl-4-isozolepropionic acid receptors

AP – Anterior-posterior

ApoE – Apoliprotein E

APP – Amyloid precursor protein

APS – Ammonium persulphate

AQP4 – Aquaporin 4

ATP – Adenosine triphosphate

BBB – Blood-brain barrier

BCA – Bicinchoninic acid assay

BDNF – Brain-derived neurotrophic factor

BSA – Bovine Serum Albumin

CA – Cornu Ammonis

Ca^{2+} – Calcium cation

CAMKII – Ca^{2+}/calmodulin-dependent protein kinase II

cAMP – cyclic adenosine monophosphate

CAPS – 3-(Cyclohexylamino)-1-propanesulfonic acid

CLAP – Cocktail of proteases inhibitors

CNS – Central nervous system

CNTF – Ciliary neurotrophic factor

CREB – cAMP response element binding

COX - Cyclooxygenase

Cx – Connexin

D-AA – D-α-aminoadipate

DG – Dentate gyrus

DH – Dorsal hippocampus

DTT – Dithiothreitol

DV – Dorsal-ventral

EAATs – Excitatory amino acid transporters

EDTA – Ethylenediaminetetraacetic acid

EGFR – Epidermal growth factor receptor

EPM – Elevated plus maze

EPSP – Excitatory postsynaptic potential

E-S – EPSP-spike

FAD – Familial Alzheimer's disease

HC – Hemichannels

HEPES – 2-[4-(2-hydroxyethyl) piperazin-1-yl]ethanesulfonic acid

HFS – High frequency stimulation

G-1/6-P – Glucose-1/6-Phosphate

GABA – Gamma-aminobutyric acid

GAT – GABA transporters

GDH – Glutamate dehydrogenase 1

GDNF – Glial cell line-derived neurotrophic factor

Glu – Glial cell-derived neurotrophic factor

GFAP – Glial fibrillary acidic protein

GFAP$^+$ – GFAP positive

GLAST – Glutamate aspartate transporter

Gln – Glutamine

GLT-1 – Glutamate transporter 1

Glu – Glutamate

GLUT – Glucose transporters

GLYT – Glycine transporters

GS – Glutamine synthetase

GSSG – GSH – Glutathione disulfide – glutathione

ICV - intracerebroventricular

IF – Intermediate filaments

IL – Interleukin

IP3 – Inositol triphosphate

ITI – Inter-trial interval

K^+ – Potassium

KCl – Potassium chloride

KHR – Krebs hepes ringer

Kir4.1 – Inward rectifying K^+ channels

L-AA – L-α-aminoadipate

LDH – Lactate dehydrogenase

LIF – Leukemia inhibitor factor

LTD – Long-term depression

LTM – Long-term memory

LTP – Long-term potentiation

MEC – Medial entorhinal cortex

mGluR – Metabotropic glutamate receptors

MPT – Mitochondrial permeability transition

mROS – Mithochondrial reactive oxygen species

mtDNA – Mitochondrial DNA

MTL – Medial temporal lobe

MV – Medial-lateral

Na^+ – Sodium cation

NaCl – Sodium chloride

NMDA – N-methyl-D-aspartate

NMDARs – N-methyl-D-aspartate receptors

NO – Nitric oxide

NOR – Novel object recognition

OD – Object displacement

PFA – Paraformaldehyde

PBS – Phosphate buffered saline

PFC – Prefrontal cortex

PKA – protein kinase A

PLC – Phospholipase C

PMSF – Phenylmethylsulfonyl fluoride

PNS – Peripheral nervous system

PSD – Postsynaptic density

PSD-95 – Postsynaptic density protein 95

RI – Recognition index

ROS – Reactive oxygen species

RT – Room temperature

S100β – S100 calcium-binding protein β

SDS – Sodium dodecyl sulfate

SNAP-25 – Synaptosomal-associated protein

SNAREs – Soluble N-ethylmaleimide-sensitive factor attachment protein receptors

STDP – Spike-timing-dependent plasticity

STM – Short-term memory

Succinyl-CoA – Succinyl-coenzyme A

TARPs – Transmembrane AMPAR regulatory proteins

TBS – Tris-buffered saline

TCA – Tricarboxylic acid

TEMED – Tetramethylethylenediamine

TGF – Transforming growth factor

UDP – Uridine diphosphate

vGluTs – Vesicular glutamate transportes

VH – Ventral hippocampus

Resumo

Os astrócitos são elementos dinâmicos envolvidos na comunicação bidirecional com os neurónios, controlando a atividade neuronal e a função cerebral. Ao interferir com a integridade da rede neurónios-glia no hipocampo, é esperado que haja disfunções, como por exemplo na aprendizagem e na memória. Em condições patológicas, onde a memória está afetada, tal como na doença de Alzheimer, existe cada vez mais a noção de que os astrócitos também possam estar envolvidos no aparecimento e progressão dos défices cognitivos. Para além disso, tem sido proposto que a patologia astrocítica, causada pela gliotoxina ácido L-α-aminoadípico (L-AA) no córtex pré-frontal ou na amígdala medeie perturbações no humor e na cognição. Porém, o papel dos astrócitos na memória, com particular foco no hipocampo, tem sido pouco investigado.

O objetivo principal deste trabalho foi investigar o impacto da disfunção dos astrócitos, causada pela gliotoxina L-AA, na memória, bem como nas alterações morfológicas e proteicas dos astrócitos no hipocampo. Assim, para induzir a disfunção astrocítica no hipocampo, administrámos intracerebroventricularmente (icv) L-AA, uma infusão por dia durante três dias consecutivos em murganhos C57BL/6 jovens adultos através de uma cânula que foi implantada num dos ventrículos laterais. De modo semelhante, os animais controlo foram icv administrados com solução salina (PBS). A seguir, os dois grupos de animais foram testados em comportamento, principalmente em testes de memória (testes do reconhecimento do objeto, do deslocamento do objeto, do labirinto em Y modificado e da esquiva inibitória). Posteriormente, foram feitas análises morfológicas e neuroquímicas no hipocampo dos dois grupos de animais. Usou-se secções hipocampais para analisar alterações na morfologia dos astrócitos (através de anticorpos que reconhecem proteínas típicas de astrócitos) por imunohistoquímica, tendo como ponto central identificar alterações ao nível das ramificações (número e tamanho) por microscopia confocal e posterior análise tridimensional da estrutura. Os níveis das proteínas astrocíticas, proteína glial fibrillar acidíca (GFAP), glutamina sintetase (GS), proteína de ligação ao cálcio S100 β e conexina 43 (Cx43) foram também avaliados no hipocampo dos dois grupos de murganhos. Para

avaliar se a gliotoxina L-AA afetava os terminais nervosos, quantificou-se também os níveis das proteínas sinápticas (sinaptofisina, SNAP-25 e PSD-95). Os resultados obtidos mostraram que os murganhos administrados icv com L-AA apresentavam défices na memória dependente do hipocampo no teste do deslocamento do objeto (OD) e no teste de labirinto em Y modificado e pareciam apresentar uma maior impulsividade. Além disso, esta gliotoxina reduziu significativamente, em aproximadamente 5–10%, o número de células marcadas positivamente para GFAP, em diferentes sub-regiões do hipocampo (CA1 oriens, CA1 stratum radiatum e CA3) e causou também uma diminuição dos níveis das proteínas astrocíticas (GFAP e Cx43), mas não alterou os níveis das proteínas sinápticas. A análise tridimensional dos astrócitos revelou ainda que murganhos administrados icv com L-AA possuem astrócitos maiores e com maior número de ramificações, sendo a sua complexidade também maior perto do corpo celular.

Apesar do presente trabalho ter sido desenvolvido no sentido de validar um modelo animal de patologia astrocítica no hipocampo (estrutura do cérebro envolvida na memória), permitiu também dar uma nova visão sobre o papel dos astrócitos na memória. Este trabalho foi também crucial para evoluir para outros estudos com o objetivo de definir se os astrócitos têm de facto um papel fundamental em doenças com declínio cognitivo, como por exemplo na doença de Alzheimer.

Palavras-chave: astrócitos; ácido L-α-aminoadípico; memória; sinapse, hipocampo

Abstract

Astrocytes are dynamic signalling elements involved in a bi-directional communication with neurons, controlling neuronal activity and metabolism and, consequently, brain function. Interfering with the integrity of the neuron-glial network in the hippocampus is known to impair integrated responses, like learning and memory. In pathological conditions where memory is impaired, such as in Alzheimer's disease, there is an increasing recognition for a role of astrocytes in the onset and progression of cognitive deficits. Astrocytic pathology has been proposed to underlie the pathogenesis of mood or cognitive disorders, as heralded by the impact of the gliotoxin, L-α-aminoadipic acid (L-AA) in brain regions, such as prefrontal cortex or amygdala. However, the impact of astrocytes on memory, with a focus in the hippocampus, has been few explored.

The major goal of this work was to investigate the impact of astrocytes blunting, triggered by L-AA, on memory and on astrocytic morphology and proteins in hippocampus. Thus, to induce a condition of astrocytes blunting in hippocampus we administrated intracerebroventricularly (icv) L-AA, one single infusion for three consecutive days in young adult C57BL/6 mice using cannula guides implanted in one of the lateral ventricles. Similarly, the control group of animals were icv administrated with saline solution (PBS, LAA-vehicle). Then, these two groups of animals were behaviourally tested, mainly regarding memory performance (object recognition, object displacement, modified y-maze and step-down inhibitory avoidance tests). Afterward, we performed morphological and neurochemical analyses of the hippocampus of described experimental animal models. Therefore, we used hippocampal sections to analyze alterations in astrocytes morphology (immunolabelling of astrocytic markers) by immunohistochemistry, with the particular focus on identifying alterations in astrocytic processes (number and length) using confocal microscopy and further analysis of tridimensional structure. In addition, we quantified the levels of hippocampal astrocytic proteins, glial fibrillary acidic protein (GFAP), glutamine synthetase (GS), S100 calcium-binding protein β (S100β) and connexin 43 (Cx43) in the two animal groups, by Western-blot analysis. To check out whether the gliotoxin L-AA was affecting nerve terminals,

levels of synaptic markers (synaptophysin, SNAP-25 and PSD-95) were also quantified. Our results showed that icv infused L-AA mice exhibited a reduced hippocampal memory performance, in the object displacement (OD) test and in the modified y-maze test and seemed had an enhanced in impulsivity. Moreover, this gliotoxin significantly decreased the number of GFAP-positive cells, by about 5–10%, in different subregions (CA1 oriens, CA1 stratum radiatum and CA3) of the hippocampus and caused a reduction in the levels astrocytic proteins (GFAP and Cx43) but had no effect in synaptic proteins. Furthermore, the tridimensional analysis of astrocytes revealed that in mice icv infused with L-AA, the hippocampal astrocytes exhibited a significant increase in the number and in the total length of processes (or ramifications), being the complexity of the processes higher near the cell body.

Although the present work was designed to validate an animal model of astrocytes pathology in the hippocampus, a brain structure involved in memory processing, it also gave novel insight about the role of astrocytes in memory. Furthermore, it will be crucial to evolve to other studies in which the focus is the definition of whether astrocytes have a key role in brain-disorders associated with cognitive decline, such as Alzheimer´s disease.

Key words: astrocytes; L-α-aminoadipate; memory; synapse, hippocampus

Chapter 1 | Introduction

1.1. Nervous system and cellular components

The nervous system is a complex network of neurons and glial cells. Neurons are electrically excitable nerve cells that transmit and process information through chemical and electrical signals, which occur at synapses whereas glial cells are considered non-neuronal cells that support and protect neurons, maintain the homeostasis and participate in neurotransmission (Virchow, 1856; Araque et al., 1999; Woolsey et al., 2017).

The nervous system includes both the Central Nervous System (CNS) and Peripheral Nervous System (PNS) (Fig. 1).

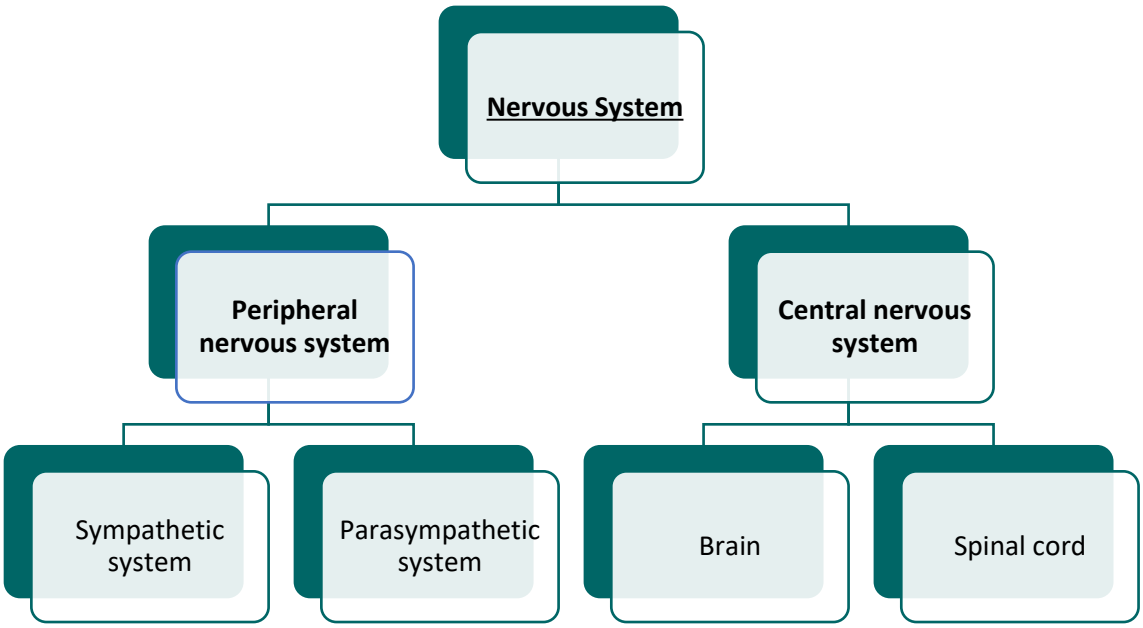

Figure 1 - Schematic representation of the Nervous system.

The CNS is constituted by the brain, which is protected with a cranial cavity of the skull and by the spinal cord. The main function of this system is to assimilate the information that is received and to coordinate the activity of all parts of the body. The CNS can be divided in white matter and gray matter, being the first mainly constituted by axons and oligodendrocytes, while the gray matter comprises mainly cell bodies of neurons, synapses and glia (Woolsey et al., 2017). It is well known the importance of neurons in receiving, processing and transmitting information of the brain. However, it is now widely accepted that glial cells are active participants in brain signaling, playing

active roles in many processes, such as metabolism, neurotransmission, immune function and blood-brain barrier signaling. Glial cells are classified in two main groups: microglia and macroglia. Microglia are macrophage-like cells that regulate the inflammatory response of the neural tissue and are located throughout the brain. Macroglia are generally subdivided into four specialized cell types: ependymal cells, Schwann cells, oligodendrocytes and astrocytes (Merrill, 1987).

There are many CNS diseases, including attention deficit hyperactivity disorder, autism, Alzheimer's disease (AD), Parkinson's disease, multiple sclerosis, Huntington's disease, frontotemporal dementia and amyotrophic lateral sclerosis (Amor et al., 2010).

1.1.1. Memory and Hippocampus

Memory is defined by the ability to recall past events, simply by the acquisition of new information that can be stored for later retrieval (McGaugh, 1966, 2000; Dudai, 2004). Initially, the new memories can be susceptible to disruption, but as the time goes by, they get strengthened (memory consolidation) and we can claim that the retrieval was successful (McGaugh, 1966, 2000; Cahill et al., 2001). Once this memory consolidation is accomplished, memory becomes enduring (conversion of short-term memory (STM) to long-term memory (LTM)) (Squire and Davis, 1981; Nader, 2003). Short-term memory can be distinguished from long-term memory in some aspects: i) STM last from seconds to hours, whereas LTM last from days to years; ii) STM is "labile" (sensitive to disruption), while LTM is consolidated and iii) STM does not need new RNA or protein synthesis, while this is a requirement for LTM (Nader, 2003). Nonetheless, if consolidated memory is reactivated, it can become vulnerable to most of the treatments that could have impaired memory consolidation after training; this constitutes the memory reconsolidation that is the maintenance and modification of long-term memory (Nader, 2003; Blake et al., 2014). After storage and retrieval, memory can influence behaviour, since different learning experiences could lead to changes in behaviour (Cahill et al., 2001).

Memory can be categorized in two classes: explicit or declarative memory and implicit or nondeclarative memory. In declarative memory, there is a conscientious

recollection of events and facts, whereas in nondeclarative memory, past events pop up in our mind due to a prior experience or behaviour without any will of retrieving the memory (Squire et al., 1992; Schacter and Buckner, 1998). Declarative memory can be itself divided in three subclasses: i) episodic, ii) semantic and iii) familiar (Tulving, 1972; Moscovitch et al., 2005). The first one refers to specific events in life that contains information about the content and spatial and temporal context, in which it occurred (Tulving, 1985). The semantic memory is associated with noncontextual content or experience, in which we have the knowledge that an event happened without the sense of experience (Cermak and O'Connor, 1983; Kopelman et al., 1989). The familiar memory is a mixture of both subclasses and corresponds to a memory that we know that is familiar but we do not have recollection of the context in which it occurred (Tulving, 1985; Moscovitch et al., 2005).

As referred before, after memory is well consolidated, different learning experiences can alter behaviour. In this way, modifications in spatial cognition may be obtained through exploratory behaviour, which is based on the expression of natural curiosity and on the necessity of obtain information when the subjects face novel environments and stimuli (Berlyne, 1950). Therefore, spatial memory is defined by the recognition, storage and recovery of spatial information (Kessels et al., 2001). In rodents, this type of memory dependent on the hippocampus can be assessed by evaluation of their behaviour in mazes, which usually have cues that allow the recognition of the environment, location within that environment and their contents, thus providing the basis for spatial memory and flexible navigation (Burgess et al., 2002; Paul et al., 2009). In contrast, recognition memory is the perception of a prior event and it is critical to our ability to record events, but also to guide prospective behaviour (Warburton and Brown, 2015). In rodents, recognition memory can be evaluated by the use of object recognition memory tasks, measuring spontaneous preference for novelty in either an arena or a maze (Dix and Aggleton, 1999; Good et al., 2007). This type of memory is affected by different types of brain regions such as i) perirhinal cortex in the medial temporal lobe (MTL) by the recognition of memory judgments for individual items, ii) hippocampus by spatial location of a previously encountered item, iii) medial prefrontal cortex and iv) medial dorsal thalamus (Aggleton and Brown, 1999; Bussey et al., 1999).

The hippocampus, as well as the adjacent cortex (temporal polar, parahippocampal, entorhinal, and perirhinal cortices) are structures of the MTL, that are known to be involved in declarative memory processes (Doxey and Kirwan, 2015). The hippocampus is responsible for encode, storage and replay of spatial knowledge in the form of a cognitive map and can be divided in ventral and dorsal hippocampus (O'Keefe, 1990). Dorsal hippocampus (DH) corresponds to the cognitive function of this brain region, whereas ventral hippocampus (VH) is related with the stress, emotion and affection. The differences between DH and VH were based on three arguments: i) distinct input and output connections in DH and VH; ii) spatial memory only depended on DH, but not on VH and iii) alterations in stress and emotional behaviour were related with lesions on VH but not on DH (Swanson and Cowan, 1977; Moser et al., 1995; Moser and Moser, 1998; Fanselow, 2010).

Hippocampus can be divided by subregions, being the most important, *Cornu Ammonis* 1 (CA1), *Cornu Ammonis* 3 (CA3) and dentate gyrus (DG) (Kesner et al., 2004). The hippocampal network consists in generation of projections to all constituents of the hippocampus by neurons in layers II and III of medial entorhinal cortex (MEC). These layer II cells project to DG and CA3, whereas cells in layer III project to CA1 and the subiculum. The trysinaptic pathway begins through the project ion to DG through layer II, which subsequently includes the mossy fibers projection from DG to CA3 and the Schaffer collateral projection from CA3 to CA1 (Fig. 2) (Witter et al., 2014).

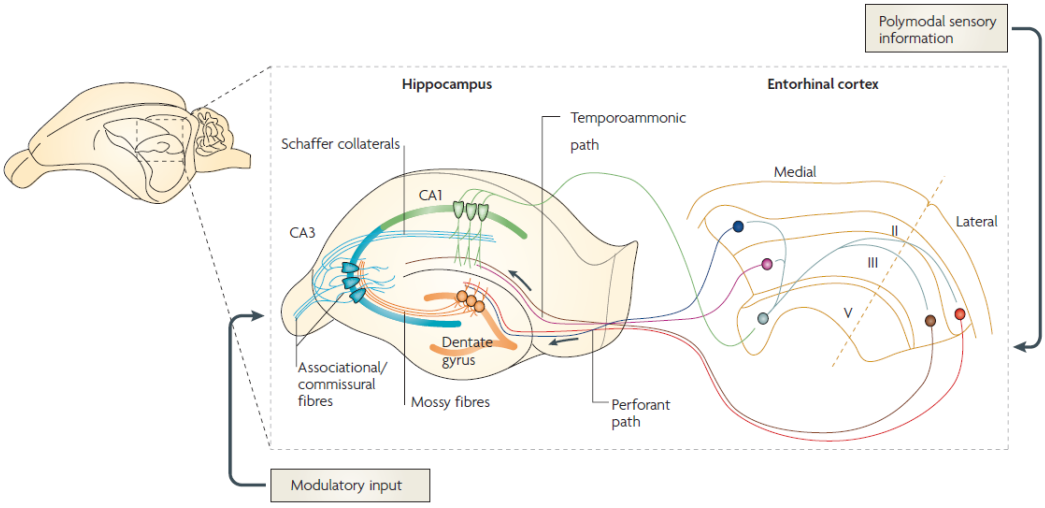

Figure 2 - Anatomy of the hippocampus. Cornu Ammonis 3 (CA3) and dentate gyrus project from layer II cells of entorhinal cortex, whereas CA1 and subiculum project from cells in layer III of entorhinal cortex. Granule cells of dentate gyrus project, through their axons (the mossy fibers), to the proximal apical dendrites of CA3 pyramidal cells which, in turn, project to ipsilateral CA1 pyramidal cells through Schaffer collaterals and to contralateral CA3 and CA1 pyramidal cells through commissural connections (Neves et al., 2008).

Synaptic plasticity is the ability of synapses to strengthen or weaken over time, in response to increases or decreases in their activity, and this event is considered to constitute the neurophysiological basis of learning and memory (Hughes, 1958; Ota et al., 2013). Long-term potentiation (LTP) is the most studied model of this process, identified in hippocampus by using electrophysiological, biochemical and molecular techniques (Bliss and Lømo, 1973; Bliss et al., 2007). LTP consists in the strengthening of the synapses using a high-frequency electrical stimulation (HFS) of afferent-fiber pathways, inducing an improvement of synaptic transmission that can last for months (Neves et al., 2008). Induction of LTP requires the activation of glutamate receptors, of subtype N-methyl-D-aspartate (NMDA) receptors and membrane depolarization. After HFS, glutamate is released from the presynaptic terminal and binds to α-amino-3-hydroxy-5-methyl-4-isozolepropionic acid (AMPA) receptors and activate them, but the same does not happen with NMDA receptors (NMDARs), since they are blocked (voltage-dependent) by magnesium (Mg^{2+}). With the activation of AMPA receptors (AMPARs), there is an influx of potassium (K^{+}) and sodium (Na^{+}), leading to membrane depolarization that further activate NMDARs. Consequently, there is an influx of calcium (Ca^{2+}) and Na^{+} to the interior of dendritic spines. Ca^{2+} stimulates cyclic adenosine monophosphate (cAMP) formation, triggering a cascade of signaling mechanisms, involving protein kinase A (PKA), cAMP response element binding protein (CREB), cAMP response element (CRE), mitogen activated protein kinase, and calcium calmodulin dependent protein kinase II (CAMKII), which in turn phosphorylates transmembrane AMPARs regulatory proteins (TARPs) that allowing the insertion of AMPARs in the membrane of synapses, which underlie the LTP phenomena (Kandel, 2001; Miyamoto, 2006; Mayford et al., 2012) .

Nonetheless, LTP is not the only form of activity-dependent plasticity, existing many others such as: i) long-term depression (LTD); ii) excitatory postsynaptic potential (EPSP)-spike (E-S) potentiation iii) spike-timing-dependent plasticity (STDP); iv) depotentiation; and v) de-depression (Abraham et al., 1985; Dudek and Bear, 1992; Montgomery and Madison, 2002; Dan and Poo, 2004). In contrast with LTP, LTD is the weakening of the synaptic transmission using a low-frequency stimulation (Neves et al., 2008). LTD is also trigger by a slight increase in Ca^{2+} by activation of NMDARs, which

stimulate phosphatases that dephosphorylate proteins involved in LTP. This causes the endocytosis of AMPARs, which is promoted by calcineurin (a phosphatase dependent of Ca^{2+}), despite NMDARs do not be affected (Malenka et al., 1999). E-S potentiation occurs at the same time as LTP after HFS, whereas STDP is a type of plasticity in which pre- and postsynaptic cells are stimulated independently, and the timing with which spikes are evoked determines the direction of plasticity. Depotentiation is the selective and time-dependent reversal of already potentiated synapses using low-frequency stimulation, while de-depression is the reversion of LTD using HFS (Neves et al., 2008).

1.2. Astrocytes: the star-shape cells of the brain

1.2.1. Arousal and evolution of the astrocytic concept

In 1856, Rudolf Virchow, the father of the modern pathology, defined the brain connective tissue, 'nervenkitt' or nerve-cement as "neuroglia", a homogenous population without cellular elements that generally supported the neuronal function (Virchow, 1856). However, Camillo Golgi established the cellular nature of neuroglia, which he defined as round cells with many fine processes extended in all directions, being some of these processes directed towards blood vessels (reviewed in Verkhratsky and Parpura, 2014).

In 1893, the term "astrocyte" was first proposed by Michael von Lenhossek, further categorized in fibrous or protoplasmic, being the astrocytes fibrous mainly present in white matter while the protoplasmic are found mainly in grey matter of the brain and spinal cord (Kölliker, 1889; Andriezen, 1893; Von Lenhossék, 1893; Ramón y Cajal, 1913; Miller and Raff, 1984).

Although the concept of neuroglia is known for a long time, our knowledge on glial cells, especially of astrocytes, is still scarce and a current matter of great research interest. One of the first roles assigned to glial cells was that they corresponded to the space that was not occupied by neurons. As the investigation in this field progressed, a new role as supporting cells was attributed to astrocytes: these glial cells are necessary

to guarantee optimal neuronal functioning; and the knowledge that they express voltage-gated channels and neurotransmitter receptors turned astrocytes as potential participants in intercellular communication in the brain (Volterra and Meldolesi, 2005;

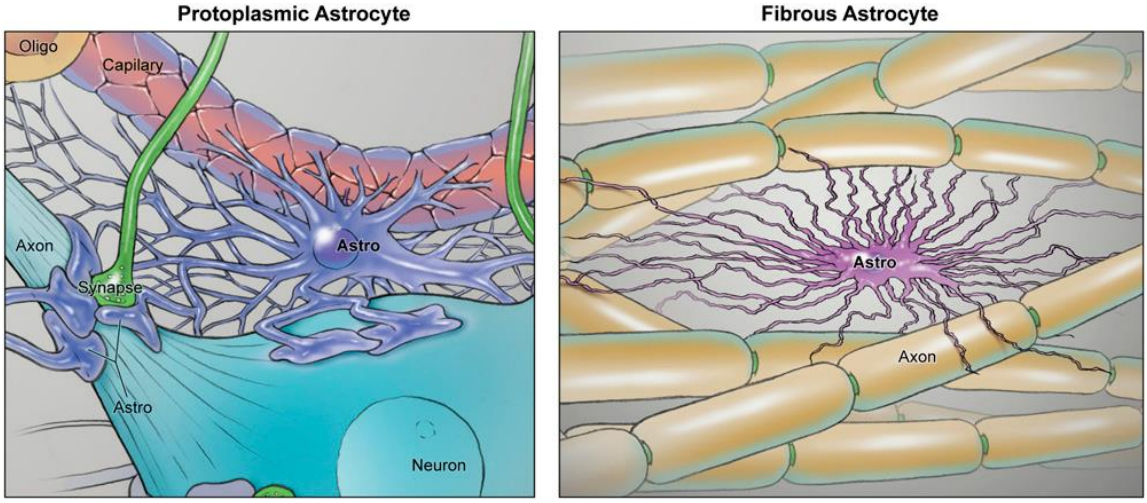

Figure 3 - **Schematic representation of protoplasmic and fibrous astrocytes in the brain**. In left panel – Protoplasmic astrocyte in close connection with a neuron and a capillary, constituting the so called ''neurovascular unit'' and highlighting the roles of astrocytes in developmental synaptogenesis and in modulating the BBB. In right panel – Fibrous astrocyte present in a white matter tract, where it may interact with oligodendrocytes to promote myelination (Molofsk et al., 2012).

Kettenmann and Verkhratsky, 2008; Molofsk et al., 2012).

1.2.2. Types and morphology of astrocytes

Radial glial cells are involved in brain development, acting as stem and progenitor cells that generates neurons and glia. These glial cells extend long processes throughout the thickness of the tissue from the outer pial surface to the inner ventricular surface of the brain; having functions in the guidance of migrating neurons and, thereby, contribute to the organized arrangement of neurons, possibly leading them to different regions of the brain, like amygdala or hippocampus. After the neurogenesis, *the radial* glial *cells* disappear, and a subset of them transforms into astrocytes (Reichenbach and Wolburg, 2005).

Mature astrocytes were mainly divided into two classes according to their morphology and anatomical location (Fig. 3): i) protoplasmic astrocytes in gray matter and ii) fibrous astrocytes in white matter (Miller and Raff, 1984). The first ones are characterized by having many branching processes that surround the synapses and

cover the blood vessels, while the fibrous astrocytes have thinner, longer and unbranched processes that sheath the nodes of Ranvier (Wang and Bordey, 2008; Sofroniew and Vinters, 2010). However, recently it has been found that in the human brain, astrocytes have a more complex morphology, being necessary to expand the criteria of classification. Thus, they have been divided in four subtypes: protoplasmic, fibrous, interlaminar, polarized. (Table 1) (Hu et al., 2016).

Table 1 - **Different types of astrocytes in human brain** (adapted from (Hu et al., 2016)).

Subtype	Location	Features
Protoplasmic astrocytes	Deep layers of the cortex (layers 2-6)	Majority of the process do not overlap
		Larger and more elaborate than their rodent counterparts.
		The processes of one protoplasmic astrocyte can cover five different blood vessels, eight neuronal cells bodies and numerous synapses
		Highly coupled by gap junction
Interlaminar astrocytes	Layer I of the cortex	Extend striking long, frequently unbranched processes throughout the layers of the cortex
		Two types of processes: one contributes to the astrocytic network near the pial surface and the other penetrates deep layers of the cortex
Polarized astrocytes	Deep layers of the cortex (near the white matter)	Extend one or two long processes away from the white matter
		The long processes are frequently unbranched or branched once
Fibrous astrocytes	White matter	Contain few primary processes
		Their fibers are straighter and less branched than those of other glia

Studies in protoplasmic astrocytes (Fig. 4) from the cerebral cortex of an adult mouse, a rhesus monkey, and a human showed that the mouse astrocyte domain (cell body and ramifications) is about 2.5 times smaller than the human astrocyte domain (Oberheim et al., 2009). These findings were obtained using immunostaining for the glial fibrillary acidic protein (GFAP), which is mainly expressed by astrocytes, and allow to observe that in cerebral cortex of rodents, the astrocytes have relatively short processes that more close to the soma. By contrast in primates, astrocytes are long, with varicosity-bearing ramifications that extend beyond the domains of the thick ramifications and extend between the cortical lamina, which have been suggested to optimize the columnar organization of the cerebral cortex of primates (Colombo and Reisin, 2004). This apparent larger size of the domains of protoplasmic astrocytes of primates could serve to limit the expansion of the astrocyte population, by controlling more synapses with fewer astrocytes cell bodies (Kimelberg and Nedergaard, 2010). Concerning the protoplasmic astrocytes in the human brain, it was observed that they are much more complex and larger when compared with rodents and primate brains. These astrocytes have approximately 10 times more ramifications and an increase in GFAP expression in their end-feet (Matyash and Kettenmann, 2010). Thus, rodents astrocytes contact with less synapses than humans astrocytes, and the fibrous astrocytes are smaller (Oberheim et al., 2009). In this way, it is possible to assume that the size of astrocytes increases with increasing complexity of brain function (Kimelberg and Nedergaard, 2010).

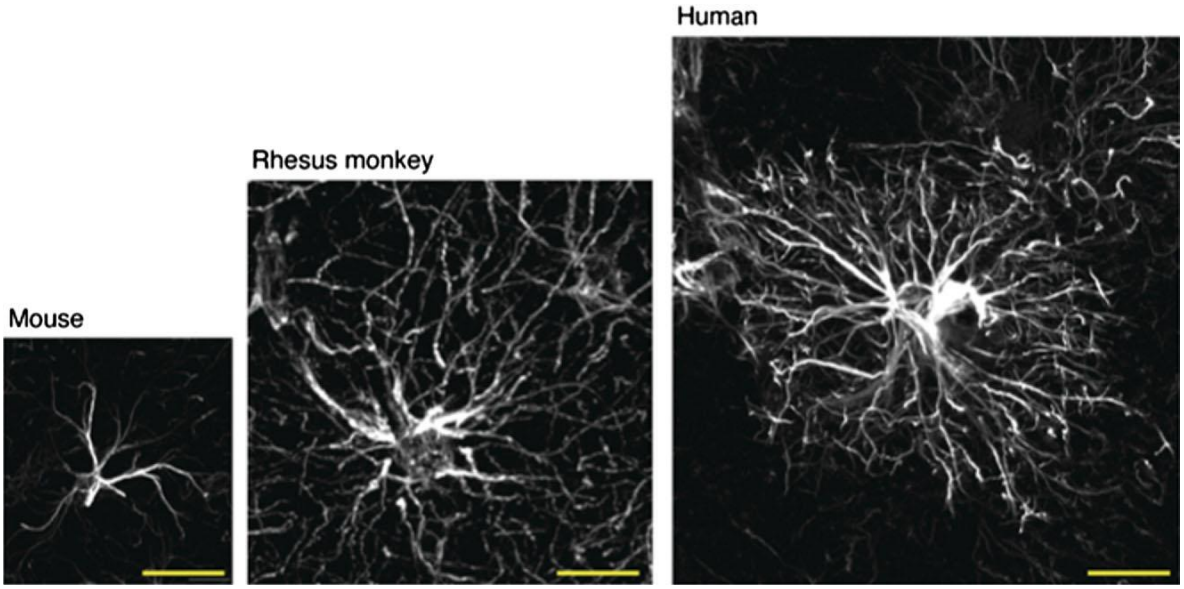

Figure 4 - **Size of astrocytes of rodents, primates and humans**. Scale bar: 50 µm (Kimelberg and Nedergaard, 2010).

Astrocytes are normally connected through gap junctions to form large intercellular networks (Seifert et al., 2006). Gap junctions participate in the intercellular communication by the docking of two hemichannels in adjacent cells (Willecke et al., 2002). Each hemichannel (or connexon) is composed of six protein subunits, called connexins (Cx), which in the case of astrocytes, are formed by connexins 43 (Cx43) and 30 (Cx30) (Giaume et al., 2010). The first one is expressed in the beginning of the development of rat radial astrocytes ramifications and its levels increase with the progression of the age, whereas Cx30 is expressed in astrocytes in juvenile rodents (Kunzelmann et al., 1999; Nagy and Rash, 2000). Both connexins are also expressed in mature astrocytes of grey matter, whereas Cx43 is expressed mainly in astrocytes of white matter (Nagy et al., 1999). The connexins, by forming hemichannels or gap junctions, have a key role in the propagation of intercellular Ca^{2+} waves that can promote the release of gliotransmitters, such as ATP, glutamate and D-serine (Nedergaard et al., 2003). Since astrocytes have many ramifications that contact with thousands of synapses simultaneously, the release of gliotransmitters synchronize the neuronal firing pattern, controlling the strength of excitatory and inhibitory synaptic transmission, through the activation of receptors present in neurons. Moreover, interactions between glia and neurons are also implicated in regulation of the local blood flow (Volterra and Meldolesi, 2005).

1.2.3. Functions of astrocytes

Astrocytes are involved in many processes, including i) synaptogenesis; ii) modulation of synaptic transmission; iii) blood-brain barrier and ionic concentrations; iv) pH regulation of the brain; v) regulation of cerebral blood flow; vi) regulation of metabolism; vii) oxidative stress and viii) cognition (Kimelberg and Nedergaard, 2010).

1.2.3.1. Synaptogenesis

Synapses are structures that allow neurons to communicate through electrical or chemical signals (Pereda, 2014). They are formed by two terminals: a pre- and a postsynaptic. The presynaptic terminal contains a matrix of proteins responsible for

anchoring synaptic vesicles, that contain glycoproteins such as synaptophysin, to the membrane and promoting their exocytosis, and consequently release of neurotransmitters to the synaptic cleft (Li and Sheng, 2003). This synaptic vesicle docking to the membrane is mediated by soluble N-ethylmaleimide-sensitive factor attachment protein receptors (SNAREs), such as synaptosomal-associated protein 25 (SNAP-25), that allows the binding of Ca^{+} to synaptogamin and consequently the exocytosis (Masliah and Terry, 1993). In the postsynaptic terminal, there is a dense matrix (postsynaptic density (PSD)) that contains scaffold proteins, such as PSD-95, which cause receptors accumulation and promote the binding between membrane proteins and cytoskeleton proteins. For example, PSD-95 has the major function of connecting NMDARs to actin cytoskeleton (Cho et al., 1992).

Synapses take time to be formed, since the majority of excitatory synaptic structures in the rodent brain appear during the second and third postnatal weeks. In this period also occurs the differentiation and maturation of astrocytes. Thus, it was possible to assume that astrocytes might contribute for the timing and extent of synapse formation in the CNS. Furthermore, astrocytes are also vital for the survival and health of neurons (Banker, 1980). Studies in mice confirmed that in the absence of astrocytes, the animals could not survive due to neurodegeneration (Li et al., 2012). Moreover, ablation of perisynaptic Schwann cells in the PNS (analogous to astrocytes in the CNS) cause synaptic transmission dysfunction and loss and degeneration of neuromuscular junctions, responsible for muscular contractions (Reddy et al., 2003).

In this way, astrocytes control different stages of the excitatory synapse formation: i) they increase the number of synaptic structures; ii) increase postsynaptic activity by inducing AMPARs insertion in the postsynaptic terminal, and iii) enhance presynaptic function by increasing probability of neurotransmitters release (Chung et al., 2015a).

1.2.3.2. Astrocytes: key players in synaptic transmission

The demonstration of a bidirectional communication between astrocytes and neurons gave rise to the concept of “Tripartite Synapse”. According with this concept, the exchange of the communication among pre- and postsynaptic neurons is modulated

by astrocytes. These glial cells interact with these synaptic elements, responding to synaptic activity and, thus, have a key role in regulation of synaptic transmission and plasticity (Fig.5) (Araque et al., 1999).

Astrocytes are one of the largest cellular populations of the brain involved in the processing, transfer and storage of information by CNS (Perea et al., 2009). These cells are located throughout the brain and are known to have several functions: enwrap most synapses, provide metabolic support to neurons, remove neurotransmitters (GABA and glutamate) from synaptic cleft, participate in ion homeostasis and control radical stress. Astrocytes also shape synaptic volume and regulate synaptic strength, through the release of gliotransmitters, such as glutamate, ATP, D-serine, GABA and neurotrophins, like brain-derived neurotrophic factor (BDNF) and glial cell line-derived neurotrophic factor (GDNF) (Araque et al., 1999; Maragakis and Rothstein, 2006; Kimelberg and Nedergaard, 2010; Ota et al., 2013).

The signaling pathway between astrocytes and neurons is mutual: astrocytes sense neuronal activity by increasing cytosolic Ca^{2+} levels and express G-protein-coupled receptors that sense the neurotransmitters released in the synaptic cleft, which in turn the neurotransmitters released by neurons can trigger astrocytic Ca^{2+} waves and the release of gliotransmitters, such as ATP, glutamate, as well as of adenosine and D-serine; which shape synaptic transmission and plasticity (Stobart and Anderson, 2013; Rudy et al., 2015 and Orellana et al., 2016).

When a synaptic transmitter is released from the presynaptic terminal, it is important to clear that transmitter from synapse to prevent receptor desensitization and maintain the reliability of synaptic transmission. For instance, one of the primary roles of astrocytes is to protect neurons from excitotoxicity, taking up excess ammonia and glutamate from the synaptic cleft (Meister, 1974; Suárez et al., 2002). Glutamine (Gln) released by astrocytes are further taken up by neurons and, by the action of phosphate-activated glutaminase, glutamate (Glu) is synthetized *de novo* from glutamine. In the presynaptic terminal of the synapse, glutamate, as a neurotransmitter, is packaged in synaptic vesicles by vesicular glutamate transporters (vGluTs) and it is released in the synaptic cleft. In this phase, glutamate has two paths: i) it can bind to ionotropic receptors (NMDARs and AMPARs) or to metabotropic receptors (mGluR1 to

mGluR8), leading to membrane depolarization and modulation of local protein synthesis, and ii) it can be cleared from synaptic cleft by astrocytes. Astrocytes express transporters for glutamate (excitatory amino acid transporters (EAATs)), that use Na^+ and K^+ gradients to promote the uptake of this transmitter into these cells (Bergles and Jahr, 1998; Hertz and Zielke, 2004). Once glutamate is taken up by astrocytes, it is converted into glutamine by glutamine synthetase (GS) and in an ATP-dependent manner the glutamine is driven back to the neurons (Hertz and Zielke, 2004; Parpura et al., 2017). This constitute the glutamate-glutamine cycle and allows efficacy to glutamatergic synapses that are coupled to both astrocytic and neuronal metabolism.

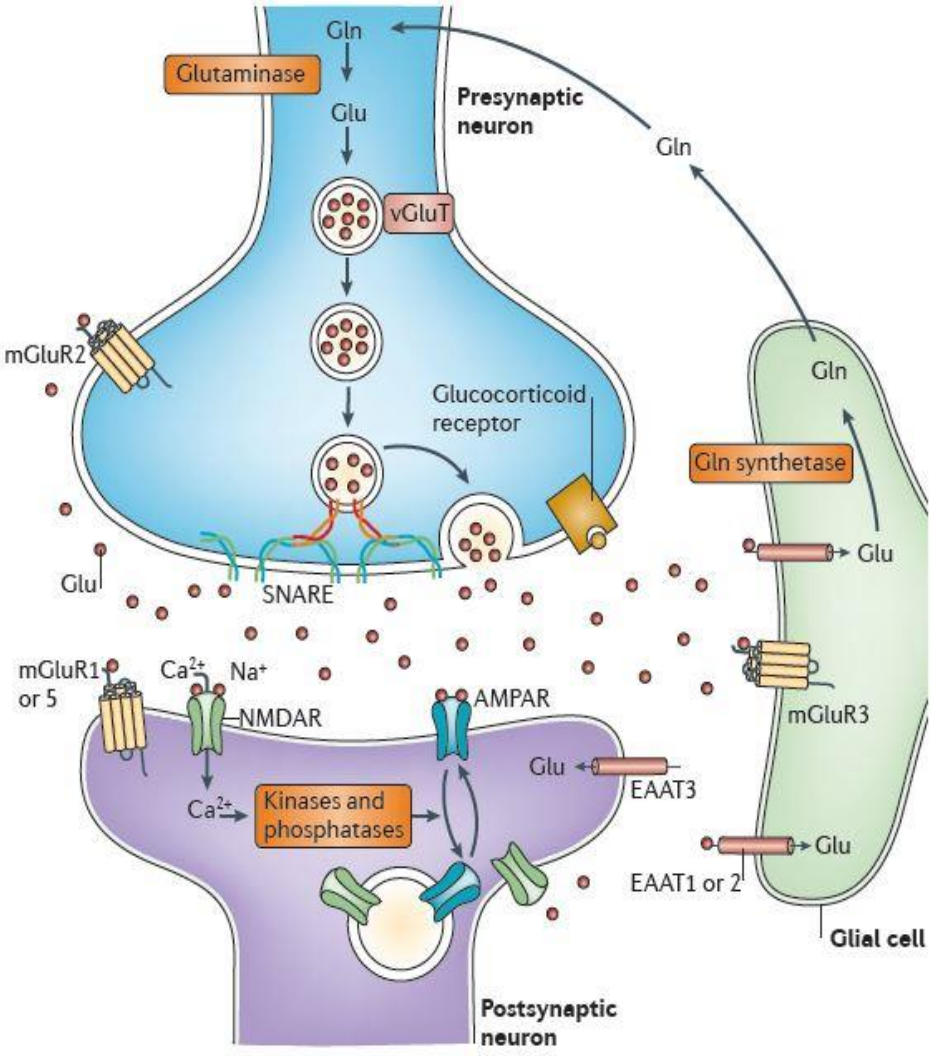

Figure 5 - The tripartite glutamate synapse. Neuronal glutamate is synthesized *de novo* from glutamine supplied by glial cells. After synthetized, glutamate is packaged into synaptic vesicles by vGluTs and it is released to the extracellular space to bind to ionotropic receptors, like NMDARs and AMPARs and metabotropic receptors (mGluR1 to mGluR8). A cascade of signaling is initiated, leading to membrane depolarization and modulation of local protein synthesis. Glutamate is cleared from the synapse through EAATs present in glial cells, mainly in astrocytes. In the astrocytes, glutamate is converted to glutamine, by glutamine synthetase, and glutamine is further delivered to neurons, initiating a new cycle (Popoli et al., 2011).

Moreover, astrocytes are also responsible for the uptake of other transmitters, like gamma-aminobutyric acid (GABA) and glycine. These cells contain GABA transporters (GAT), like GAT-1 and GAT-3, as well as glycine transporters, such as GLYT-1 (Minelli et al., 1995, 1996). By having these GABA transporters, astrocytes can affect inhibitory neurotransmission. However, the specific mechanism is not well characterized due to, in part, to the expression of identical GABA transporters on both neurons and glial cells (Schousboe et al., 1979).

1.2.3.3. Blood-brain barrier and ionic concentrations

The BBB is a selective barrier formed by these endothelial cells that line cerebral microvessels that control molecular traffic, permitting or facilitating the entry of required nutrients, and excluding or effluxing potentially harmful compounds (Abbott and Romero, 1996; Abbott, 2002; Hawkins and Davis, 2005). This barrier allows the diffusion of small gaseous molecules, such as O_2 and CO_2 , through the lipid membranes, and of small lipophilic agents, including drugs such as barbiturates and ethanol (Abbott et al., 2006). There is strong evidence, particularly from studies in cultured cells, that astrocytes can upregulate many BBB features, leading to tighter tight junctions (physical barrier) and the expression and polarized localization of transporters, including P-glycoprotein 24 and glucose transporter 1 (GLUT1) (transport barrier) (Dehouck et al., 1990; McAllister et al., 2001).

Studies in cultured cells demonstrated that astrocytes have much higher capacity to uptake K^+ than neurons, since that when an increase of extracellular K^+ was promoted, a higher concentration of this ion was found within astrocytes (Walz and Hertz, 1984). So, in these cells, exclusive K^+ permeability endorses the ability of astrocytes to maintain the extracellular K^+ concentration constant, when in the face of neuronal activity its concentration would increase (Orkand et al., 1966).

There are two major mechanisms, by which astrocytes can control K^+ buffering: i) uptake by Na^+/K^+ pump or ii) channel-mediated uptake of increased K^+ and Cl^- driven by the Donnan potential (distribution of ion species between two ionic solutions separated by a semipermeable membrane). In the first case, inward rectifying K^+

channels (Kir channels) are responsible for the regulation of baseline K^+ concentration, whereas Na^+/K^+ pump determines its rate of recovery after excessive neuronal firing in hippocampal slice (Walz and Wuttke, 1999; Walz, 2000; D'Ambrosio et al., 2002). However, this pump is more responsive to changes in intracellular Na^+ concentration to pump out, whereas its outside K^+ binding site is ~90% saturated. So, this clearance of K^+ must be accompanied by increases in intracellular Na^+ (Bergles and Jahr, 1997; Fischer et al., 2009). The second mechanism requires Cl^- and K^+ channels. However, there is no many evidences of the opening Cl^- channels under elevated K^+ concentrations, during normal neuronal activity (Amzica and Massimini, 2002).

Astrocytes can also express high levels of water channels (aquaporins). When intramembranous particles formed orthogonal arrays in perivascular membranes of astrocytes around capillaries and arterioles, a specific isoform of aquaporins (aquaporin 4, AQP4) was found (Amiry-Moghaddam and Ottersen, 2003). This aquaporin channel is composed by membrane proteins that transport, mainly water and, in some cases, also small solutes, e.g. glycerol (Verkman, 2005). Moreover, aquaporins have other functions like facilitating the flux of gases, including O_2, CO_2 and nitric oxide (NO) (Verkman, 2009).

One of the subunits of the family of inward rectifying K^+ channels, Kir4.1 is mainly localized in astrocytic ramifications that surround capillaries and synapses in the CNS (Higashi et al., 2001). It is necessary that these channels (Kir4.1) work in a coordinated way with AQP4, a water channel protein, to astrocytes maintain K^+ and water homeostasis (Nagelhus et al., 1999; Amiry-Moghaddam et al., 2004). Studies with *Aqp4* knock-out mice demonstrated reduced water permeability, whereas water transport in neurons is slow, which is consistent with the limited expression of aquaporins in neurons (Aitken et al., 1998; Kimelberg, 2004). However, its expression in the vascular end-feet of astrocytes suggests that these cells are highly responsible for water transport into and out of the brain (Kimelberg and Nedergaard, 2010).

1.2.3.4. Regulation of pH of the brain

Regulation of brain pH was proposed based on a localization of carbonic anhydrase in astrocytes at the blood-brain barrier, involving transport of HCO_3^- linked to acceleration of intra-astrocytic CO_2 hydration. Moreover, studies revealed Na^+/H^+ and

Cl^-/HCO_3^- exchangers and carbonic anhydrase activity in primary astrocyte cultures, which explain the astrocytic swelling under pathological conditions (Kimelberg, 1981; Kimelberg et al., 1982). Other studies showed some ways in which astrocytes can regulate pH through: i) an electrogenic sodium proton co-transporter ($3\ HCO3^- + 2\ Na^+$) that could acidify the extracellular space when stimulated by an increased K^+-dependent depolarization, and the subsequent alkalinization of cytosol; ii) a sodium-dependent Cl^-/HCO_3^-exchange and iii) the sodium independent Cl^-/HCO_3^- exchanger (Schmitt et al., 2000; Parker et al., 2008). Astrocytes can also efflux lactate through H^+ transporter, allowing its further uptake by neurons proposed in the astrocyte–neuron lactate shuttle hypothesis. Since lactate is co-transported with H^+, and this transport regulates pH levels (Pellerin and Magistretti, 2004).

1.2.3.5. Regulation of cerebral blood flow

Astrocytes foot ramifications surround blood vessels in the brain, such as the pre-capillary arterioles that regulate blood flow (Reichenbach and Wolburg, 2009; Kimelberg and Nedergaard, 2010). This control must be made in arterioles, since capillaries lack the smooth muscle responsible for the contractions and relaxations to change blood vessel diameter (Traystman, 1997). Interaction between astrocytes and blood vessels is initiated when, in early development, blood vessels breach the brain parenchyma and attract the end-feet of astrocytic ramifications (Abbott, 2002). This interaction is thought to be the major responsible for the formation of BBB through the development of endothelial tight junctions (Kimelberg and Nedergaard, 2010). However, it has been shown that in adult animals, astrocytic ramifications continue to surround blood vessels. Thus, it has been assumed that astrocytes are transducers of changes in neuronal activity, affecting the arteriole diameter and, consequently, their flow. Furthermore, it has been suggested that the increases in calcium concentrations in astrocytes by mGluR may activate phospholipase 2 to generate arachidonic acid and prostaglandin 2, through cyclooxygenase-1 (COX-1), to ultimately dilate vascular smooth muscle (Koehler et al., 2009).

1.2.3.6. Regulation of metabolism

Glycogen is a polysaccharide that acts as a cellular storage depot for glucose, either for the cells own use or for export to other cells. When high levels of glucose are present, it can be stored as glycogen; and when a period of starvation exists, glycogen can be metabolized to release energy substrate in the form of glucose. In this way the food ingested in excess can be stored so that the excessive calories do not go to waste (Brown and Ransom, 2007). Although glycogen exists in high levels in liver and skeletal muscle, lower amounts are also present in the brain (Cruz and Dienel, 2002; Chryssanthopoulos et al., 2004; McKenna et al., 2012). Thus, it is possible to assume that brain glycogen does not have the same function as liver glycogen in supporting blood glucose levels (Nilsson and Hultman, 1973).

The cellular enzyme that metabolize brain glycogen, such as glycogen phosphorylase is localized in astrocytes, as well as glycogen synthase that synthetizes this polysaccharide (Pellegri et al., 1996; Pfeiffer-Guglielmi et al., 2003). Glucose enters in CNS through the perivascular end-feet of astrocytic ramifications that have glucose transporters (Vannucci et al., 1997). Glycogen metabolism begins when glucose is converted in glucose-6-phosphate and, consequently, it is converted to glucose-1-phosphate by phosphoglucomutase. Then, the glucose-1-phosphate combines with uridine triphosphate to form uridine diphosphate (UDP) glucose in a reaction catalyzed by UDP glucose pyrophosphorylase. Finally, glycogen is catalyzed by glycogen synthase. This process is reversible since glycogen can give rise to glucose (Brown and Ransom, 2007).

Brain glycogen has two major roles: i) provide energy substrate under hypoglycemic conditions when delivery of blood-borne glucose is insufficient to meet immediate energy requirements (Brown et al., 2003; Choi et al., 2003) and ii) during periods of increased tissue energy demand, when ambient glucose is insufficient to meet the transient elevation in energy needs (Brown et al., 2003).

Astrocytes also participate in the astrocyte-neuron lactate shuttle, one of the major interactions between the cells. In this hypothesis, there is glucose entry in the CNS and, when glucose is converted in lactate, it can be served as energy supply of neurons

(Magistretti et al., 1994; Voutsinos-Porche et al., 2003). In a more detailed way, glucose is converted in pyruvate and ATP. Then, pyruvate is converted in lactate by the action of lactate dehydrogenase (LDH). Both lactate and glutamine are released and taken up by neurons, where the first one is converted again in pyruvate by LDH, producing ATP (Kimelberg and Nedergaard, 2010).

The enzymes involved in this lactate shuttle are also present in high amounts in the tricarboxylic acid (TCA) cycle in astrocytes (Kimelberg and Nedergaard, 2010). In this cycle, glutamate also acts as an energy substrate leading to ATP production following the metabolism of its carbon skeleton through the action of glutamate dehydrogenase 1 (GDH) and aspartate aminotransferase (AAT), two enzymes localized in mitochondria (McKenna, 2013). Although it has been highly discussed which of these enzymes is the main responsible for the conversion of glutamate to alpha-ketoglutarate (α-KG), ATP production is higher when the initial step of glutamate metabolism is catalyzed by GDH rather than AAT (McKenna, 2013). The cycle begins with the conversion pyruvate in acetyl-coenzyme A (acetyl-CoA) that catalyzes the transformation of oxaloacetate in citrate, along with citrate synthetase. Citrate is converted in isocitrate by aconitase and further converted into α-KG by isocitrate dehydrogenase. Then, α-KG is converted in succinyl-coenzyme A (succinyl-CoA), by α-ketoglutarate dehydrogenase, or it can also be converted into glutamate by glutamate dehydrogenase, and vice-versa. When succinyl-CoA is transformed in succinate through succinyl-CoA synthetase, ATP is released, and succinate is converted in fumarate by succinate dehydrogenase. Afterwards, fumarate is transformed in malate by fumarase, which is further converted into oxaloacetate by malate dehydrogenase, beginning a new cycle (Fig. 6).

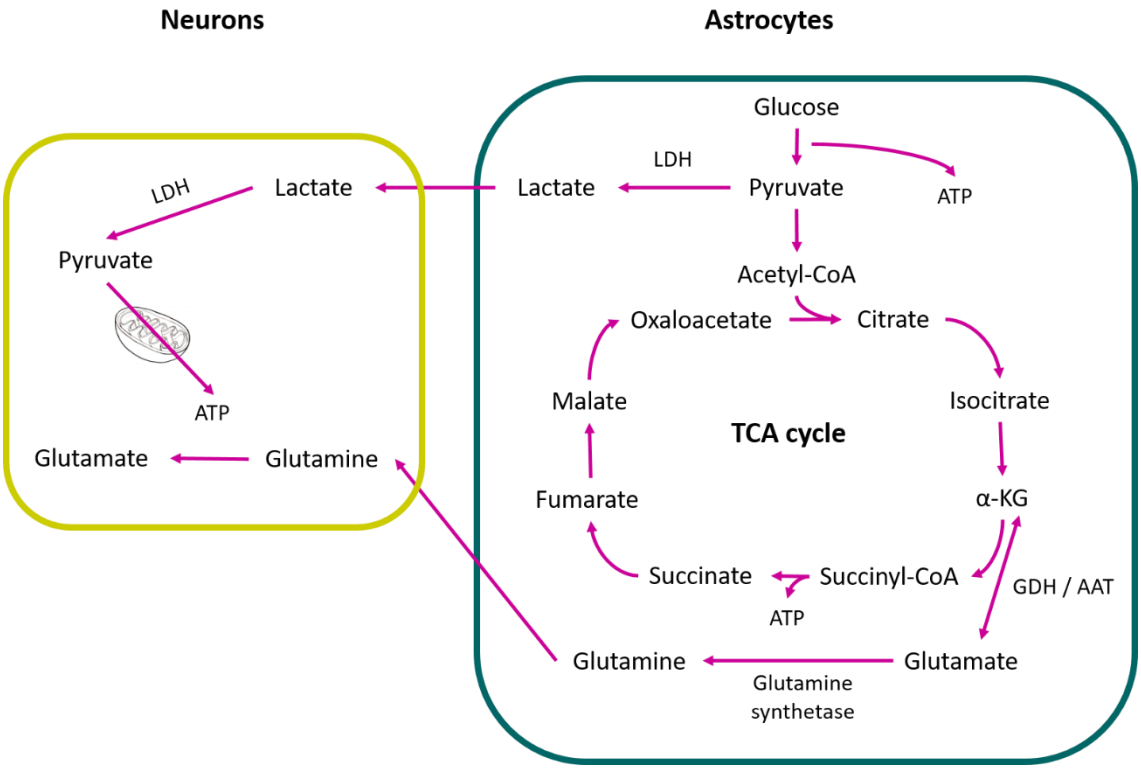

Figure 6 - **Astrocytes-neurons lactate shuffle and astrocytic involvement in the tricarboxylic acid (TCA) cycle.** α-KG: α-ketoglutarate; AAT: Aspartate aminotransferase; acetyl-CoA: acetyl-coenzyme A; ATP: adenosine triphosphate; GDH: Glutamate dehydrogenase; LDH: lactate dehydrogenase; succinyl-CoA: succinyl-coenzyme A.

Moreover, glutamate and ATP are recognized by astrocytic metabotropic receptors, activating phospholipase C (PLC) and producing inositol triphosphate (IP3), which in turn, could trigger the release Ca^{2+} from endoplasmic reticulum (intracellular Ca^{2+} store), leading to the opening of hemichannels and the exocytotic Ca^{2+}-dependent gliotransmitters release (Orellana and Stehberg, 2014).

1.2.3.7. Role in oxidative stress

Mitochondrial reactive oxygen species (mROS) are generated by the respiratory chain during ATP synthesis due to the leakage of electrons from complex I, complex II and complex III to molecular oxygen (Boveris et al., 1972; Chance et al., 1979; Yankovskaya et al., 2003). Normally, the levels of mROS are low due to antioxidants and enzymatic antioxidant systems. But, when these systems fail, there is an increase in the levels of these reactive oxygen species (ROS), which are the major stimulators of cell injury (Chance et al., 1979). Mitochondrial oxidative stress leads not only to the interruption of the energy supply, but also to severe damage of mitochondrial components, including proteins, lipids and mitochondrial DNA (mtDNA). In addition,

oxidative stress is often accompanied by Ca^{2+} stress, another important apoptotic inducer (Duchen, 2000; Maassen et al., 2004). Subsequently, there is the activation of mitochondrial permeability transition (MPT)-dependent and/or MPT-independent release of mitochondrial potential noxious proteins, including cytochrome c that promotes apoptosis (Kroemer et al., 2007).

Astrocytes are connected with gap junctions, which allows intercellular propagation of intracellular signaling molecules including Ca^{2+} and ROS. However, these cells are also involved in maintaining the intracellular levels of antioxidants (Giaume and McCarthy, 1996; Verkhratsky and Kettenmann, 1996; Bennett et al., 2003; Brady et al., 2004). Thus, astrocytes have antioxidant systems, such as glutathione disulfide – glutathione (GSSG – GSH), superoxide dismutase (SOD; metabolizes superoxide into oxygen and hydrogen peroxide) and catalase (decomposes hydrogen peroxide into water and oxygen) (Anderson et al., 2003; Cahoy et al., 2008). So, in order to prevent the neurological injury by ROS, it is necessary to improve antioxidation function of astrocytes or limit their capacity of producing ROS.

1.2.3.8. Astrocytic functions in cognition

To understand how astrocytes take part in in memory and learning, it might be useful to elucidate better the mechanisms behind these cognitive processes. Although, it is known that learning depends on states of attention, motivation, sleep cycles and arousal; glia cells, in particular astrocytes, can alter the formation and consolidation of memories (Meltzoff et al., 2009). It is known that in astrocytes, the activation of intracellular Ca^{2+} signaling can further enhance or diminish both inhibitory and excitatory synaptic transmission, and consequently the states of sleep and working memory (Halassa et al., 2009). Astrocytic signaling is also involved in LTP in hippocampus and cortex, as well as in hippocampal LTD, that may influence working memory (Han et al., 2012).

1.3. Reactivity of astrocytes

In neurological disorders, astrocytes react in a defensive manner called reactive astrogliosis that can be defined as constitutive, graded and multistage process, which is evolutionarily conserved. It also accompanies many pathological situations that affect the CNS, such as trauma, ischemic damage, and neurodegenerative disorders. Moreover, the activation of these cells, like of microglia cells, can trigger a neuroinflammatory process, in which the neurons usually start degenerating (Verkhratsky and Butt, 2013). Reactive astrocytes, when compared with nonreactive astrocytes, exhibit altered expression of many genes and distinct morphological and functional features (Eddleston and Mucke, 1993; Rosario Hernandez et al., 2002; Pekny and Nilsson, 2005; Sofroniew and Vinters, 2010).

GFAP is a cytoskeletal protein present in astrocytes and is thought to provide structural support for maintenance of cell shape and, when astrocytes become reactive this protein is upregulated and, besides occurring morphological changes, it might happen alterations in intracellular trafficking of organelles and proteins (Eng and Ghirnikar, 1994). Furthermore, increase of GFAP in astrocytes also occurs gradually throughout the aging of rodents and humans (Nichols et al., 1993). *In vitro* studies using neuron-astrocyte co-cultures have shown that inhibition in GFAP synthesis led to a reduction of astroglial hypertrophy and blockade of neuritic outgrowth diminished, that normally is observed after a lesion (Lefrançois et al., 1997). However, GFAP does not exist only in astrocytes but also, in ependymal cells, like tanycytes and in immature neurons (Eng and Ghirnikar, 1994; Liu et al., 2010). Furthermore, it was also shown that in many neurological conditions, such as hypoxia, ischemia and epilepsy, the astrocytic protein GS is also altered. However, alterations in this enzyme expression are specific of the region of the brain and does not positively correlates with GFAP expression, suggesting that it is not a good marker for reactive astrogliosis (Rose et al., 2013). Although GS plays an important role in neurotransmission (see section 1.2.3.2.), it is also involved in the assimilation of ammonia by the brain. Ammonia is a metabolite mainly produced in the gastrointestinal system, through protein degradation and amino acid deamination and it is primarily regulated by the urea cycle, found exclusively in the liver

(Eng and Ghirnikar, 1994). When ammonia concentration increases, GS activity intensifies to prevent toxicity and neurological dysfunction (Cudalbu et al., 2012).

Cytokines, such as transforming growth factor (TGF), ciliary neurotrophic factor (CNTF), interleukin (IL)-6, leukemia inhibitory factor (LIF) and oncostatin M, trigger astrocyte activation in rodents brain (Balasingam et al., 1994; Winter et al., 1995; Klein et al., 1997; Rabchevsky et al., 1998). Epidermal growth factor receptor (EGFR) is also detected in reactive astrocytes and in inactivated microglia/macrophages, and when upregulated, allows the transition of astrocytes from nonreactive to the reactive state (Planas et al., 1998; Erschbamer et al., 2007). When its signaling is inhibited, there is axonal regeneration and functional recovery after CNS injury (Koprivica et al., 2005; Erschbamer et al., 2007).

Reactive astrocytes usually surround the damaged area, forming glial scars as an attempt to isolate the damage area and allow it regeneration (Rodriguez et al., 2009; Osborn et al., 2016; Rodríguez-Arellano et al., 2016). These alterations will result in a gain or loss of function of astrocytes. Since although the glial scars create conditions to occur brain regeneration, they might also contribute to the reduction of synaptic coverage and homeostatic support, which together may lead to synaptic weakness and loss, affecting thus the connectivity of neuronal networking and associated information processing that might underlie memory impairment (Sofroniew and Vinters, 2010; Zorec et al., 2015, 2017).

Besides GFAP and GS, there are several molecular markers for the identification of astrocytes or of their function state, such as S100β, a calcium binding protein only expressed by a subtype of mature astrocytes; the glutamate transporters: glutamate aspartate transporter (GLAST; or excitatory amino acid transporter type 1 (EAAT1) in humans) and glutamate transporter 1 (GLT-1; or EAAT2 in humans), and the metabolic enzyme, aldehyde dehydrogenase 1 family member L1 (Aldh1L1) (Wang and Bordey, 2008; Sofroniew and Vinters, 2010; Garwood et al., 2017). The S100β is a calcium-binding peptide, used as a parameter of glial activation or death in many disorders of the CNS, since there is evidence that extracellular S100β might participate in brain inflammation by activating astrocytes, microglia and neurons (Donato, 2001). This

peptide can also inhibit protein phosphorylation, regulate enzyme activity and Ca^{2+} homeostasis (Gerke and Weber, 1985; Wilder et al., 1998; Donato, 2001).

Although the number of reactive astrocytes is increased in neuropathological conditions, it remains unclear whether astrocytic dysfunction contribute for the disorder by providing detrimental signals, such as glutamate, pro-inflammatory cytokines and reactive oxygen and nitrogen species, or if the activation of astrocytes prevents the disease by being supportive and attempting to reverse the early cellular damages (Minagar et al., 2002). Thus, it is crucial to understand the role of astrocytes to understand their function in pathophysiological states.

1.3.1. Astrocytes and brain disorders

Increasing evidences point out that different type of astrocytes with particular properties are found in a given brain region, and that their properties can vary in different subregions (Seifert et al., 2006). Thus, for each neurological disorder, astrocytes can be differentially dysfunctional with diverse pathological consequences.

In brain disorders like depression, epilepsy, schizophrenia, Alzheimer's disease and Parkinson's disease, the astrocytes morphology and protein expression, in particular GFAP, were shown to be altered (Tian et al., 2005; Volterra and Meldolesi, 2005; Webster et al., 2005; Sastre et al., 2006; Seifert et al., 2006; Banasr and Duman, 2008; Lee et al., 2010). Since gliotransmission is now known as a modulatory factor of synaptic communication, changes in this event may be considered an important mechanism underlying pathological processes (Fellin, 2009).

Regarding epilepsy, it was shown that when there was an increase in GFAP, there was hypertrophy and proliferation of astrocytes (reactive astrocytes), being possible to correlate with the increase of seizure frequency (Cohen-Gadol et al., 2004). Moreover, astrocytic glutamate release can participate in the generation of paroxysmal depolarization shifts (abnormal prolonged depolarizations with repetitive spiking that are reflected as interictal discharges in the encephalogram), and consecutively, contribute to epileptic seizures. It was also observed that the frequency of astrocytic

Ca^{2+} oscillations increases in isolated brain slices that exhibit epileptiform activity (Rogawski and Löscher, 2004; Tian et al., 2005). GS activity and expression in this disease can be region-selective, depending on the kind of epilepsy (Rose et al., 2013).

In the case of bipolar disorder and major depression, the expression of GFAP was diminished (Johnston-Wilson et al., 2000; Webster et al., 2005). Also, in depression, the expression of brain glutamate-ammonia ligase mRNA that codifies GS was decreased (Klempan et al., 2009; Sequeira et al., 2009). In schizophrenia, the levels of S100β and of GFAP as well as Aldh1L1 mRNA were found to be increased (Barley et al., 2009; Qi et al., 2009).

Alzheimer's disease (AD) is characterized by the accumulation of amyloid-β (Aβ) peptides, which form fibrils that make up the amyloid plaques. Accumulating evidences suggest that Aβ peptides trigger structural and morphological alterations in astrocytes, activating reactive astrogliosis (Pekny and Nilsson, 2005). Astrocytes play an important role in the clearance of Aβ peptides and can also form a protective barrier between amyloid deposits and neurons (Wyss-Coray et al., 2003; Roßner et al., 2005). Moreover, the astrocytes activation is associated with the development of amyloid plaques and the reactive astrocytes may initiate a neuroinflammatory process (Nagele et al., 2004). Moreover, some of causal and risk factor genes for AD, such as genes coding the amyloid-β precursor protein (APP) and the presenilins-1 and 2 that constitute the γ-secretase complex, an enzyme involved in proteolytic processing of APP and subsequent formation of Aβ, as well as the ε4 allele of the Apoe gene (risk factor for AD) are not only expressed by neurons but also by astrocytes, corroborating the idea that astrocytes are important players in AD pathogenesis (Boyles et al., 1985; Patel and Ridgeway, 1993). In post-mortem brain tissue from patients with this disease, it was demonstrated that there was a reduction in GS and this reduction was correlated with a greater number of amyloid deposits (Hensley et al., 1995; Le Prince et al., 1995; Olabarria et al., 2011). In contrast, it was shown that Aβ peptides stimulate the synthesis of both S100β mRNA and S100β protein in astrocyte cultures (Peña et al., 1995).

1.4. Pharmacological tools to abrogate astrocytic function

There are several pharmacological tools that can abrogate astrocytes function, such as the L-α-Aminoadipate (L-AA) and its D-isomer D-α-Aminoadipate (D-AA), trifluoroacetic acid and inhibitors of glutamate transporters.

Interfering with the glutamate clearance by astrocytes might have harmful consequences in synaptic transmission. There are two main glutamate transporters in astrocytes, GLT-1 and GLAST (Rothstein et al., 1994). These astroglial glutamate transporters are important in maintaining low extracellular glutamate concentrations, since glutamate is supposed to be recycled by astrocytes preventing excitotoxicity. Neurons have less capacity to uptake extracellular glutamate when compared with astrocytes. So, loosing these GLT-1 or GLAST could lead to persistent synaptic depolarization, disrupting neural circuitry (Rothstein et al., 1996). Furthermore, mice lacking glutamate transporter GLT-1 die within weeks after birth as a consequence of repeated seizures, suggesting that pharmacological manipulation of the transmitter represents a therapeutic target (Rothstein et al., 1996).

1.4.1. The gliotoxin L-α-aminoadipate

L-AA is an amino acid similar to L-glutamate that results from the metabolism of lysine in the brain (Chang, 1976, 1978). L-AA and its isomer D-AA are well known as CNS gliotoxins that affect the Müller cells in the retina (Olney et al., 1971). D-AA is a NMDARs antagonist that may be neuroprotective (Olney et al., 1980). In fact, the L-isomer was considered to be more toxic than the D-isomer (Bridges et al., 1992). Studies *in vitro* also showed that its cytotoxic effects occurred in astrocytes, but not in neurons (Huck et al., 1984; Khurgel et al., 1996). It was also observed that each isomer had different toxic mechanisms, L-AA was more toxic to protoplasmic astrocytes through the sodium dependent glutamate transport, whereas D-AA was only toxic to mitotic astrocytes (proliferating astrocytes), by interference with protein synthesis needed for cell division (Connor et al., 1990; Brown and Kretzschmar, 1998).

Two mechanisms are involved in the gliotoxicity induced by L-AA: i) high affinity glutamate transporter and ii) inhibition of cystine/ glutamate antiporter. The first takes into account that L-AA structure is similar to glutamate, so it could be taken up by astrocytes through Na^+-dependent glutamate transporters, like GLT-1 and GLAST, being a direct competitor (McBean, 1994). When accumulated in these cells, L-AA began to exert its toxic effects by inhibiting the action of GS that is supposed to convert glutamate into glutamine (McBean, 1994) (Fig. 7). The second is based in the ability of inhibit Na^+-independent cystine/glutamate exchange, which is mediated by cystine/glutamate antiporter. This antiporter transports glutamate to the extracellular space and cystine to cell inside, maintaining cellular concentrations of glutathione. Thus, high concentrations of glutamate inhibit cystine uptake leading to a reduction of glutathione levels and to an increase of oxidative stress, promoting apoptotic cell death (Kato et al., 1993; Brown and Kretzschmar, 1998). Moreover, these levels of glutathione can also vary due to the inhibition of γ-glutamylcysteine synthetase, also responsible for the maintenance of glutathione levels, due to the similarities with GS (Meister and Tate, 1976; McBean, 1994; Chang et al., 1997).

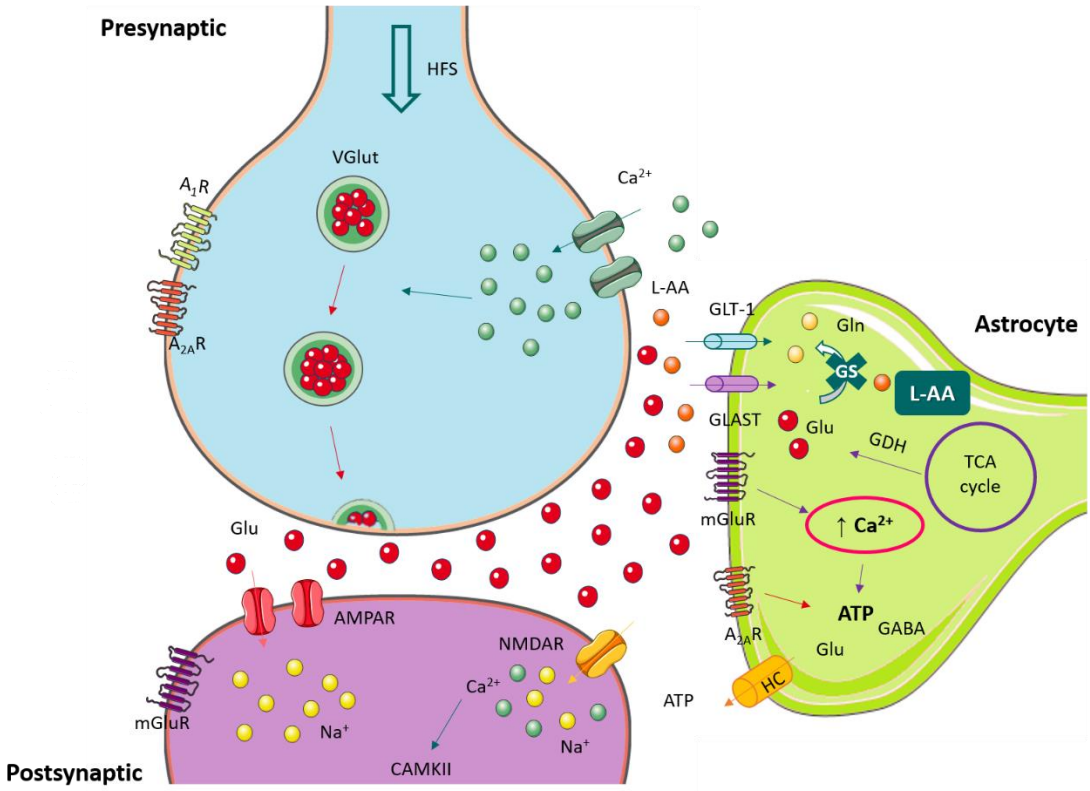

Figure 7 - Mechanism of astrocytes toxicity by L-AA. L-AA is taken up by astrocytes through sodium-dependent glutamate transporters (GLT-1 and GLAST), inhibiting the conversion of glutamate (Glu) into glutamine (Gln) by glutamine synthetase (GS).

Chapter 2 | Aims of work

In this work, we aim to investigate the impact of astrocytes blunting on memory and hippocampal astrocytic proteins and morphology.

To achieve these goals, we use an astrocytic pathology mice model, consisting in the icv administration of L-AA for three consecutive days. Alterations in mice behaviour were evaluated and compared between mice icv administrated with L-AA or with vehicle. The hippocampal astrocytic proteins levels and of astrocytes morphology were also evaluated to infer about the impact of L-AA on astrocytes function and viability. In addition to confirm if the alterations in memory was not related with synaptic loss triggered by L-AA we also checked for putative changes in synaptic proteins.

In the first task, we administrated intracerebroventricularly L-AA or vehicle (as a control) for three consecutive days in young adult mice, using cannula guides implanted in one of the lateral ventricles. Then these two groups of animals were behaviourally tested, mainly regarding memory performance (object recognition, object displacement, modified y-maze and step-down inhibitory avoidance tests). In a second task, we performed morphological and neurochemical analyses of hippocampus of the described experimental animal models. Therefore, we used hippocampal sections to analyze alterations in astrocytes morphology (label of GFAP) by immunohistochemistry, with particular focus on identifying alterations in astrocytic process (number and size) and astrocyte tridimensional structure analysis, using confocal microscopy. In addition, we also quantified the levels of hippocampal astrocytic proteins (GFAP, GS, S100β and Cx43) and of synaptic markers (synaptophysin, SNAP-25 and PSD-95), in the two animal groups, by Western-blot analysis.

Although the present work was designed to validate an animal model of astrocytes pathology in hippocampus, a brain structure involved in memory processing; it also gives novel insight about the role of astrocytes in memory. Furthermore, it will be crucial to evolve to other studies in which the focus is the definition of whether astrocytes have a key role in brain-disorders associated with cognitive decline, such as Alzheimer´s disease.

Chapter 3 | Material and Methods

3.1. Animals

Male C57BL/6 mice (8–12 weeks) (Fig. 8) were obtained from Charles River (Charles River Laboratories, Barcelona, Spain). Animals were maintained under controlled environment (22 ± 2°C; 12 h light/dark cycle, relative humidity of 55% and *ad libitum* access to food and water) and handled according to European Union guidelines (2010/63/EU) that were approved by the Ethics Committee of the Center for Neuroscience and Cell Biology of Coimbra.

Figure 8 - C57BL/6 mice.

3.2. Reagents

Table 2 - List of reagents used.

Reagent	Supplier
(2R,3R,4S,5S,6R)-2-[(2S,3S,4S,5R)-3,4-dihydroxy-2,5bis(hydroxymethyl)oxolan-2-yl] oxy-6-(hydroxymethyl)oxane-3,4,5-triol (Sucrose)	Sigma-Aldrich
(2R,3S,4R,5R)-2,3,4,5,6-Pentahydroxyhexanal (Glucose)	Sigma-Aldrich
2-(Bis(2-hydroxyethyl)amino)acetic acid (Bicine)	Sigma-Aldrich
2,6-dibromo-4-[3-(3,5-dibromo-4-hydroxyphenyl) -1,1-dioxo-2,1λbenzoxathiol-3-yl]phenol (Bromophenol blue)	Sigma-Aldrich
2-[2-[3,4-bis(2-hydroxyethoxy) oxolan-2-yl]-2-(2hydroxyethoxy)ethoxy]ethyl dodecanoate (Tween 20)	Sigma-Aldrich
2-[2-[Bis(carboxymethyl)amino]ethyl} (carboxymethyl)amino]acetic acid (EDTA) tetrasodium	Sigma-Aldrich
2-[4-(2,4,4-trimethylpentan-2-yl)phenoxy]ethanol (Triton X-100)	Sigma-Aldrich
2-Amino-2-hydroxymethyl-propane-1,3-diol (Trizma base)	Sigma-Aldrich
3-(cyclohexylamino)propane-1-sulfonic acid (CAPS)	Sigma-Aldrich
30% Acrylamide/Bis solution	Bio Rad
4-(2-hydroxyethyl)-1-piperazineethanesulfonic acid (HEPES)	Sigma-Aldrich
Ammonium Persulfate (APS)	Sigma-Aldrich
Bicinchoninic acid (BCA) kit	Thermo Fisher Scientific
Bovine Serum Albumin (BSA)	Sigma-Aldrich
Protease inhibitor cocktail (CLAP)	Sigma-Aldrich
Dithiothreitol (DTT)	Sigma-Aldrich
Pierce ECL Western Blotting substrate	Thermo Fisher Scientific
Horse Serum Substrate	Invitrogen
Hydrogen Chloride (HCl)	Sigma-Aldrich
Methanol	Sigma-Aldrich
N,N,N′,N′-Tetramethylethane-1,2-diamine (TEMED)	Sigma-Aldrich
Paraformaldehyde	Sigma-Aldrich
Percoll	GE Healthcare
Phenylmethanesulfonyl fluoride (PMSF)	Sigma-Aldrich
Ponceau S	Sigma-Aldrich
Potassium Chloride (KCl)	Sigma-Aldrich
Potassium phosphate monobasic (KH_2PO_4)	Sigma-Aldrich

Prolong Gold Antifade Reagent	Invitrogen
Glycerol	Sigma-Aldrich
Sodium Chloride (NaCl)	Sigma-Aldrich
Sodium Dodecyl Sulfate (SDS)	Bio Rad
Sodium Hydroxide (NaOH)	Merck
Sodium phosphate dibasic heptahydrate ($Na_2HPO_4 \cdot 7H_2O$)	Sigma-Aldrich
2,2,2-Tribromoethanol	Sigma-Aldrich
2-Methyl-2-butanol	Sigma-Aldrich
Sodium deoxycholate	Sigma-Aldrich
DAKO fluorescent mounting medium	DAKO
Luminata Forte Western HRP substrate	Millipore
Ethanol	Emsure
L-α-aminoadipate	Sigma-Aldrich

3.3. Experimental Design

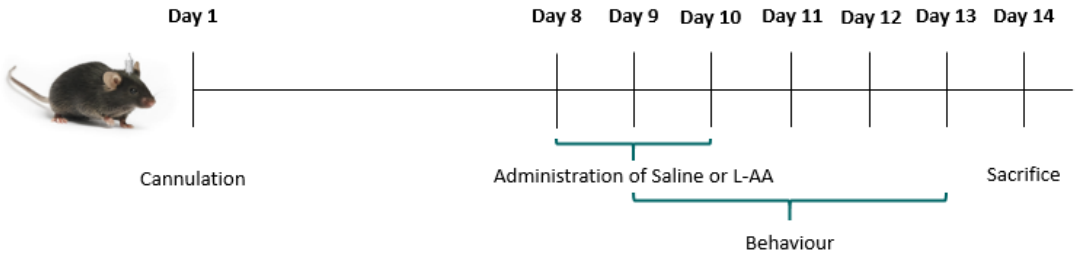

Figure 9 - Experimental design.

3.4. Preparation and administration of gliotoxin

3.4.1. Stereotaxic surgery

To establish the astrocyte pathology model, mice were surgically implanted with cannula guides in the lateral ventricle to further perform the intracerebroventricular administration of gliotoxin L-AA (Fig. 10). Briefly, animals were anesthetized with tribromoethanol (Avertin, 12-14 µl/g body weight, intraperitoneal (i.p.) max 250 mg/kg) and placed on a stereotaxic frame (Stoeling). A stainless-steel cannula (26G, Plastics One) was implanted unilaterally and fixed to the skull with dental cement, according to the following coordinates:

Figure 10 - Stereotaxic surgery with cannula implantation.

anterior – posterior (AP) -0.58 mm; medial – lateral (MV) -1.13 mm; dorsal – ventral (DV) -2.00 mm (Paxinos and Franklin, 1997).

3.4.2. L-AA preparation and administration

To prepare L-α-aminoadipate drug solution, we solubilized this L-AA in PBS and adjusting the pH to 7.4 to help to dissolve the aminoadipate (Khurgel et al., 1996).

Animals were allowed to recover from surgery before proceeding with one administration for three consecutive days of saline solution (PBS) or 40 µg/µl of L-AA, being infused a total volume of 4 µl at a rate of 0.5 µl/minute, controlled by a micro-pump (53100V, Stoeling).

The animals were gently restrained by hand and these administrations were accomplished using a 10 µL Hamilton microsyringe, connected to a double internal cannula (that projected 1 mm from the tip of cannula guide) through a polyethylene tubbing. The double internal cannula was slowly withdrawn 1 minute after infusion completion to avoid the displacement of the injected fluid by capillarity.

Since L-AA has an effect 4 hours following injection and persists up to three days (Khurgel et al., 1996), this gliotoxin was infused in the mice brains three days before starting the behaviour analysis, to mimic the window of time of L-α-aminoadipate effect.

3.5. Behaviour analysis

Each behavioural test was performed in sound-attenuated room with controlled dimmed lighting conditions, predominantly set with a red source of light. All environmental cues in the room were held constant throughout testing.

Before initiating behaviour studies, animals were handled once a day and before each test they were up to red light habituation for one hour.

To remove the smell traces left by mice, the floor and walls of the equipment and used objects were carefully cleaned with 70% ethanol before testing the next

animal. To avoid influence of the circadian rhythms on performance of the animals, each behavioural test was carried out between 8 a.m. and 1 p.m. All the behaviour tests were carried out after the injections of PBS or L-AA.

Activity of the animals was recorded by a video camera and software. For each test with two parts, an inter-trial interval (*ITI*) of 90 minutes, between sample trial and test trial, was chosen since we wanted to evaluate short-term memory dependent of hippocampus (Assini et al., 2009).

3.5.1. Open Field test

The open field test was designed to assess the locomotor activity, hyperactivity and exploratory behaviour. It can also be used to evaluate anxiety and/or impulsivity, since mice don't appreciate bright illuminated, novel and open spaces (Cummins and Walsh, 1976; Belzung and Griebel, 2001). This test is a trial test with no impact on the animal's subsequent behaviour.

Locomotor activity of C57BL/6 mice was monitored in three consecutive days in an open field arena (Fig. 11) and the exploratory behaviour was evaluated by the total distance travelled in a 10 minute period and by the total time mice spent in the center and periphery of the open field arena (Coelho et al., 2014).

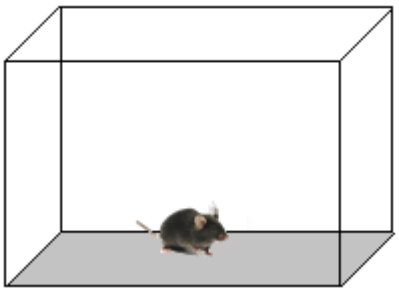

Figure 11 - Open field habituation test.

This test was carried before Novel object recognition (NOR) test and Object displacement (OD) test, functioning also as habituation to the arena.

3.5.2. Novel Object Recognition test

The NOR test has become a widely used model to assess memory performance for the investigation of memory alterations (Silvers et al., 2007) Animals without any neurological alterations prefer novelty since they are very curious (Ennaceur, 2010).

This test evaluates the hippocampus and cortex-dependent memory and consists in two phases described below: i) sample trial and ii) test trial (Clark et al., 2000; Buckmaster, 2004) (Fig. 12):

i) In the sample trial, mice were placed in the open field arena with two identical objects in two opposite corners, which mice could explore freely for 10 minutes.

ii) In the test trial (90 minutes later), mice were placed again in the open field arena and in this time one of the objects (novel) was different from the other (familiar); mice were allowed to explore for 5 minutes.

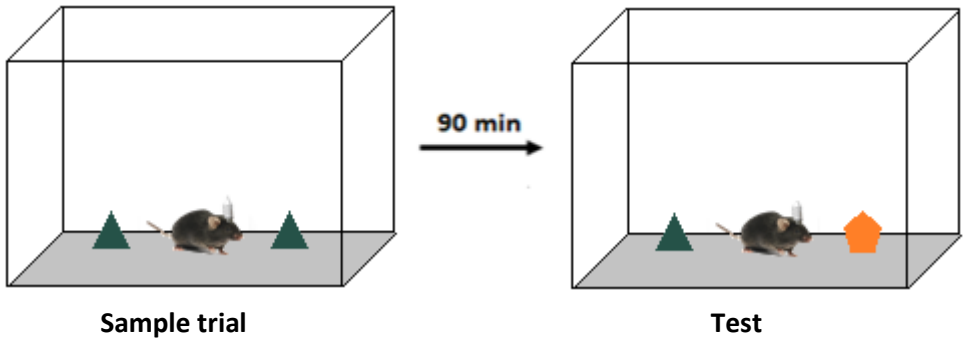

Figure 12 - Novel object recognition test, with an ITI of 90 minutes between the two sessions.

The criteria for the exploration of the objects was defined as directing the nose to the object at distance equal to or less than 1 cm from the object and/or touching it with the nose. The time exploring and number of interactions with each object was quantified manually in both sample and test trials by a blinded observer to the experimental groups. Recognition index (RI), which corresponds to the percentage of time mice spent exploring the novel object, was calculated as (total time spent with the novel object / total time spent with both objects) multiplied by 100. The same was done for number of interactions with the objects.

3.5.3. Object Displacement test

Hippocampus-dependent memory was evaluated in the object displacement test (Fig. 13). This test consists in two phases described below: i) sample trial and ii) test trial:

i) In the sample trial, C57BL/6 mice were placed in the open field arena with two identical objects in two opposite corners, which animals could explore freely for 10 minutes.

ii) In the test trial, 90 minutes later, mice were placed again in the open field arena, except that this time one of the objects was moved from its original position, and mice were allowed explore the objects for 5 minutes.

The criteria to define the exploration of the objects was the same as used for the object recognition test. The time exploring and the number of interactions mice with each object was quantified manually in both sample trial and test trial by blinded observer to the experimental groups. Displacement index was calculated as (total time mice spent with the displaced object / total time mice spent with both objects), multiplied by 100. The same was done for the interactions with the objects.

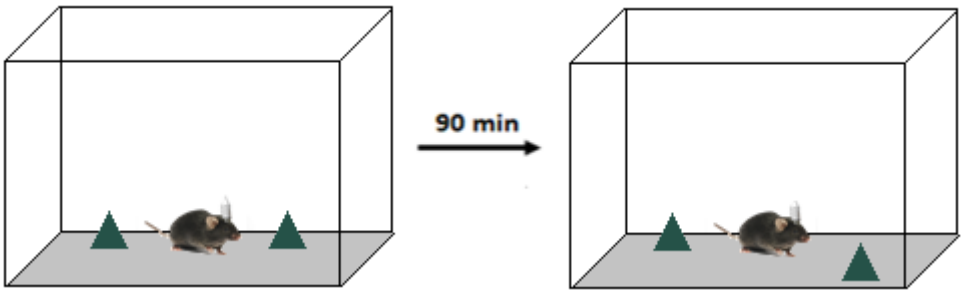

Figure 13 - Object Displacement test, with an ITI of 90 minutes between sample trial and test trial.

3.5.4. Elevated Plus Maze test

Anxious-like behaviour was assessed in the elevated plus maze (EPM) test, which is based on the propensity of mice to approach closed and dark spaces and to avoid open and high spaces (Barnett, 1975). Briefly, C57BL/6 mice were placed in the center of a plus-like elevated apparatus (Fig. 14), with two opposing closed and two opposing open arms, which mice freely explored the maze for 5 minutes. The time, the number of entries and the travelled distance mice

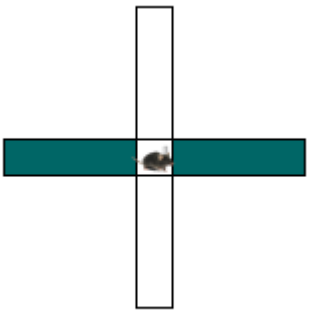

Figure 14 - **Elevated plus maze test.** With two open (white) and two closed arms.

spent in the open and closed arms was recorded (Dawson and Tricklebank, 1995). The latency to enter in open arms, as well as the number of head dippings (each time that mice evaluates the risk inside the open arms) and stretch-attend posture (each time that mice evaluates the risk in the center of the elevated plus maze) was also evaluated.

Percentage of time, entries and distance mice spent in the open arms was calculated as (total time/entries/distance spent in the open arms) divided by (total time/entries/distance spent in open and closed arms), multiplied by 100.

3.5.5. Modified Y-maze test

The Y-maze used is a three-arm black apparatus in which the three arms converged to a same point with an equal angle between them.

Modified Y-maze test evaluates working memory for spatial location, it depends of the hippocampus and it is based on the innate tendency of mice to explore novelty (Dellu et al., 1992, 1997). This test consists in two phases described below: i) sample trial and ii) test trial, with a ITI of 90 min (Fig. 15):

i) In this phase (sample trial) only two arms of the apparatus were available for exploration ("start arm" and "other arm"), being the third arm closed. C57BL/6 mice were placed in "start arm" and allowed to explore for 5 minutes.
ii) 90 minutes later, the test was performed with a third arm ("novel arm") open. The animals were placed again in the "start arm" and left for exploration for another 5 minutes.

The time, number of entries and distance travelled in each arm was recorded (Dawson and Tricklebank, 1995). Percentage of time, entries and distance mice spent in the novel arm was calculated as (total time/entries/distance spent in the novel arm) divided by (total time/entries/distance spent in the three arms), multiplied by 100.

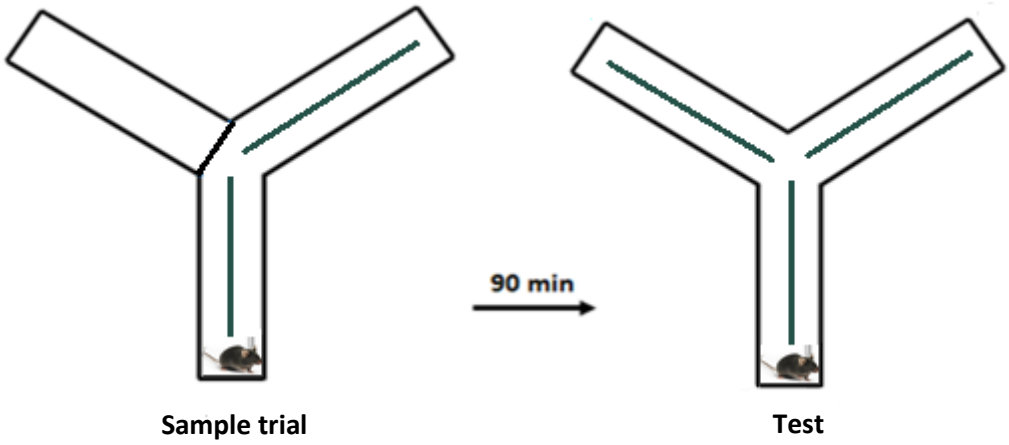

Figure 15 - **Modified Y-maze test**, with an ITI of 90 minutes between sample trial and test trial.

3.5.6. Step-down Inhibitory avoidance test

In the training session, mice were gently placed at the platform in the middle of the apparatus (Pagnussat et al., 2015) (Fig. 16). When they stepped down, placing their four paws on the grid, they received a 2 second 0.5 mA scrambled foot electric shock and then were immediately removed from the apparatus. The test session was carried out 90 minutes after the training session. The procedure was the same, but the foot electric shock was omitted. In both training and in test, the maximal step-down latency was 180 seconds. Latency to step down from the platform was recorded, as a measure of retention, using an automated stopwatch.

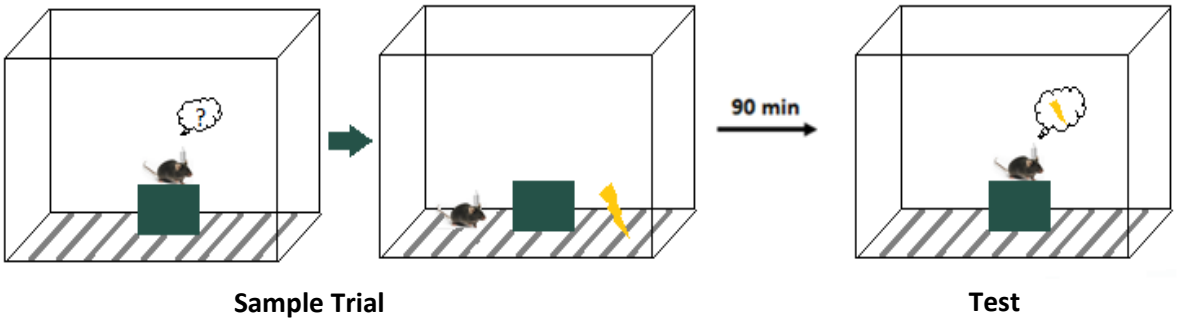

Figure 16 - Step-down inhibitory avoidance test, with an ITI of 90 minutes between sample trial and test. In the platform (green) the electric shock is not sensed.

3.6. Neurochemical studies

Immunohistochemistry and immunoblot (Western blot) assays were performed to assess alterations, triggered by the gliotoxin L-AA, in the morphology and/or number of astrocytes and to determine alterations in the levels of astrocytic and synaptic markers, respectively. The levels of astrocytic markers were measured in total extracts of hippocampus, whereas the levels of synaptic markers were determined in synaptosomes purified by a 45% percoll gradient, enriched in membranes of pre-synaptic and postsynaptic terminals (Canas et al., 2009; Rodrigues et al., 2014). These neurochemical studies were performed, 24h after behavioural tests and 96h after L-AA or vehicle administration.

3.6.1. Brain fixation and Immunohistochemistry

Brain fixation was obtained through transcardial perfusion with a paraformaldehyde (PFA) solution, as previously described (Cunha et al., 2006). Briefly, mice were anaesthetized with tribromoethanol, their heart was exposed and after clamping the descending aorta, a catheter was inserted into the ascending aorta. The mice were perfused PBS) solution (while opening the right atria to allow the outflow of the internal blood) and further perfused with 4% PFA in PBS. After fixation, the brain was removed and maintained in 4% PFA in PBS solution for 24h at 4ºC, and then 48h in a 30% sucrose solution (in PBS). Finally, the brain was frozen in dry ice and 30 µm coronal sections were obtained using a Leica CM1850 cryostat (Leica Microsystems).

After selecting the brain slices to be used and placed them in a multiwell plate, it was necessary to wash them three times with PBS, under gentle agitation for 5 minutes. Then, the slices were permeabilized with 0.1% Triton in PBS for 15 minutes and afterwards, blocked with 10% horse serum and 0.1% Triton in PBS, for one hour at room temperature (RT). Later, the brain slices were incubated with the primary antibody overnight at 4ºC. After this incubation, the slices were washed once again with blocking solution and they were incubated with the secondary antibody for two hours at RT and protected from the light. In the table 3 it is stated the dilution of primary and secondary

antibodies used. Then, they were washed three times with PBS for 5 minutes and they were incubated with DAPI (1: 5000, nucleus marker) for 10 minutes at RT under gentle agitation and washed again with PBS. These slices were mounted on slides, pre-coated with 2% gelatin in a 0.08% chromalin solution (chromium and potassium sulfate), with DAKO fluorescent mounting medium or Prolong gold antifade reagent and allowed to dry at room temperature, and further stored at -20°C until use (Canas et al., 2009).

Table 3 - **Antibodies used in immunohistochemistry.**

Primary Antibodies	Host	Supplier	Reference	Dilution
Glial fibrillary acidic protein (GFAP)	rabbit	Millipore	AB5804	1:1000
Glutamine synthetase	rabbit	Thermo Scientific	PA1-46165	1:1000
Secondary Antibodies	**Host**	**Supplier**	**Reference**	**Dilution**
Alexa Fluor 488 conjugate anti-rabbit	donkey	Invitrogen	A-21206	1:10000
Alexa Fluor 594 conjugate anti-rabbit	donkey	Invitrogen	A-21207	1:10000

3.6.1.1. Image acquisition and quantification of immunolabelled brain slices

For the evaluation of the number of GFAP postitive ($GFAP^+$) cells and the immunoreactivity of glutamine synthetase, the image acquisition was made using a Zeiss Axiovert 200 microscope equipped with a 63x oil objective, an AxioCam HRm camera and using Axiovision software 4.6. Each brain slice (four per experiment) was analyzed in both hemispheres and in different regions of the hippocampus: CA1 oriens, CA1 radiatum, CA3 and dentate gyrus. For each region, an area was defined to count the number of astrocytes (represented by $GFAP^+$ cells) or to measure the immunoreactivity of glutamine synthetase.

For the assessment of astrocytic morphology, images of each brain slice (four per experiment) were obtained using a Zeiss 710 Confocal Microscope, equipped with a 63x oil objective (Plan Apo 63X/1.4 oil DICII) and using Zen software. The selection criteria used to choose the astrocytes drew were: i) GFAP-stained structure encloses a single DAPI-stained nucleus; ii) the main structure cannot have truncated ramifications; iii) reconstruct the first five astrocytes per animal that fulfill the criteria mentioned above. The images were analyzed in order to draw the 5 astrocytes per animal that were referred previously in both hemispheres and in CA1 region of the hippocampus, and the data obtained were quantified using Image J software and Simple Neurite Tracer was used to draw the astrocytes (Tavares et al., 2016). The number of ramifications and the

total length of the ramifications in each astrocyte was evaluated. Sholl analysis was also performed to assess the number of intersections existing in each radius (Tavares et al., 2016).

3.6.2. Preparation of total extracts and synaptosomes of hippocampus

Animals were sacrificed, under profound anesthesia (in halothane atmosphere), and the brain was dissected out on ice, and the hippocampi were immediately isolated. The tissue was stored with RIPA buffer (50 mM Tris, 150 mM NaCl, 1% IGEPAL (NP-40), 0.5% Sodium Deoxycholate, 1 mM EDTA and 0.1% SDS) with protease inhibitors (PMSF (1 mM in ethanol and 0.001% of CLAP (containing 1 µg/ml of leupeptin, pepstatin A, chymostatin, and antipain) and DTT (1mM; to prevent protein oxidation), until further use.

For total extracts preparation, 100 µl of RIPA buffer with protease inhibitors were added to the tissue, that was placed in a potter for homogenization (700 – 900 rpm). The homogenate was sonicated until a homogeneous suspension was obtained. The suspension was further centrifuged for 20 minutes at 16000 x *g* at 4ºC, and the obtained supernatant was collected (Rodrigues et al., 2014).

To prepare synaptosomes, the hippocampus was placed in centrifuge tube with 5 ml of sucrose solution (0.32 M sucrose, 1 mM EDTA-Na and 10 mM HEPES and 1 mg/ml BSA) and homogenized. Then, the mixture was centrifuged at 3000 x *g* for 10 minutes at 4ºC, discarding the obtained pellet that contains mainly nuclei and unbroken cells. The obtained supernatant was further centrifuged at 14000 x *g* for 12 minutes at 4ºC, and the pellet was collected resuspended in 1 ml Percoll 45% (45% v/v Percoll in Krebs Hepes Ringer (KHR) solution, composed by 140 mM NaCl, 1 mM EDTA-Na, 10 mM HEPES, 5 mM KCl and 5 mM glucose, pH 7.4). The pellets were centrifuged for 2 minutes at 16,000 x *g* at 4ºC and the top layer was collected and resuspended in 1 ml of KHR solution. Afterwards, this top layer, containing the synaptosomes, was centrifuged again at 14,000x *g* for 2 minutes and the obtained pellet was resuspended in the appropriate volume of RIPA buffer with protease inhibitors. All solutions used had a of pH 7.4 at 4ºC (Rodrigues et al., 2014).

3.6.2.1. BCA Method for protein quantification

The bicinchoninic acid (BCA) assay is a method for colorimetric detection and quantification of total protein (Fig. 17). Bovine serum albumin (BSA) was used as protein standard, being done a standard curve of 2, 1, 0.5, 0.25, 0.125, 0.0625 and 0 µg/µL of BSA. After incubation of the samples with the mixed reagents (reagent A and reagent B) from the BCA protein assay kit (Pierce ® BCA Protein Assay, Thermo Scientific), for 30 minutes at 37°C, absorbance was read at 570 nm in a spectrophotometer. The resulting standard curve was then used to determine the protein concentration of each sample in µg/µL. The samples were normalized to place the same amount of protein in the gel.

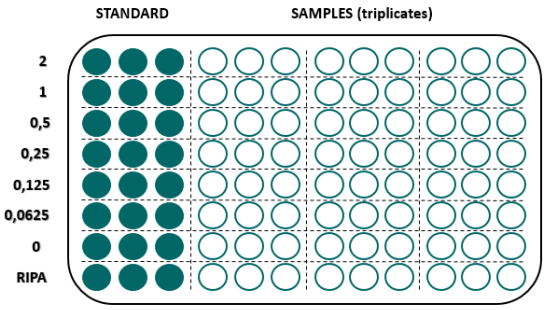

Figure 17 - **BCA method for protein quantification.**

3.6.2.2. Western blot

After protein quantification, the samples were prepared for Western blotting by adding sample buffer 6x (30% glycerol, 10.3% SDS, 500 mM Tris, 0.6M DTT, 0.012% bromophenol blue), followed by heating the samples at 70°C for 20 minutes. Samples were stored at -20°C until they were used.

Gel electrophoresis was carried out in a 10% polyacrylamide resolving gel with a 4% polyacrylamide stacking gel (see Table 4). The proteins were transferred to nitrocellulose membranes, with a constant current of 1A, for 2 hours at, approximately, 4°C. Samples moved through stacking and resolving gel sequentially in the presence of running buffer (see Table 5). The samples were in their respective wells and run at 80V for 15 minutes and then changed to 120V for 45 minutes to 1 hour, using an electrophoresis system and power sources (both from Biorad).

Table 4 - Gel electrophoresis preparation.

Formulation (1 gel)	Resolving Gel (10%)	Stacking Gel (4%)
Acrylamide 30%	3.3 mL	1.3 mL
Tris-buffer 1.5 M (pH 8.8)	2.5 mL	-
Tris-buffer 0.5 M (pH 6.8)	-	2.5 mL
Water	4.1 mL	6.1 mL
SDS 10 %	100 µL	100 µL
TEMED	5 µL	10 µL
APS 20 % (freshly prepared, water diluted)	100 µL	100 µL

After electrophoresis, proteins were transferred to nitrocellulose membranes with transfer buffer (Table 5), with a constant electric current of 1A, for 2 hours at, approximately, 4°C. Membranes were then incubated with Ponceau S to stain the protein, and then washed in distilled water. Prior to the incubation with the primary antibody, membranes were blocked in a solution containing 5% low-fat milk in TBS-T, for 1 hour at RT with agitation.

Table 5 - Solutions used for Western blotting assays.

Running Buffer	Transfer buffer	CAPS	Blocking solution	Washing solution (TBS-Tween)	Tris-buffered saline (TBS)
3 g/l Trizma	250 ml CAPS	22.1 g CAPS	5g low-fat milk	100 ml TBS	20 mM Tris-HCl
31.33 g Bicine	250 ml Methanol (10% v/v)	1l H_2O	100 ml TBS-T	900 ml H_2O	137 mM NaCl
1g/l SDS	1.5 l H_2O	pH 11		1 ml Tween-20	H_2O
H_2O					pH 7.6
pH 8.3					

Primary antibody (see dilution in Table 6) was diluted in a solution of 1% milk in TBS-T and the membranes immersed in it, overnight, at 4°C. After being washed with TBS-T, membranes were incubated with the appropriate secondary antibody (Table 6) diluted in 1% milk in TBS-T, for 2 hours at RT. The immunolabelled bands in the membranes were revealed with an ECL (enhanced chemiluminescent substrate for detection of horseradish peroxidase) Western Blotting substrate kit and then visualized in a ChemiDoc system (Bio Rad).

Table 6 - Antibodies used for Western blotting assays.

Primary antibodies	Host	Supplier	Reference	Dilution	Protein Band Size (kDa)
β-actin	mouse	Sigma-Aldrich	A5316	1:20000	42
Connexin 43	rabbit	Sigma-Aldrich	C6219	1:10000	43
GFAP	rabbit	Millipore	AB5804	1:20000	50
Glutamine synthetase	rabbit	Thermo Scientific	PA1-46165	1:5000	42
Postsynaptic density protein 95 (PSD-95)	mouse	Sigma-Aldrich	P-246	1:10000	95
Synaptosomal-associated protein 25 (SNAP-25)	mouse	Sigma-Aldrich	S5187	1:10000	25
Synaptophysin	mouse	Sigma-Aldrich	S 5768	1:20000	38
S100 calcium-binding protein β (S100β)	mouse	Abcam	ab66028	1:300	11
Secondary antibodies	**Host**	**Supplier**	**Reference**	**Dilution**	**Protein Band Size (kDa)**
Anti-mouse IgG peroxidase conjugated	goat	Thermo Scientific	31432	1:5000	-
Anti-rabbit IgG peroxidase conjugated	goat	Thermo Scientific	31462	1:5000	-

To probe for other proteins in the same nitrocellulose membranes such as β-actin for protein normalization, the membranes were reprobed. Briefly, membranes were washed with a stripping solution (15 g/L glicine, 1 g/L SDS and 10 ml/L Tween 20) and then blocked in a 5% milk in TBS-T solution, followed by an overnight incubation with the primary antibody. The remaining steps, from incubation with the secondary antibody and to determine the immunoreactivity of bands in the membrane, are performed as described above.

3.7. Statistical Analysis

Data are expressed as mean ± SEM of the indicated number of independent experiments. A Two-way ANOVA followed by Holm-Sidak's post-hoc test for multiple comparisons were used in to compare the response of the two group of mice in all habituations. To compare the mean value of a single group with a hypothetical value of 100, a one-sample *t* test was performed. A Student's *t* test was used to test the significance of the difference between two independent groups. In the tridimensional analysis, multiple *t* tests were used to evaluate the number of ramifications intersections along the radius from the center of the cell body. Statistical differences were considered significant at $p < 0.05$ and all tests were performed using the GraphPad Prism Software® (StatSoft Inc., La Jolla, CA, USA).

Chapter 4 | Results

4.1. Behaviour analysis

4.1.1. Open field test

To evaluate locomotor activity and anxiety-related behaviour, which might affect the performance of mice in memory tasks, three open field habituations were performed to assess possible locomotor changes between saline and L-AA-treated animals. The total distance mice travelled in the open field arena was measured, along with the time they spent in the center and periphery of the arena to evaluate anxious-like behaviour in mice. Results showed that saline animals travelled significant ($p < 0.05$) less distance along the habituations performed in three consecutive days, which did not happen with L-AA-treated animals since they travelled the same distance in every habituation (Figure 18 A and 18 B). No significant differences were observed in the time mice spent in the center of the arena between the two groups of animals (Figure 18 C).

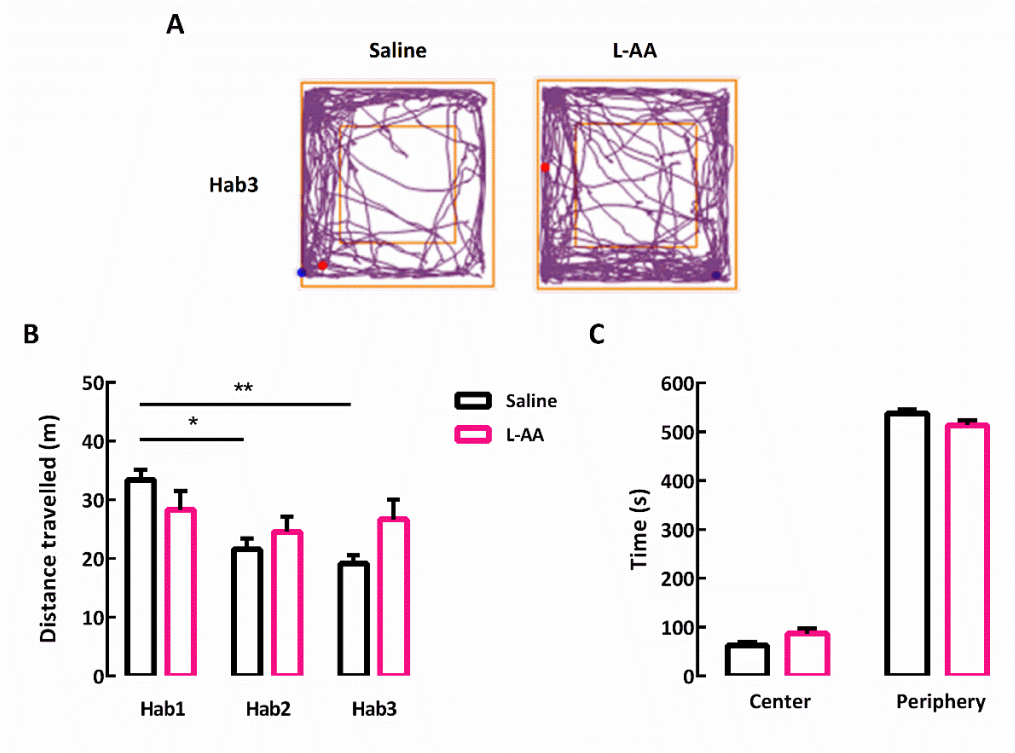

Figure 18 – L-AA-treated mice did not accustom to the open field arena when compared with saline animals. (A) Distance travelled in the third habituation of the open field test by saline and L-AA-treated animals. **(B)** Total distance travelled by saline and L-AA-treated mice (L-AA) in the open field test. **(C)** Time mice spent in the center and periphery of the arena in the open field test. Data are presented as mean ± SEM of n = 11-13 animals per group, ** $p < 0.01$, * $p < 0.05$, using a Two-way ANOVA, followed by Holm-Sidak's post-hoc test for multiple comparisons.

These data indicate that the L-AA-treated mice had neither motor complications nor an anxious behaviour. However, the L-AA-treated mice appear to not accustom to open field, since as compared with saline there were no decrease in travelled distance during the habituation of days 2 and 3 (Hab 2 and Hab 3); the “normal” behaviour is a decrease in the distance travelled over the days of habituation (Cummins and Walsh, 1976), which might indicate an impulsive behaviour in L-AA-treated mice.

4.1.2. Elevated plus maze test

The elevated plus maze (EPM) test was also performed to assess putative alterations in anxious state of the animals, since L-AA-treated mice did not familiarize with the open field arena (see Figure 18 B). This test can measure anxiety and impulsivity levels of mice, by measuring the percentage of time mice spent in the open arms. Additionally, the percentage of distance and entries in the open arms as well as the latency to first entry in the open arms, the number of head dippings (each time that mice evaluates the risk inside the open arms) and stretch-attend posture (each time that mice evaluates the risk in the center of the elevated plus maze) were also quantified (Walf and Frye, 2007).

No significant differences were observed in the percentage of time and entries in the open arms (Figure 19 B and 19 C) as well as in the number of head dippings and stretch-attend posture between the two groups of animals (Figure 19 F and 19 G). Despite the lack of differences in these parameters, it was possible to observe a tendency for L-AA-treated mice to enter and spend more time in the open arms ($p = 0.2694$) as well as for evaluating the risk in the open arms ($p = 0.2132$) when compared with saline mice (Figure 19 B and 19 F). In contrast, saline animals had a tendency to evaluate more the risk but in the center of the elevated plus maze when compared with L-AA-treated animals ($p = 0.1093$) (Figure 19 G). However, there was a significant increase in the percentage ($p < 0.05$, $13.16 \pm 5.27\%$) of distance in the open arms (Figure 19 D) and a decrease in the latency to first entry in open arms ($p < 0.05$, $-15.31 \pm 5.37\%$) in L-AA-treated mice when compared with saline mice (Figure 19 E).

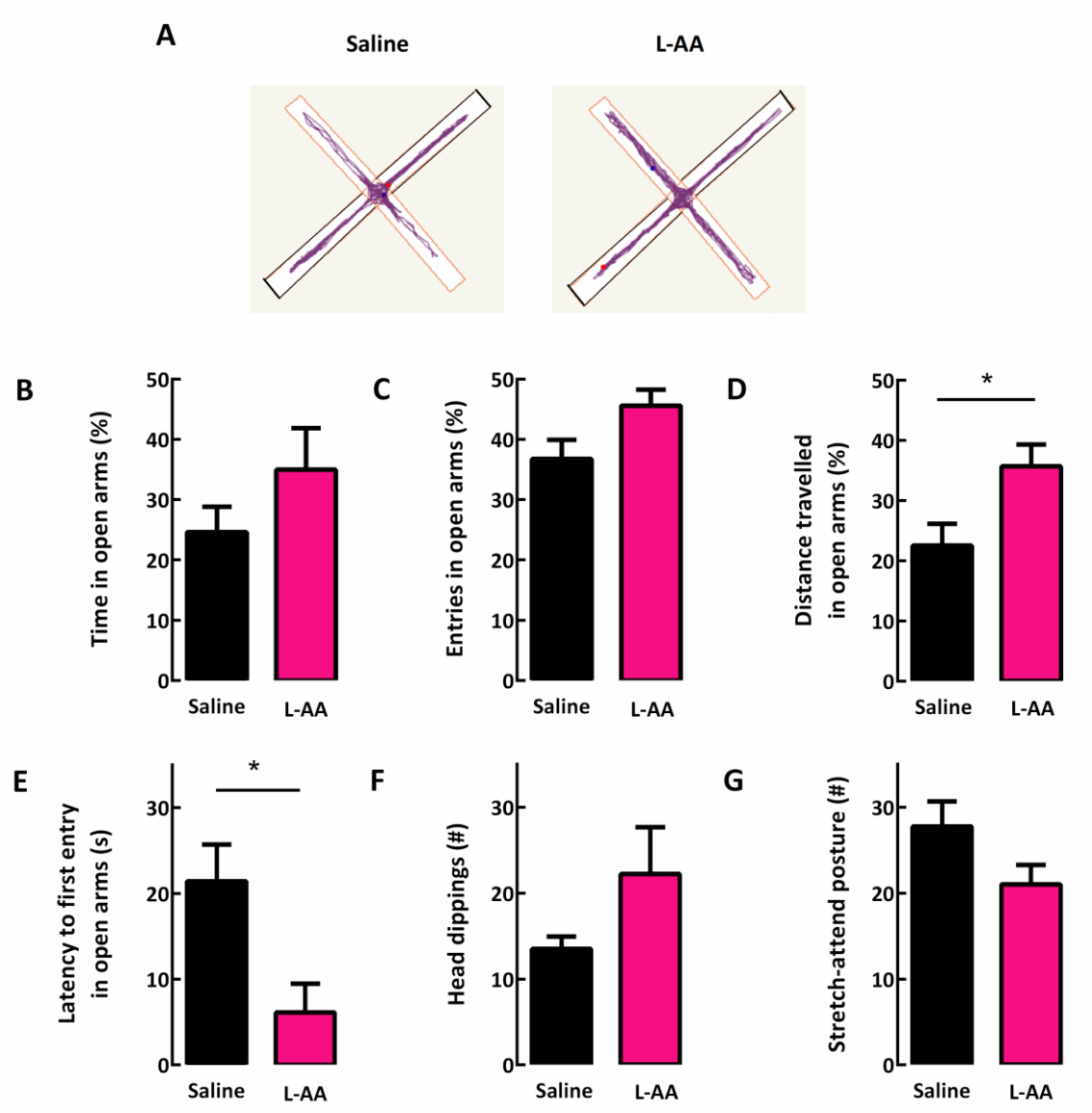

Figure 19 - L-AA-treated mice travelled more in the open arms and took less time to enter in the open arms, suggesting a great impulsivity. (A) Representative distance travelled by saline and L-AA-treated mice. **(B)** Percentage of time spent in the open arms of the elevated plus maze. **(C)** Percentage of entries in the open arms of the elevated plus maze. **(D)** Percentage of distance travelled in the open arms. **(E)** Latency to first entry in the open arms of elevated plus maze. **(F)** Number of head dippings. **(G)** Number of stretch-attend posture. Data are presented as mean ± SEM of n = 4-5 animals per group, * $p < 0.05$, using an unpaired Student's *t* test.

4.1.3. Novel object recognition test

To evaluate L-AA's effect on memory performance, a novel object recognition test was performed. In the sample trial, the time that mice spent in each object was measured to perceive if they displayed a preference for one object in particular, although they were the same. Then, in the test trial, the percentage of time and

interactions mice spent exploring the novel object, as well as the distance mice travelled in the open field arena during the test were quantified.

In the sample trial, no significant differences were observed in the exploration of both objects between saline- and L-AA-treated mice (Figure 20 A). Regarding the test trial, no significant differences were also observed in the Recognition index as well as in the percentage of interactions with the novel object nor in the distance between the two groups of animals (Figure 20 B, 20 C and 20 D).

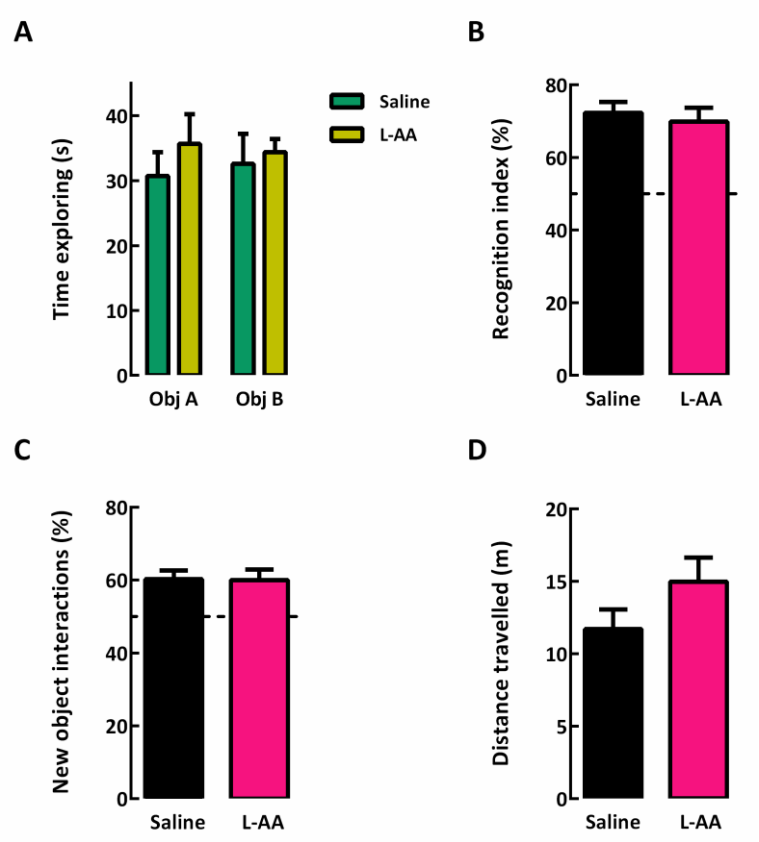

Figure 20 - No significant differences were observed between saline and L-AA-treated mice in NOR test , assessing hippocampus and cortex-dependent memory. (A) Time mice spent exploring both objects in the sample trial. **(B)** Percentage of time mice spent exploring the novel object in the novel object recognition test. **(C)** Percentage of interactions mice had with the novel object in the novel object recognition test. **(D)** Distance travelled in the open field arena during the novel object recognition test. Data are presented as mean ± SEM of n = 12 animals per group, $p > 0.05$, using an unpaired Student's *t* test.

4.1.4. Object Displacement test

To assess hippocampal-dependent memory performance, an object displacement test was performed. In the sample trial, the time mice spent in each object

was measured to see if they displayed a preference. Then, in the test, percentage of time and interactions mice spent exploring the displaced, as well as the distance mice travelled in the open field arena during the test were quantified.

Results showed no significant differences were observed in the exploration of both objects between the two groups of animals (LAA-treated and saline-treated) in the sample trial, as well in the percentage of interactions mice had with the displaced object and distance travelled during the test (Figure 21 A, 21 C and 21 D). However, L-AA-treated animals displayed a significant decrease of ($p < 0.05$; -15.31 ± 7.11%) in the percentage of time mice spent exploring the displaced object. These data indicate that LAA-treated mice had memory impairments (Figure 21 B).

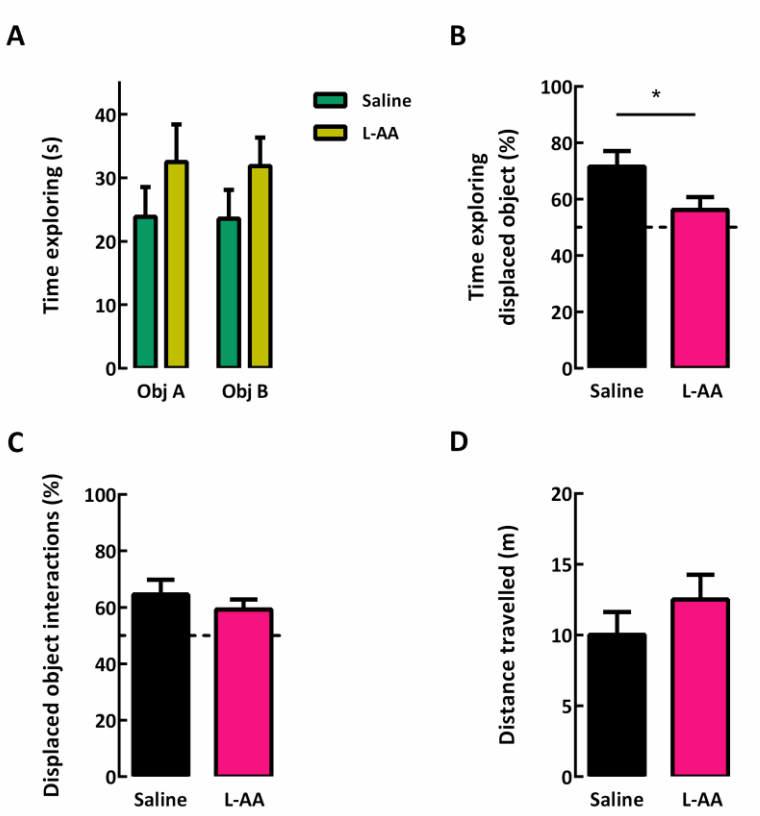

Figure 21 – L-AA-treated animals spent less time exploring the displaced object, indicated that these mice had memory deficits (A) Time mice spent exploring both objects in the sample trial. **(B)** Percentage of time mice spent exploring the displaced object in the object displacement test. **(C)** Percentage of interactions mice had with the displaced object in the object displacement test. **(D)** Distance travelled in the open field arena during the object displacement test. Data are presented as mean ± SEM of n = 9-10, * $p < 0.05$, using an unpaired Student's *t* test.

4.1.5. Modified y-maze test

To evaluate hippocampal-dependent working memory for spatial location, a modified Y-maze test was performed (Conrad et al., 1996; Dellu et al., 1997). The percentage of time mice spent in the novel arm, as well as the percentage of entries and distance travelled in the same arm were measured.

Results showed that L-AA-treated mice spent significant ($p < 0.05$, -17.29 ± 6.65%) less time in the novel arm when compared with saline mice (Figure 22 A). No significant differences were observed in the percentage of entries and distance travelled in the novel arm between the groups of animals (Figure 22 B and 22 C).

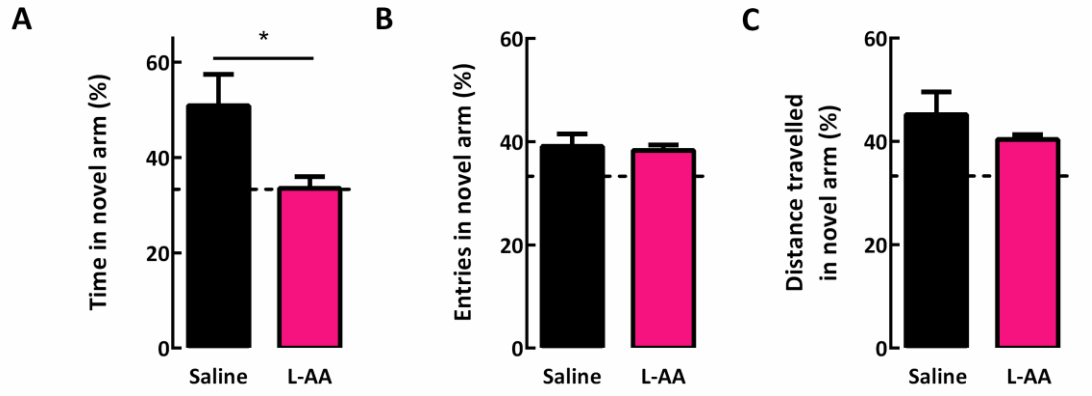

Figure 22 - L-AA-treated mice spent less time in the novel arm. (A) Percentage of time spent in the novel arm of modified y-maze test. **(B)** Percentage of entries in the novel arm of the modified y-maze test. **(C)** Percentage of distance travelled in the novel arm. Data are presented as mean ± SEM of n = 12-14, * $p < 0.05$, using an unpaired Student's *t* test.

4.1.6. Step-down inhibitory avoidance

To evaluate learning and memory processes in these animals, a step-down inhibitory avoidance test was performed. In both sample trial and test, the latency to step down the platform was measured.

No significant differences were observed in both phases of the step-down inhibitory avoidance test (Figure 23 A), but it was possible to observe a tendency in L-AA-treated mice to take less time ($p = 0.0618$) to step down the platform when compared with saline mice (Figure 23 B). These data indicate a great impulsivity in L-AA-

treated mice, which are in accordance with the data gathered in EPM and also, in OF tests.

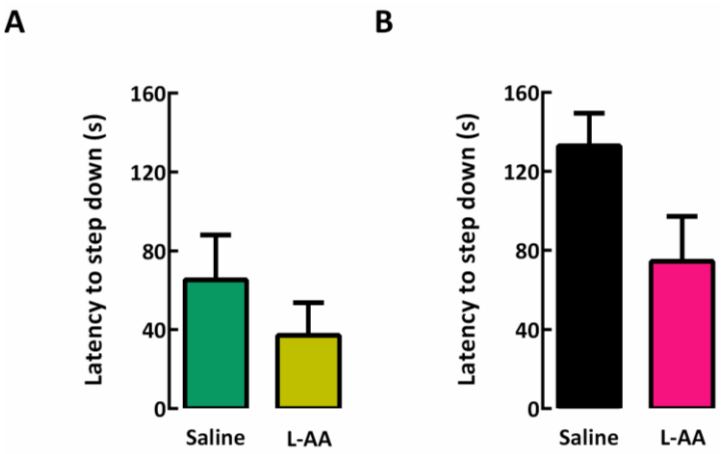

Figure 23 - L-AA-treated mice had a tendency to take less time to step down of the platform when compared with saline mice. (A) Latency to step down of the platform in the sample trial. **(B)** Latency to step down of the platform in the test. Data are presented as mean ± SEM of n = 9-11, $p > 0.05$, using an unpaired Student's *t* test.

4.2. Neurochemical studies

4.2.1. Immunohistochemistry

4.2.1.1. Number of GFAP⁺ cells and immunoreactivity of glutamine synthetase

Since L-AA is a gliotoxin, it was important to assess the impact of its administration on astrocytes number and morphology and also in the levels of GFAP and glutamine synthetase (GS) in the hippocampus. GFAP is an astrocytic protein usually used to label astrocytes and its reactivity, whereas GS is a protein present in astrocytes involved in the glutamate-glutamine cycle. Thus, immunohistochemistry analyses were performed to assess the percentage of $GFAP^+$ cells and the levels of GS immunoreactivity of in L-AA-treated mice when compared with saline animals. For both evaluations, four regions of the hippocampus (CA1 oriens, CA1 stratum radiatum, CA3 and dentate gyrus) were analyzed.

Results showed that there was a significant ($p < 0.05$) decrease in the number of $GFAP^+$ cells in CA1 oriens (-10.97 ± 3.32, n = 5), CA1 stratum radiatum (-5.04 ± 0.89, n = 5) and CA3 (-9.72 ± 2.70, n = 5) regions of the hippocampus in L-AA-treated mice when

compared with saline mice, which did not happen in dentate gyrus (9.31 ± 3.80, n = 5) (Figure 24 A and 24 B). In contrast, no significant differences were observed in the immunoreactivity of glutamine synthetase in any of the regions of the hippocampus (CA1 oriens: -4.67 ± 3.61, n = 5; CA1 stratum radiatum: -4.34 ± 4.22, n = 5; CA3: -5.37 ± 5.05, n = 5; dentate gyrus: -9.12 ± 7.03, n = 5) between the two groups of animals (Figure 24 A and 24 C).

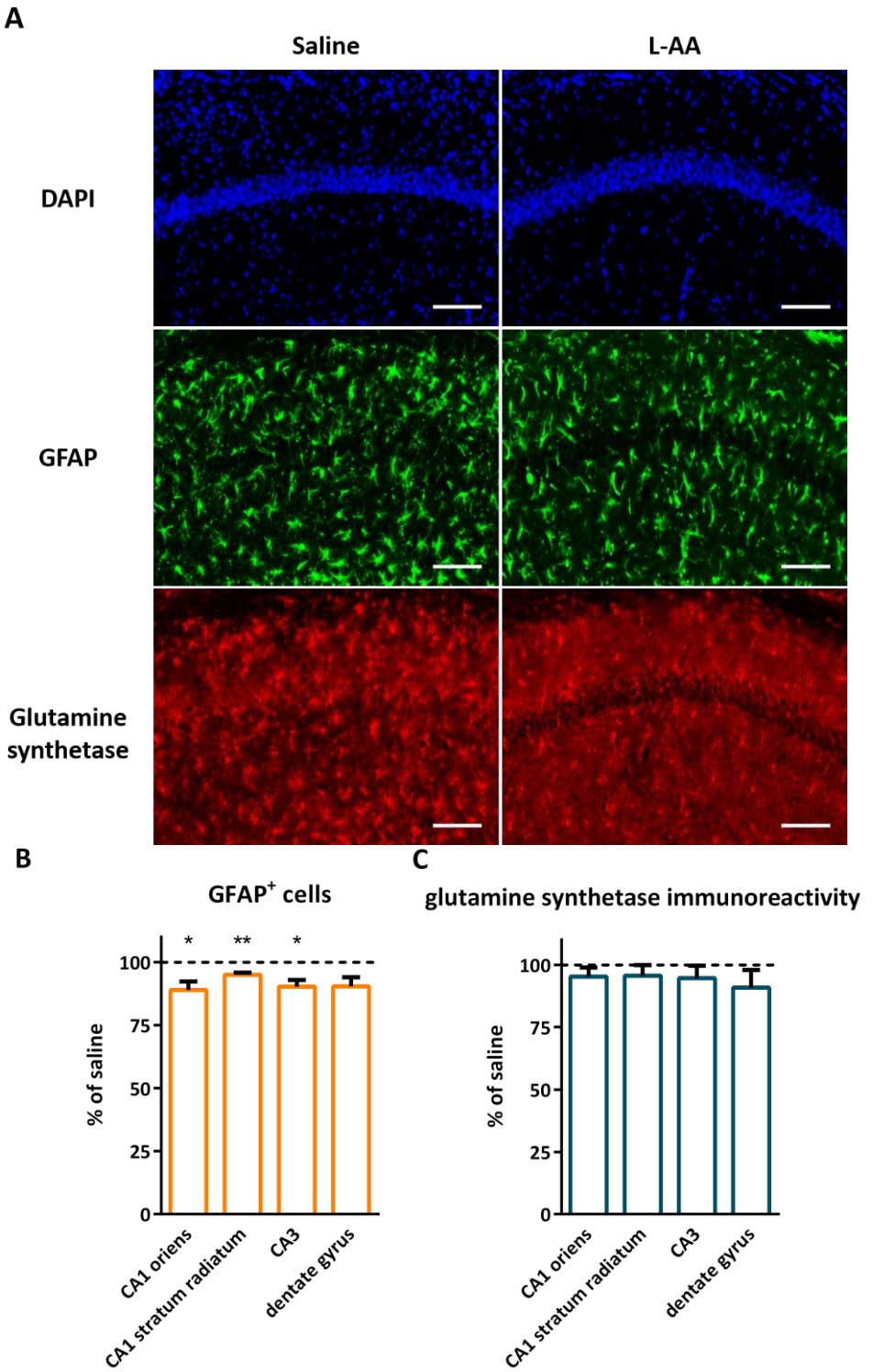

Figure 24 - Effect of L-AA administration in GFAP⁺ cells and in glutamine synthetase immunoreactivity. (A) Representative images of immunohistochemical labelling of brain slices with DAPI (nuclei marker, first line, blue), GFAP (second line, green) and glutamine synthetase (third line, red). **(B)** Percentage of GFAP⁺ cells in the four regions of the hippocampus of L-AA-treated animals when compared with saline animals. **(C)** Percentage of glutamine synthetase immunoreactivity in the four regions of the hippocampus of L-AA-treated animals when compared with saline animals. Results are presented as percentage of saline. The images were taken in a fluorescence microscope with a magnification of 40x. Scale bar - 100 µm. Data are expressed as mean ± SEM of n = 4-5, ** $p < 0.01$, * $p < 0.05$ using a one sample *t*-test compared with the hypothetical value of 100.

4.2.1.2. Astrocytic morphology

To evaluate possible modifications in astrocytic morphology, upon L-AA administration, an immunohistochemistry was performed (Fig. 25). In this case, we wanted to evaluate the number and total length of ramifications as well as the number of intersections per radius and the maximum radius of the ramifications in the CA1 region of the hippocampus. The maximus radius represents the value more distant from the center of the cell body that each astrocyte reaches. For that, we first identified the center of the cell body and then we drew every ramification that came from within (as described in material and methods, section 3.6.1.1.).

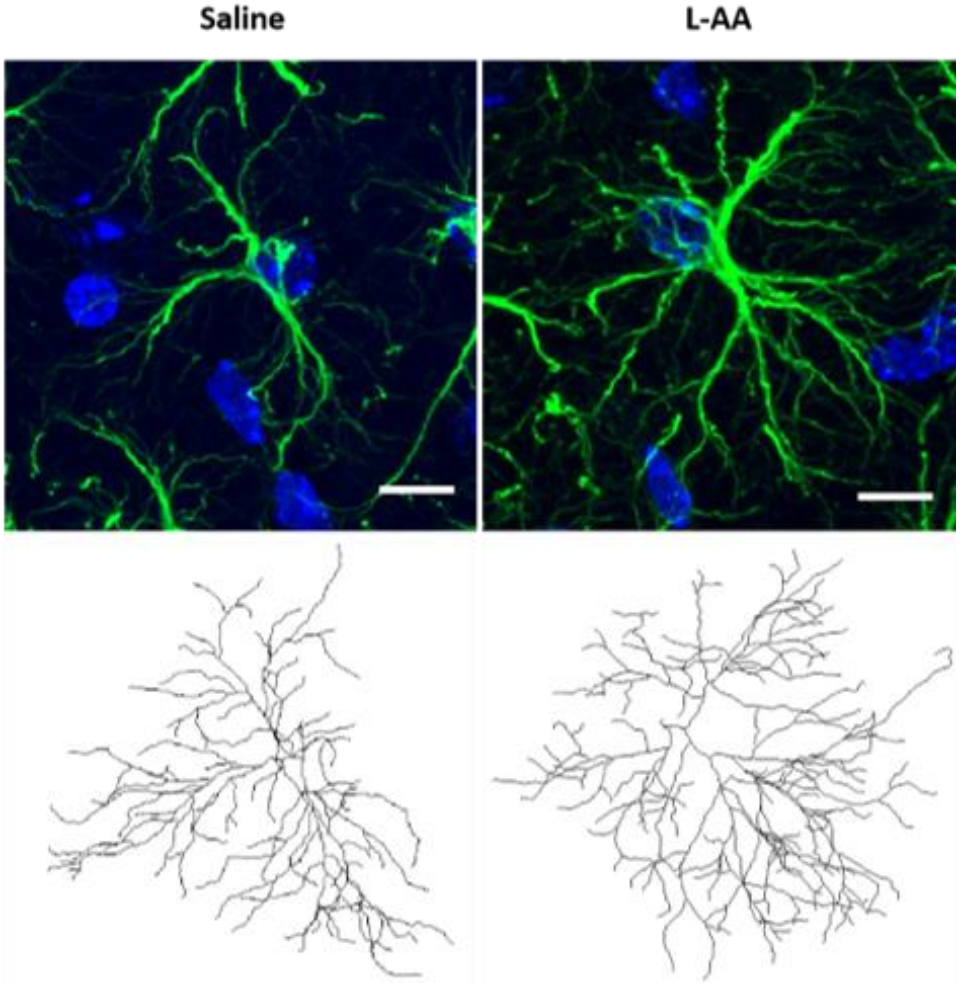

Figure 25 - Hippocampal astrocytes morphology is altered under L-AA infusion. (A) Representative images of immunohistochemical labelling of brain slices with DAPI (nuclei marker, blue) and GFAP (ramifications, green). The images were taken in a confocal microscope with a magnification of 63x and a tridimensional analysis was performed. Scale bar - 10 µm.

Results showed that L-AA-treated animals had more (saline = 99.31 ± 5.67; L-AA = 118.60 ± 4.69) and longer (saline = 1312 ± 66; L-AA = 1502 ± 39) ramifications that

saline animals (Figure 25, 26 A and 26B). No differences were observed in the maximum radius of astrocytes ramifications (saline = 41,43 ± 1,08; L-AA = 41,54 ± 1,67) between the two groups (Figure 26 C). Regarding the number of intersections of ramifications per radius, L-AA-treated mice had more intersections at 4 µm and 16 µm of distance from the center of the cell body, as shown by the sholl analysis, when compared with saline mice (Figure 26 D).

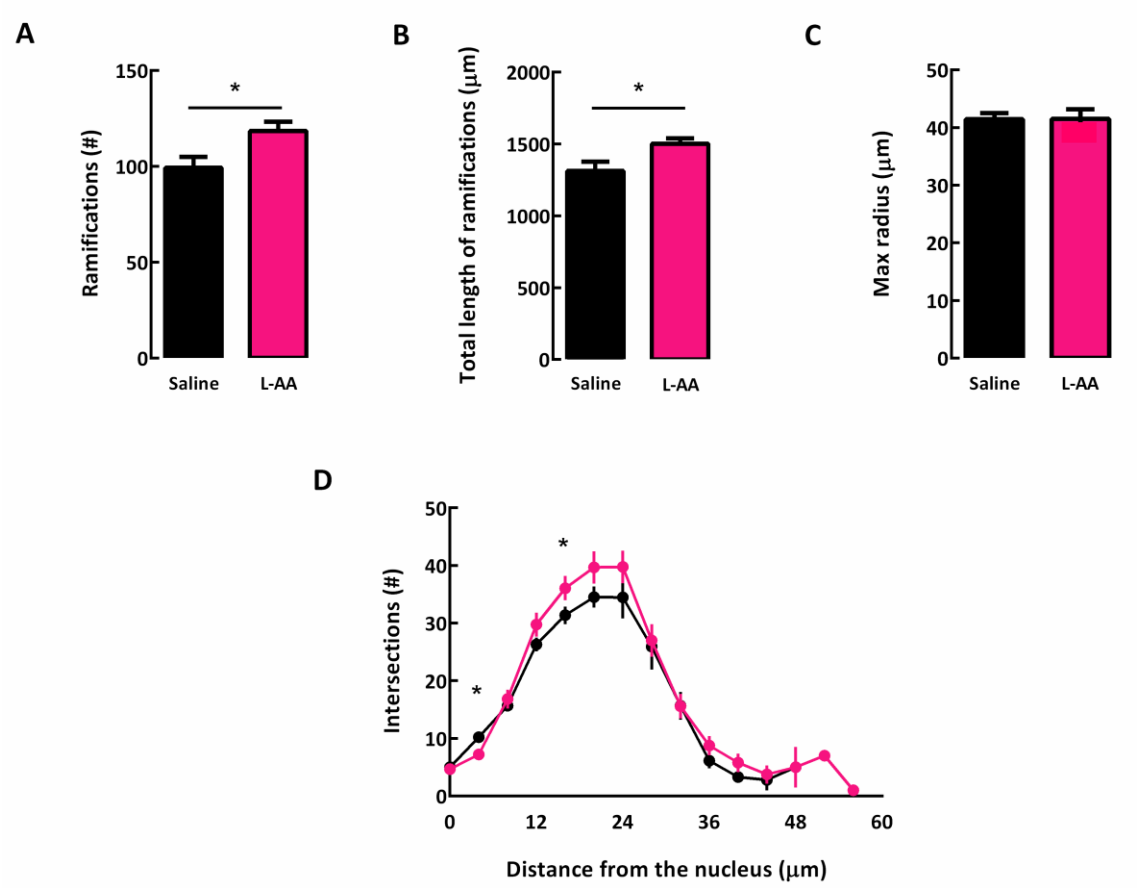

Figure 26 - L-AA administration affected hippocampal astrocytes morphology. L-AA-treated mice had more and longer ramifications than saline animals. **(A)** Number of ramifications in astrocytes of both groups of animals. **(B)** Total length of ramifications of astrocytes of both groups. **(C)** Maximum radius of the ramifications of astrocytes. **(D)** Number of intersections of ramifications per radius, assessed by Sholl analysis. The images were taken in a confocal microscope with a magnification of 63x. Scale bar - 10 µm. Data are expressed as mean ± SEM of n = 13, * $p < 0.05$ using an unpaired Student's *t* test for comparisons between two groups and multiple *t* tests for comparisons between each group of animals and each radius.

4.2.2. Quantification of protein levels by Western blot

4.2.2.1. Astrocytic markers

To evaluate if astrocytic pathology model impacted on its protein levels in hippocampus, a Western blot analysis was performed. Relative densities of proteins expressed by astrocytes, such as GFAP, S100β, GS and connexin 43, were quantified.

No significant differences were found in S100β (3.70 ± 24.01%, n = 5) and in glutamine synthetase (5.10 ± 5.23 %, n = 6) immunoreactivity between L-AA-treated mice and saline mice (Figure 26). In contrast, both GFAP (-26.97 ± 8.58, n = 6) and connexin 43 (-16.36 ± 6.36, n = 6) were significantly ($p < 0.05$) downregulated in L-AA-treated mice when compared with saline mice (Figure 27).

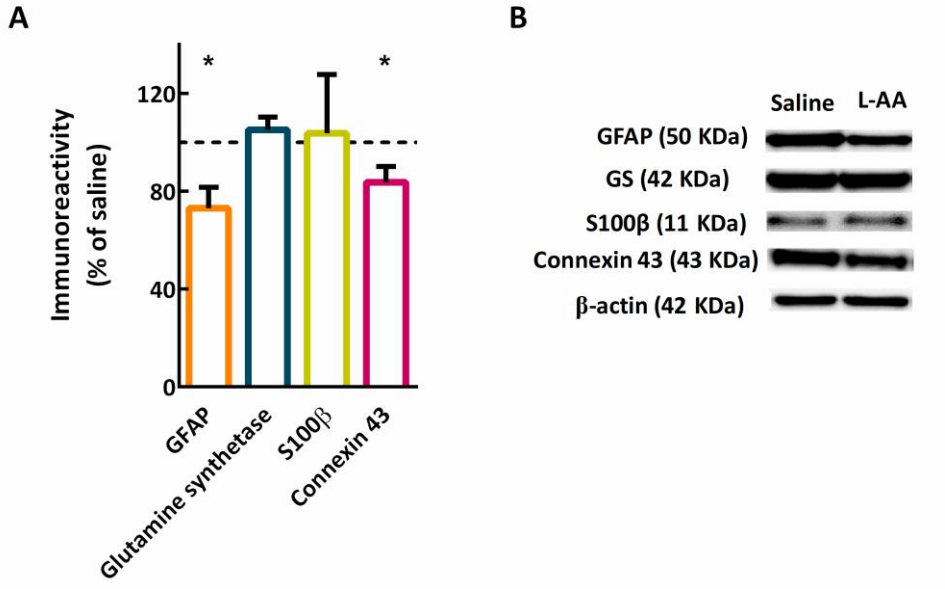

Figure 27 - GFAP and connexin 43 are downregulated in the hippocampus in L-AA-treated mice. (A) Density of GFAP, glutamine synthetase, S100β and connexin 43 in L-AA-treated mice in the hippocampus. **(B)** Representative Western blot of GFAP, glutamine synthetase, S100β, connexin 43 and β-actin levels in total extracts membranes of saline animals and L-AA-treated animals (L-AA). β-actin was used as control for protein loading. Results are presented in percentage of saline total extracts. Data are expressed as mean ± SEM of n = 5-6 per group, * $p < 0.05$ using a one sample *t*-test compared with the hypothetical value of 100.

4.2.2.2. Synaptic markers

To gain further insight to whether the astrocytic pathology model impacted at the synaptic level in the hippocampus, a Western blot analysis was performed. Relative densities of presynaptic proteins, synaptophysin and SNAP-25, were quantified. The first

protein is present in synaptic vesicles, and the second is a component of the SNARE protein complex, which is involved in vesicle fusion to cell membrane, respectively (Masliah and Terry, 1993). Additionally, we addressed whether this model affected the density of PSD-95, a general postsynaptic marker of excitatory neurons (Cho et al., 1992). No significant differences were found in the immunoreactivity of any of the synaptic proteins, SNAP-25 (14.50 ± 12.22%, n = 5), synaptophysin (10.00 ± 17.40%, n = 5) and PSD-95 (13.20 ± 11.60%, n = 5) between L-AA-treated animals compared to saline animals (Figure 28).

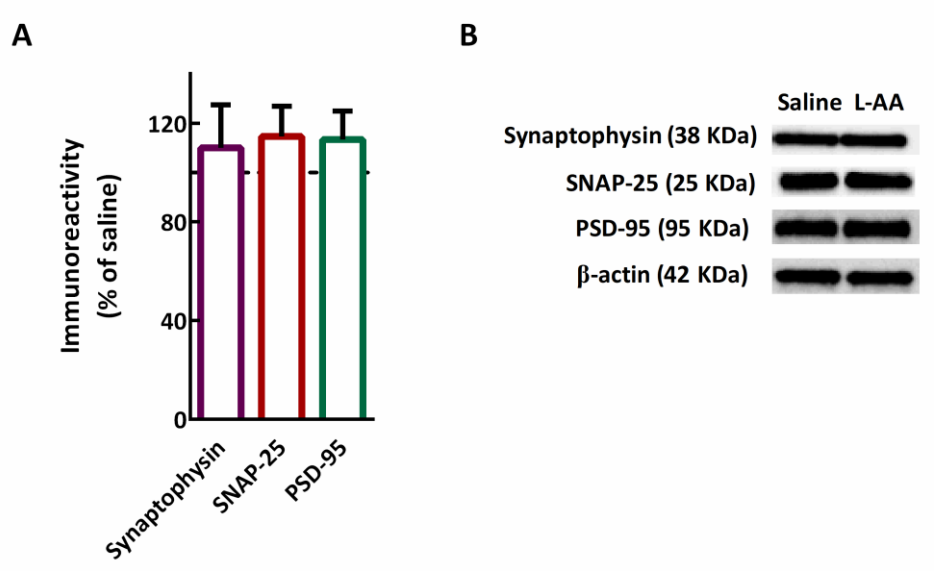

Figure 28 - No significant differences were observed in synaptic proteins in L-AA-treated animals (A) Density of synaptophysin, SNAP-25, and PSD-95 in L-AA-treated mice in the hippocampus. **(B)** Representative Western blot of Synaptophysin, SNAP-25, PSD-95 and β-actin levels in synaptosomal membranes of saline animals and L-AA-treated animals (L-AA). β-actin was used as control for protein loading. Results are presented as percentage of saline total extracts. Data are expressed as mean ± SEM of n = 5 per group, $p > 0.05$, using a one sample *t*-test compared with the hypothetical value of 100.

Chapter 5 | Discussion

Nowadays, it is accepted that astrocytes make part of the synapse, having a crucial role in the regulation of synaptic transmission through the uptake of glutamate and GABA, and also by the release of gliotransmitters, such as ATP and glutamate (Wang and Bordey, 2008; Orellana et al., 2016). Synaptic plasticity, which consists in modifications of synaptic strengths through cellular mechanisms of long-term potentiation (LTP) and long-term depression (LTD), is widely believed to be the neurophysiological basis of memory formation and storage (Martin et al., 2000; Morris et al., 2003). Astrocytes dynamically interact with neuronal synapses via fine processes, being currently known that in response to synaptic plasticity, these glial cells rapidly move towards and enwrap active synapses, supporting the stabilization and the preservation of active synaptic connections (Allen, 2014). It is widely known that synapse dysfunction and loss are early events associated with memory deficits in several brain disorders associated with cognitive deficits, such as in Alzheimer´s disease, which usually occurs before signs of neuropathology of amyloid deposits and neuronal death (Terry et al., 1991; Chung et al., 2015b). However, there are lacking of experimental evidences supporting that the abnormal function of astrocytes could impact on hippocampal synaptic plasticity, and consequenty in memory.

The present study was planned to study the impact of hippocampal astrocytic dysfunction on memory, correlating this alteration with morphological and molecular (astrocytic proteins) alterations of astrocytes. Thus, we used an astrocytic pathology model, consisting in the intracerebroventricular administration of a selective astrocyte toxin, L-α-aminoadipate (L-AA), previously validated by our group (Pereira, 2017) as a trigger of astrocyte dysfunction. This gliotoxin that is taken up by astrocytes through glutamate transporters and inhibits the glutamine synthetase, causing alteration in glutamate homeostasis. There are reports that this gliotoxin trigger and a decrease in astrocytes in prefrontal cortex, which impairs cognition of adult , and also in amygdala of rats (Khurgel et al. 1996; Lima et al. 2014); however, studies about the impact of astrocytes blunting on hippocampus and memory are scarce.

During the establishment of our model of hippocampal astrocytic pathology model, it was necessary to adjust several parameters: i) cannula implementation in the in the middle of the left lateral ventricle (choice of stereotaxic coordinates), since we

wanted the dispersion of the gliotoxin throughout a region close to hippocampus (Feinberg and Mark, 1987) and the method of fixing the cannula to the skull to hinder its removal by animal, ii) surgery recovery period before L-AA or saline infusion; iii) L-AA or saline administration (concentration and infusion rate, as well as the method for restraint mice during the drug infusion, to minimize mice discomfort and stress , iv) lag phase between L-AA or saline infusions and behavioural testing (so this period do not exceed the three days in which L-AA has effect (Khurgel et al., 1996). Nevertheless, after all parameters were defined, the experiments carried out with this model of pharmacological astrocytic ablation provided us several interesting results.

From the behaviour analysis of the mice subjected to the icv infusions of L-AA, we could observe that astrocytic blunting led to impairments in memory and cognition. When the open field habituations were performed, we expected to see a reduction in locomotor activity through all the habituations in both saline and L-AA-treated mice, since we did not want mice to be anxious or stressed (Cummins and Walsh, 1976). Both saline and L-AA-treated mice showed no motor difficulties or anxious behaviour. However, we observed that animals infused with L-AA could not habituate in the same way as saline animals, since they travelled the same distance in the three habituations, which might suggest that L-AA-treated animals could be more impulsive. So, to confirm this putative impulsivity, the elevated plus maze test was performed and results showed that animals infused with L-AA travelled more in the open arms, took less time to enter in those arms and had a tendency to spend more time and evaluating the risk in the open arms when compared with saline animals. These results seems to indicate that the L-AA infused mice in the lateral ventricle had an increased impulsivity that is mainly a behaviour more related with the striatum and substantia nigra and with the dopaminergic system (Cho et al., 2014). Nevertheless, we did not have time to explore putative alterations in these area in our mice model of astrocytic pathology.

Regarding memory performance, we observed that L-AA-treated animals had no memory deficits in Novel Object Recognition (NOR) test, however, this group of animals have a significant reduction in the performance of carried out Object Displacement (OD) test. These two tests, despite appearing very similar, they have some differences: i) in the objects during test trial: the NOR test has two dissimilar objects, whereas OD has

two similar objects, but one of them was displaced; ii) the brain regions that both tests assess are different: OD is more hippocampal dependent, being necessary for encoding, consolidation and retrieval of memory and it is sensitive to manipulations in CA1 region (Assini et al., 2009; Haettig et al., 2011; Vogel-Ciernia and Wood, 2015), whereas NOR depends on insular cortex, perirhinal cortex and ventromedial prefrontal cortex, besides hippocampus (Winters et al., 2004; Bermudez-Rattoni et al., 2005; Akirav and Maroun, 2006; Balderas et al., 2008). Furthermore, we also observed memory impairments in L-AA-treated animals, since they spent significant less time in the novel arm of Modified Y-Maze test, as compared with saline animals. We also saw that in the step-down Inhibitory avoidance, L-AA-treated animals had a tendency to take less time to step down of the platform when compared with saline animals. Taken together, these data indicate that the hippocampal-dependent memory was particularly affected in mice chronically infused in one lateral ventricle with the gliotoxin, L-AA.

It is well-known that hippocampus has an important role in certain forms of memory (Scoville and Milner, 2016). However, this region of the brain has gain more insight, not only in the formation of memories, but also in information processing and the subsequent regulation of behaviour (Bannerman et al., 2004). Increasing evidences showed that the ventral hippocampus plays an important role in fear and/or anxiety (McHugh et al., 2004). Lesions in this subregion of the hippocampus had demonstrated diminished levels of freezing after the delivery of a mild foot shock, anxiolytic properties in anxiety tests and reduced plasma corticosterone levels following exposure to a stressful situation (Richmond et al., 1999; Kjelstrup et al., 2002; Bannerman et al., 2003; McHugh et al., 2004). Thus, it is possible that when administrating L-AA, mice lose astrocytes in the hippocampus, resulting in short-term memory impairments and in greater impulsivity, defined by lower anxiety.

Concerning the immunohistochemistry assays, we assessed the impact of L-AA administration on astrocytic levels of GFAP and glutamine synthetase (GS) in the four regions of the hippocampus (CA1 oriens, CA1 stratum radiatum, CA3 and dentate gyrus), as well as astrocytes number and morphology. We obtained a significant decrease in GFAP positive cells in CA1 oriens, CA1 stratum radiatum and CA3 regions of the hippocampus in L-AA-treated mice compared with saline mice, whereas the GS

immunoreactivity was not affected in none of the regions studied. These data are in accordance with those obtained by immunoblot assays, where we measured the levels of GFAP and GS in hippocampus lysates (of the hemisphere infused), and it was found that L-AA-treated mice had significant lower GFAP levels, but not of GS, compared with control animals (vehicle injected). Accordingly, it was reported that GS expression does not positively correlate with the expression or levels of GFAP (Rose et al., 2013). Changes in the expression/activity of GS, which regulates astrocytic glutamate–glutamine cycle and consequently glutamate uptake from synaptic cleft by astrocytes, are associated with neurodegenerative diseases and mental disorders (Rose et al., 2013; Pekny and Pekna, 2014); however, our model was not properly a model of a chronic brain disorder. Beside the significant decrease in the levels of GFAP, we also observed a significant reduction in connexin 43 levels in the hippocampus of L-AA mice. The connexin 43 is main component of hemichannels, which can form also gap junctions (joining of two hemichannels of adjacent cells), which are crucial to form an astrocytic syncytium (Giaume and Liu, 2012). Curiously it was reported that downregulation of connexin 43 impair the syncytium formation, and this syncytiopathy is responsible for memory impairment in patients with severe depression (Mitterauer, 2010). Furthermore, our data showing decreased levels of connexin 43 matched with those observed in GFAP reduction (positive cells and density) and in the memory impairment observed in L-AA mice. Regarding the protein S100β, no alterations were observed in its levels when compared L-AA-treated and vehicle-treated mice, although a considerable variation of this protein levels was detected (high SEM, see Fig. 26). S100β is secreted by astrocytes upon brain injury or disease and can have pro-survival or pro-apoptotic effects depending on the concentration reached in the extracellular environment (Villarreal et al., 2011); thus, the quantification of S100β did not allow us to draw significant conclusion about astrocytes blunting or ablation.

For synaptic levels, we observed that L-AA did not affect synaptic proteins, mainly the synaptophysin, SNAP-25 and PSD-95, since no significant differences were observed in the levels of these proteins between saline and L-AA-treated mice. Although, in some studies, it was referred that the L-isomer of α-aminoadipate exerted its toxic effects in glial cells and in neurons, unlike the D-isomer that only affected non-

neuronal cells (Olney et al., 1980); this contradictory data might be due to the high L-AA doses used or to the age of animals that were used. Indeed, there were more studies that proved otherwise (Huck et al., 1984; Takada and Hattori, 1986; Khurgel et al., 1996). Experiments performed in cell cultures shown that this L-isomer (L-AA) did not affect neurons, since the loss of most of the astrocytes present in cultures did not disturb the survival of neurons, (Huck et al., 1984).

Other aim of our work was the assessment of alterations in hippocampal astrocytes morphology triggered by the gliotoxin L-AA, since it is known that morphological alterations in the astrocytes reflects in part changes in astrocytes function (Heller and Rusakov, 2015; Khakh and Sofroniew, 2015). Moreover, our group have data showing that L-AA treatment of hippocampal slice of mice affect the synaptic plasticity, of LTP and LTD type (Pereira et al., 2018, poster). Thus, we used one recent validated tool to assess tridimensional structure of GFAP-labeled astrocytes in CA1 region of hippocampus (visualized by confocal microscopy) in a simple, efficient and semi-automated manner in order to determine alterations in the number and length of astrocytes ramifications (Tavares et al., 2016). The tridimensional analysis of hippocampal astrocytes of L-AA-infused and vehicle-infused control mice revealed that the first group of animals had a significant increase in the number and length of the ramifications, as compared with control group (see Fig. 25). Although in both animal groups the number (5-6) of astrocytic primary branches were similar, L-AA also increased the number of intersections in radius closer to the cell body, suggesting a higher complexity of astrocytes near the cell body. It should be referred that we are aware of GFAP labeling might underestimate the number of and length of astrocytic ramifications, since other studies using fluorescent dye to fill the astrocytes and electron microscopic examination confirmed that GFAP delineates only about 15% of the total volume of the astrocyte (Rusakov et al., 2014). However, the method we used was rigorously validated and is widely used by others, and we did a comparative study between the L-AA-treated and vehicle-treated (control) mice.

Chapter 6 | Conclusions and Future Perspectives

Conclusions:

- The gliotoxin, L-α-aminoadipate impaired hippocampal-dependent memory, and also increased the impulsivity in mice;

- L-AA significantly downregulated the astrocytic protein markers, GFAP and connexin 43, but did not affect the levels of synaptic protein markers, suggesting that it did not affect neurons;

- L-AA increased the number and length of astrocytes ramifications, as well as, the level of ramifications complexity near the cell body.

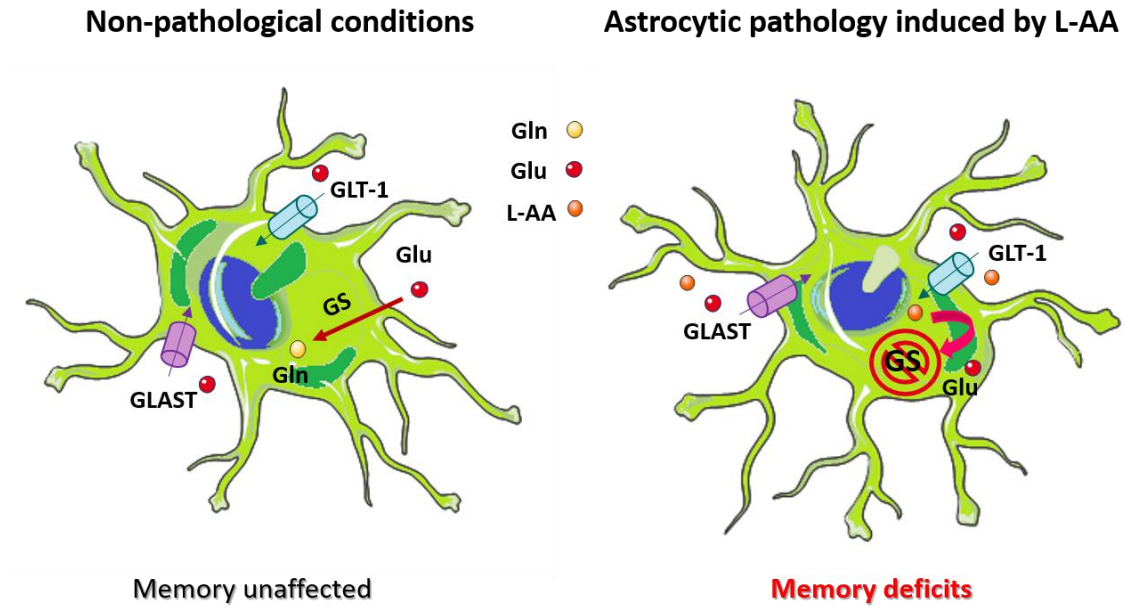

Figure 29 - Astrocytes in non-pathological conditions vs. pathology induced by L-α-aminoadipate. In an astrocytic pathology induced by L-AA, there is the competition between this gliotoxin and glutamate to enter in astrocytes through Na^+-dependent glutamate transporters, GLT-1 and GLAST. L-AA inside the astrocytes inhibits glutamine synthetase (GS) and consequently the conversion of glutamate (Glu) into glutamine. The exposure to L-AA cause an increase in the number and length of hippocampal astrocytic ramifications, which go along with memory deficits.

Future perspectives:

- Assess the impact of astrocytes blunting in a mice model of Alzheimer´s disease;

- Evaluate the role of an astrocytic pathology in other brain regions, particularly in the striatum (due to impulsivity observed in icv L-AA infused mice).

References

Abbott, N.J. (2002). Astrocyte – endothelial interactions and blood –brain barrier permeability. J. Anat *200*, 629– 638.

Abbott, N.J., and Romero, I.A. (1996). Transporting therapeutics across the blood-brain barrier. Mol. Med. Today *2*, 106–113.

Abbott, N.J., Rönnbäck, L., and Hansson, E. (2006). Astrocyte-endothelial interactions at the blood-brain barrier. Nat. Rev. Neurosci. *7*, 41–53.

Abraham, W.C., Bliss, T.V.P., and Goddard, G. V. (1985). Heterosynaptic changes accompany long-term but not short-term potentiation of the perforant path in the anaesthetized rat. J. Physiol. *363*, 335–349.

Aggleton, J.P., and Brown, M.W. (1999). Episodic memory, amnesia, and the hippocampal-anterior thalamic axis. Behav. Brain Sci. *22*, 425–444.

Agostinho, P., Cunha, R. a, and Oliveira, C. (2010). Neuroinflammation , Oxidative Stress and the Pathogenesis of Alzheimer ' s Disease. Curr. Pharmacutical Des. *16*, 2766–2778.

Aitken, P.G., Borgdorff, A.J., Juta, A.J.A., Kiehart, D.P., Somjen, G.G., and Wadman, W.J. (1998). Volume changes induced by osmotic stress in freshly isolated rat hippocampal neurons. Pflugers Arch. J. Physiol. *436*, 991–998.

Akirav, I., and Maroun, M. (2006). Ventromedial prefrontal cortex is obligatory for consolidation and reconsolidation of object recognition memory. Cereb. Cortex *16*, 1759–1765.

Allen, N.J. (2014). Synaptic plasticity: Astrocytes wrap it up. Curr. Biol. *24*, 697–699.

Amiry-Moghaddam, M., and Ottersen, O.P. (2003). The molecular basis of water transport in the brain. Nat. Rev. Neurosci. *4*, 991–1001.

Amiry-Moghaddam, M., Frydenlund, D.S., and Ottersen, O.P. (2004). Anchoring of aquaporin-4 in brain: Molecular mechanisms and implications for the physiology and pathophysiology of water transport. Neuroscience *129*, 999–1010.

Amor, S., Puentes, F., Baker, D., and Van Der Valk, P. (2010). Inflammation in neurodegenerative diseases. Immunology *129*, 154–169.

Amzica, F., and Massimini, M. (2002). Glial and neuronal interactions during slow wave and paroxysmal activities in the neocortex. Cereb. Cortex *12*, 1101–1113.

Anderson, M.F., Blomstrand, F., Blomstrand, C., Eriksson, P.S., and Nilsson, M. (2003). Astrocytes and stroke: Networking for survival? Neurochem. Res. *28*, 293–305.

Andriezen, W.L. (1893). The Neuroglia Elements in the Human Brain. Br. Med. J. *2*, 227–230.

Araque, A., Parpura, V., Sanzgiri, R.P., and Haydon, P.G. (1999). Tripartite synapses : glia, the unacknowledged partner. Trends Neurosci. *22*, 208–215.

Assini, F.L., Duzzioni, M., and Takahashi, R.N. (2009). Object location memory in mice: Pharmacological validation and further evidence of hippocampal CA1 participation. Behav. Brain Res. *204*, 206–211.

Balasingam, V., Tejada-Berges, T., Wright, E., Bouckova, R., and Yong, V.W. (1994). Reactive astrogliosis in the neonatal mouse brain and its modulation by cytokines. J. Neurosci. *14*, 846–856.

Balderas, I., Rodriguez-ortiz, C.J., Salgado-tonda, P., Balderas, I., Rodriguez-ortiz, C.J., Salgado-tonda, P., Chavez-hurtado, J., Mcgaugh, J.L., and Bermudez-rattoni, F. (2008). The consolidation of object and context recognition memory involve different regions of the temporal lobe The consolidation of object and context recognition memory involve different regions of the temporal lobe. Learn. Mem. 618–624.

Banasr, M., and Duman, R.S. (2008). Glial Loss in the Prefrontal Cortex Is Sufficient to Induce Depressive-like Behaviors. Biol. Psychiatry *64*, 863–870.

Banker, G.A. (1980). Trophic interactions between astroglial cells and hippocampal neurons in culture. Science (80-.). *209*, 809–810.

Bannerman, D.M., Grubb, M., Deacon, R.M.J., Yee, B.K., Feldon, J., and Rawlins, J.N.P. (2003). Ventral hippocampal lesions affect anxiety but not spatial learning. Behav. Brain Res. *139*, 197–213.

Bannerman, D.M., Rawlins, J.N.P., McHugh, S.B., Deacon, R.M.J., Yee, B.K., Bast, T., Zhang, W.N., Pothuizen, H.H.J., and Feldon, J. (2004). Regional dissociations within the hippocampus - Memory and anxiety. Neurosci. Biobehav. Rev. *28*, 273–283.

Barley, K., Dracheva, S., and Byne, W. (2009). Subcortical oligodendrocyte- and astrocyte-associated gene expression in subjects with schizophrenia, major depression and bipolar disorder. Schizophr. Res. *112*, 54–64.

Barnett, S. (1975). The rat : a study in behavior. Univ. Chicago Press *287*, 43–48.

Belzung, C., and Griebel, G. (2001). Measuring normal and pathological anxiety-like behaviour in mice: A review. Behav. Brain Res. *125*, 141–149.

Bennett, M.V.L., Contreras, J.E., Bukauskas, F.F., and Sáez, J.C. (2003). New roles for astrocytes: Gap junction hemichannels have something to communicate. Trends Neurosci. *26*, 610–617.

Bergles, D.E., and Jahr, C.E. (1997). Synaptic Activation of Glutamate Transporters in Hippocampal Astrocytes. Neuron *19*, 1297–1308.

Bergles, D.E., and Jahr, C.E. (1998). Glial contribution to glutamate uptake at Schaffer collateral-commissural synapses in the hippocampus. J. Neurosci. *18*, 7709–7716.

Berlyne, D.E. (1950). Novelty and Curiosity As Determinants. Br. J. Psychol *41*, 68–80.

Bermudez-Rattoni, F., Okuda, S., Roozendaal, B., and Mcgaugh, J.L. (2005). Insular cortex is involved in consolidation of object recognition memory Insular cortex is involved in consolidation of object recognition memory. Cold Spring Harb. Lab. Press *12*, 447–449.

Blake, M.G., Krawczyk, M.C., Baratti, C.M., and Boccia, M.M. (2014). Neuropharmacology of memory consolidation and reconsolidation: Insights on central cholinergic mechanisms. J. Physiol. Paris *108*, 286–291.

Bliss, T.V.P., and Lømo, T. (1973). Long-lasting potentiation of synaptic transmission in the dentate area of the anaesthetized rabbit following stimulation of the perforant path. J. Physiol. *232*, 331–356.

Bliss, T., Collingridge, G., and Morris, R. (2007). Synaptic Plasticity in the Hippocampus. In The Hippocampus Book, P. Anderson, R. Morris, D. Amaral, T. Bliss, and J. O'Keefe, eds. (New York: Oxford University Press), pp. 343–473.

Boveris, A., Oshino, N., and Chance, B. (1972). The cellular production of hydrogen peroxide. Biochem. J. *128*, 617–630.

Boyles, J.K., Pitas, R.E., Wilson, E., Mahley, R.W., and Taylor, J.M. (1985). Apolipoprotein E associated with astrocytic glia of the central nervous system and with nonmyelinating glia of the peripheral nervous system. J. Clin. Invest. *76*, 1501–1513.

Brady, N.R., Elmore, S.P., Van Beek, J.J.H.G.M., Krab, K., Courtoy, P.J., Hue, L., and Westerhoff, H. V. (2004). Coordinated behavior of mitochondria in both space and time: A reactive oxygen species-activated wave of mitochondrial depolarization. Biophys. J. *87*, 2022–2034.

Bridges, R.J., Hatalski, C.G., Shim, S.N., Cummings, B.J., Vijayan, V., Kundi, A., and

Cotman, C.W. (1992). Gliotoxic actions of excitatory amino acids. Neuropharmacology *31*, 899–907.

Brown, A.M., and Ransom, B.R. (2007). Astrocyte Glycogen and Brain Energy Metabolism. Glia *55*, 1263–1271.

Brown, D.R., and Kretzschmar, H.A. (1998). The glio-toxic mechanism of alpha-aminoadipic acid on cultured astrocytes. J. Neurocytol. *27*, 109–118.

Brown, A.M., Tekkök, S.B., and Ransom, B.R. (2003). Glycogen regulation and functional role in mouse white matter. J. Physiol. *549*, 501–512.

Buckmaster, C.A. (2004). Entorhinal Cortex Lesions Disrupt the Relational Organization of Memory in Monkeys. J. Neurosci. *24*, 9811–9825.

Burgess, N., Maguire, E.A., and O'Keefe, J. (2002). The Human Hippocampus and Spatial and Episodic Memory. Neuron *35*, 625–641.

Bussey, T.J., Muir, J.L., and Aggleton, J.P. (1999). Functionally dissociating aspects of event memory: the effects of combined perirhinal and postrhinal cortex lesions on object and place memory in the rat. J Neurosci *19*, 495–502.

Cahill, L., McGaugh, J.L., and Weinberger, N.M. (2001). The neurobiology of learning and memory: Some reminders to remember. Trends Neurosci. *24*, 578–581.

Cahoy, J.D., Emery, B., Kaushal, A., Foo, L.C., Zamanian, J.L., Christopherson, K.S., Xing, Y., Lubischer, J.L., Krieg, P.A., Krupenko, S.A., et al. (2008). A Transcriptome Database for Astrocytes, Neurons, and Oligodendrocytes: A New Resource for Understanding Brain Development and Function. J. Neurosci. *28*, 264–278.

Canas, P.M., Porciuncula, L.O., Cunha, G.M.A., Silva, C.G., Machado, N.J., Oliveira, J.M.A., Oliveira, C.R., and Cunha, R.A. (2009). Adenosine A2A Receptor Blockade Prevents Synaptotoxicity and Memory Dysfunction Caused by -Amyloid Peptides via p38 Mitogen-Activated Protein Kinase Pathway. J. Neurosci. *29*, 14741–14751.

Cermak, L.S., and O'Connor, M. (1983). The anterograde and retrograde retrieval ability of a patient with amnesia due to encephalitis. Neuropsychologia *21*, 213–234.

Chance, B., Sies, H., and Boveris, A. (1979). Hydroperoxide metabolism in mammalian organs. Physiol. Rev. *59*, 527–605.

Chang, Y. -F (1978). Lysine Metabolism in the Rat Brain: the Pipecolic Acid-Forming Pathway. J. Neurochem. *30*, 347–354.

Chang, Y.F. (1976). Pipecolic acid pathway: The major lysine metabolic route in the rat

brain. Biochem. Biophys. Res. Commun. *69*, 174–180.

Chang, Y.F., Cauley, R.K., Chang, J.D., and Rao, V. V. (1997). L-α-aminoadipate inhibits kynurenate synthesis in rat brain hippocampus and tissue culture. Neurochem. Res. *22*, 825–829.

Cho, H.S., Baek, D.J., and Baek, S.S. (2014). Effect of exercise on hyperactivity, impulsivity and dopamine D2 receptor expression in the substantia nigra and striatum of spontaneous hypertensive rats. J. Exerc. Nutr. Biochem. *18*, 379–384.

Cho, K.O., Hunt, C.A., and Kennedy, M.B. (1992). The rat brain postsynaptic density fraction contains a homolog of the drosophila discs-large tumor suppressor protein. Neuron *9*, 929–942.

Choi, I.-Y., Seaquist, E.R., and Gruetter, R. (2003). Effect of insulin-induced hypoglycemia on protein metabolism in vivo. J. Neurosci. Res. *72*, 25–32.

Chryssanthopoulos, C., Williams, C., Nowitz, A., and Bogdanis, G. (2004). Skeletal muscle glycogen concentration and metabolic responses following a high glycaemic carbohydrate breakfast. J. Sports Sci. *22*, 1065–1071.

Chung, W., Allen, N.J., and Eroglu, C. (2015a). Astrocytes Control Synapse Formation, Function, and Elimination. Cold Spring Harb Perspect Biol.

Chung, W.S., Welsh, C.A., Barres, B.A., and Stevens, B. (2015b). Do glia drive synaptic and cognitive impairment in disease? Nat. Neurosci. *18*, 1539–1545.

Clark, R.E., Zola, S.M., and Squire, L.R. (2000). Impaired recognition memory in rats after damage to the hippocampus. J. Neurosci. *20*, 8853–8860.

Coelho, J.E., Alves, P., Canas, P.M., Valadas, J.S., Shmidt, T., Batalha, V.L., Ferreira, D.G., Ribeiro, J.A., Bader, M., Cunha, R.A., et al. (2014). Overexpression of adenosine A2A receptors in rats: Effects on depression, locomotion, and anxiety. Front. Psychiatry *5*.

Cohen-Gadol, A.A., Pan, J.W., Kim, J.H., Spencer, D.D., and Hetherington, H.H. (2004). Mesial temporal lobe epilepsy: a proton magnetic resonance spectroscopy study and a histopathological analysis. J. Neurosurg. *101*, 613–620.

Colombo, J.A., and Reisin, H.D. (2004). Interlaminar astroglia of the cerebral cortex: A marker of the primate brain. Brain Res. *1006*, 126–131.

Connor, J.R., Menzies, S.L., St. Martin, S., and Mufson, E.J. (1990). The cellular distribution of transferrin, ferritin and iron in the human brain. J. Neurosci. Res.

27, 595–611.

Conrad, C.D., Galea, L.A.M., Kuroda, Y., and McEwen, B.S. (1996). Chronic stress impairs rat spatial memory on the Y maze, and this effect is blocked by tianeptine pretreatment. Behav. Neurosci. *110*, 1321–1334.

Cruz, N.F., and Dienel, G.A. (2002). High glycogen levels in brains of rats with minimal environmental stimuli: Implications for metabolic contributions of working astrocytes. J. Cereb. Blood Flow Metab. *22*, 1476–1489.

Cudalbu, C., Lanz, B., Duarte, J.M.N., Morgenthaler, F.D., Pilloud, Y., Mlynárik, V., and Gruetter, R. (2012). Cerebral glutamine metabolism under hyperammonemia determined in vivo by localized1H and15N NMR spectroscopy. J. Cereb. Blood Flow Metab. *32*, 696–708.

Cummins, R.A., and Walsh, R.N. (1976). The Open-Field Test: a critical review. Psvchological Bull. *83*, 482–504.

Cunha, G.M.A., Canas, P.M., Oliveira, C.R., and Cunha, R.A. (2006). Increased density and synapto-protective effect of adenosine A2Areceptors upon sub-chronic restraint stress. Neuroscience *141*, 1775–1781.

D'Ambrosio, R., Gordon, D.S., and Winn, H.R. (2002). Differential role of KIR channel and Na(+)/K(+)-pump in the regulation of extracellular K(+) in rat hippocampus. J. Neurophysiol. *87*, 87–102.

Dan, Y., and Poo, M.M. (2004). Spike timing-dependent plasticity of neural circuits. Neuron *44*, 23–30.

Dawson, G.R., and Tricklebank, M.D. (1995). Use of the elevated plus maze in the search for novel anxiolytic agents. Trends Pharmacol. Sci. *16*, 33–36.

Dehouck, M. -P, Méresse, S., Delorme, P., Fruchart, J. -C, and Cecchelli, R. (1990). An Easier, Reproducible, and Mass-Production Method to Study the Blood–Brain Barrier In Vitro. J. Neurochem. *54*, 1798–1801.

Dellu, F., Mayo, W., Cherkaoui, J., Lemoal, M., and Simon, H. (1992). A Two Trial Memory Task with Automated Recording: Study in Young and Aged Rats. Brain Res. *588*, 132–139.

Dellu, F., Fauchey, V., Le Moal, M., and Simon, H. (1997). Extension of a new two-trial memory task in the rat: Influence of environmental context on recognition processes. Neurobiol. Learn. Mem. *67*, 112–120.

Dix, S.L., and Aggleton, J.P. (1999). Extending the spontaneous preference test of recognition: Evidence of object-location and object-context recognition. Behav. Brain Res. *99*, 191–200.

Donato, R. (2001). S100: A multigenic family of calcium-modulated proteins of the EF-hand type with intracellular and extracellular functional roles. Int. J. Biochem. Cell Biol. *33*, 637–668.

Doxey, C.R., and Kirwan, C.B. (2015). Structural and functional correlates of behavioral pattern separation in the hippocampus and medial temporal lobe. Hippocampus *25*, 524–533.

Drejer, J., Larsson, O.M., and Schousboe, A. (1982). Characterization of L-glutamate Uptake into and Release from Astrocytes and Neurons Cultured from Different Brain Regions. Exp. Brain Res. *47*, 259–269.

Duchen, M.R. (2000). Mitochondria and calcium: from cell signaling to cell death. J Physiol *529*, 57–68.

Dudai, Y. (2004). The Neurobiology of Consolidations, Or, How Stable is the Engram? Annu. Rev. Psychol. *55*, 51–86.

Dudek, S.M., and Bear, M.F. (1992). Homosynaptic long-term depression in area CA1 of hippocampus and effects of N-methyl-D-aspartate receptor blockade. Proc. Natl. Acad. Sci. U. S. A. *89*, 4363–4367.

Eddleston, M., and Mucke, L. (1993). Molecular profile of reactive astrocytes-Implications for their role in neurologic disease. Neuroscience *54*, 15–36.

Eng, L.F., and Ghirnikar, R.S. (1994). GFAP and Astrogliosis. Brain Pathol. *4*, 229–237.

Ennaceur, A. (2010). One-trial object recognition in rats and mice: Methodological and theoretical issues. Behav. Brain Res. *215*, 244–254.

Erschbamer, M., Pernold, K., and Olson, L. (2007). Inhibiting Epidermal Growth Factor Receptor Improves Structural, Locomotor, Sensory, and Bladder Recovery from Experimental Spinal Cord Injury. J. Neurosci. *27*, 6428–6435.

Fanselow MS, D.H. (2010). Are the dorsal and ventral hippocampus functionally distinct structures? Neuron *65*, 7–19.

Feinberg, D.A., and Mark, A.S. (1987). Human brain motion and cerebrospinal fluid circulation demonstrated with MR velocity imaging. Radiology *163*, 793–799.

Fellin, T. (2009). Communication between neurons and astrocytes: Relevance to the

modulation of synaptic and network activity. J. Neurochem. *108*, 533–544.

Fischer, W., Appelt, K., Grohmann, M., Franke, H., Nörenberg, W., and Illes, P. (2009). Increase of intracellular Ca2+by P2X and P2Y receptor-subtypes in cultured cortical astroglia of the rat. Neuroscience *160*, 767–783.

Garwood, C.J., Ratcliffe, L.E., Simpson, J.E., Heath, P.R., Ince, P.G., and Wharton, S.B. (2017). Review: Astrocytes in Alzheimer's disease and other age-associated dementias: a supporting player with a central role. Neuropathol. Appl. Neurobiol. *43*, 281–298.

Gerke, V., and Weber, K. (1985). Calcium-dependent conformational changes in the 36-kDa subunit of intestinal protein I related to the cellular 36-kDa target of Rous sarcoma virus tyrosine kinase. J. Biol. Chem. *260*, 1688–1695.

Giaume, C., and Liu, X. (2012). From a glial syncytium to a more restricted and specific glial networking. J. Physiol. Paris *106*, 34–39.

Giaume, C., and McCarthy, K.D. (1996). Control of gap-junctional communication in astrocytic networks. Trends Neurosci. *19*, 319–325.

Giaume, C., Koulakoff, A., Roux, L., Holcman, D., and Rouach, N. (2010). Astroglial networks: A step further in neuroglial and gliovascular interactions. Nat. Rev. Neurosci. *11*, 87–99.

Good, M.A., Barnes, P., Staal, V., McGregor, A., and Honey, R.C. (2007). Context- but not familiarity-dependent forms of object recognition are impaired following excitotoxic hippocampal lesions in rats. Behav. Neurosci. *121*, 218–223.

Haettig, J., Stefanko, D.P., Multani, M.L., Figueroa, D.X., McQuown, S.C., and Wood, M.A. (2011). HDAC inhibition modulates hippocampus-dependent long-term memory for object location in a CBP-dependent manner. Learn. Mem. *18*, 71–79.

Halassa, M.M., Florian, C., Fellin, T., Munoz, J.R., Lee, S.Y., Abel, T., Haydon, P.G., and Frank, M.G. (2009). Astrocytic Modulation of Sleep Homeostasis and Cognitive Consequences of Sleep Loss. Neuron *61*, 213–219.

Han, J., Kesner, P., Metna-Laurent, M., Duan, T., Xu, L., Georges, F., Koehl, M., Abrous, D.N., Mendizabal-Zubiaga, J., Grandes, P., et al. (2012). Acute cannabinoids impair working memory through astroglial CB 1 receptor modulation of hippocampal LTD. Cell *148*, 1039–1050.

Hawkins, B.T., and Davis, T.P. (2005). The Blood-Brain Barrier / Neurovascular Unit in

Health and Disease. Pharmacol. Rev. *57*, 173–185.

Heller, J.P., and Rusakov, D.A. (2015). Morphological plasticity of astroglia: Understanding synaptic microenvironment. Glia *63*, 2133–2151.

Hensley, K., Hall, N., Subramaniam, R., Cole, P., Harris, M., Aksenov, M., Aksenova, M., Gabbita, S.P., Wu, J.F., Carney, J.M., et al. (1995). Brain Regional Correspondence Between Alzheimer's Disease Histopathology and Biomarkers of Protein Oxidation. J. Neurochem. *65*, 2146–2156.

Hertz, L., and Zielke, H.R. (2004). Astrocytic control of glutamatergic activity: Astrocytes as stars of the show. Trends Neurosci. *27*, 735–743.

Higashi, K., Fujita, A., Inanobe, A., Tanemoto, M., Doi, K., Kubo, T., and Kurachi, Y. (2001). An inwardly rectifying K^+ channel, Kir4.1, expressed in astrocytes surrounds synapses and blood vessels in brain. Am. J. Physiol. Physiol. *281*, C922–C931.

Hu, X., Yuan, Y., Wang, D., and Su, Z. (2016). Heterogeneous astrocytes: Active players in CNS. Brain Res. Bull. *125*, 1–18.

Huck, S., Grass, F., and Hatten, M.E. (1984). Gliotoxic effects of α-aminoadipic acid on monolayer cultures of dissociated postnatal mouse cerebellum. Neuroscience *12*.

Hughes, J.R. (1958). Post-Tetanic Potentiation. Physiol. Rev. *38*, 91–113.

Johnston-Wilson, N., Sims, C., Hofmann, J.-P., Anderson, L., Shore, A., Torrey, E., and Yolken, R. (2000). Disease-specific alterations in frontal cortex brain proteins in schizophrenia, bipolar disorder, and major depressive disorder. Mol. Psychiatry *5*, 142–149.

Kandel, E.R. (2001). The molecular biology of memory storage: A dialogue between gene and synapses. Science (80-.). *294*, 1030–1038.

Kato, S., Ishita, S., Sugawara, K., and Mawatari, K. (1993). Cystine/Glutamate antiporter expression in retinal Müller glial cells: implications for DL-alpha-aminoadipate toxicity. Neuroscience *57*, 473–482.

Kesner, R.P., Lee, I., and Gilbert, P. (2004). A behavioral assessment of hippocampal function based on a subregion analysis. Neurosciences *15*, 333–351.

Kessels, R.P.C., De Haan, E.H.F., Kappelle, L.J., and Postma, A. (2001). Varieties of human spatial memory: A meta-analysis on the effects of hippocampal lesions. Brain Res. Rev. *35*, 295–303.

Kettenmann, H., and Verkhratsky, A. (2008). Neuroglia: the 150 years after. Trends

Neurosci. *31*, 653–659.

Khakh, B.S., and Sofroniew, M. V. (2015). Diversity of astrocyte functions and phenotypes in neural circuits. Nat. Neurosci. *18*, 942–952.

Khurgel, M., Koo, A.C., and Ivy, G.O. (1996). Selective ablation of astrocytes by intracerebral injections of alpha-aminoadipate. Glia *16*, 351–358.

Kimelberg, H.K. (1981). Active accumulation and exchange transport of chloride in astroglial cells in cultures. Biochim. Biophys. Acta *646*, 179–184.

Kimelberg, H.K. (2004). Water homeostasis in the brain: Basic concepts. Neuroscience *129*, 851–860.

Kimelberg, H.K., and Nedergaard, M. (2010). Functions of Astrocytes and their Potential As Therapeutic Targets. Neurotherapeutics *7*, 338–353.

Kimelberg, H.K., Stieg, P.E., and Mazurkiewicz, J.E. (1982). Immunocytochemical and biochemical analysis of carbonic anhydrase in primary astrocyte cultures from rat brain. J Neurochem *39*, 734–742.

Kjelstrup, K.G., Tuvnes, F.A., Steffenach, H.-A., Murison, R., Moser, E.I., and Moser, M.-B. (2002). Reduced fear expression after lesions of the ventral hippocampus. Proc. Natl. Acad. Sci. *99*, 10825–10830.

Klein, M.A., Möller, J.C., Jones, L.L., Bluethmann, H., Kreutzberg, G.W., and Raivich, G. (1997). Impaired neuroglial activation in interleukin-6 deficient mice. Glia *19*, 227–233.

Klempan, T.A., Sequeira, A., Canetti, L., Lalovic, A., Ernst, C., Ffrench-Mullen, J., and Turecki, G. (2009). Altered expression of genes involved in ATP biosynthesis and GABAergic neurotransmission in the ventral prefrontal cortex of suicides with and without major depression. Mol. Psychiatry *14*, 175–189.

Koehler, R.C., Roman, R.J., and Harder, D.R. (2009). Astrocytes and the regulation of cerebral blood flow. Trends Neurosci. *32*, 160–169.

Kölliker, A. (1889). Handbuch der Gewebelehre des Menschen. Leipzig W. Engelmann *3*.

Kopelman, M.D., Wilson, B.A., and Baddeley, A.D. (1989). The autobiographical memory interview: a new assessment of autobiographical and personal semantic memory in amnesic patients. J. Clin. Exp. Neuropsychol. Off. J. Int. Neuropsychol. Soc. *11*, 724–744.

Koprivica, V., Cho, K.S., Park, J.B., Yiu, G., Atwal, J., Gore, B., Kim, J.A., Lin, E., Tessier-Lavigne, M., Chen, D.F., et al. (2005). Neuroscience: EGFR activation mediates inhibition of axon regeneration by myelin and chondroitin sulfate proteoglycans. Science (80-.). *310*, 106–110.

Kroemer, G., Galluzzi, L., and Brenner, C. (2007). Mitochondrial Membrane Permeabilization in Cell Death. Physiol. Reveiw 99–163.

Kunzelmann, P., Schröder, W., Traub, O., Steinhäuser, C., Dermietzel, R., and Willecke, K. (1999). Late onset and increasing expression of the gap junction protein connexin30 in adult murine brain and long-term cultured astrocytes. Glia *25*, 111–119.

Lee, H.J., Suk, J.E., Patrick, C., Bae, E.J., Cho, J.H., Rho, S., Hwang, D., Masliah, E., and Lee, S.J. (2010). Direct transfer of α-synuclein from neuron to astroglia causes inflammatory responses in synucleinopathies. J. Biol. Chem. *285*, 9262–9272.

Lefrançois, T., Fages, C., Peschanski, M., and Tardy, M. (1997). Neuritic outgrowth associated with astroglial phenotypic changes induced by antisense glial fibrillary acidic protein (GFAP) mRNA in injured neuron-astrocyte cocultures. J. Neurosci. *17*, 4121–4128.

Von Lenhossék, M. (1893). Die Nervenendigungen in den Maculae und Cristae acusticae. Anat. Hefte *3*, 230–266.

Li, Z., and Sheng, M. (2003). Some assembly required: The development of neuronal synapses. Nat. Rev. Mol. Cell Biol. *4*, 833–841.

Li, X., Newbern, J.M., Wu, Y., Morgan-Smith, M., Zhong, J., Charron, J., and Snider, W.D. (2012). MEK Is a Key Regulator of Gliogenesis in the Developing Brain. Neuron *75*, 1035–1050.

Lima, A., Sardinha, V.M., Oliveira, A.F., Reis, M., Mota, C., Silva, M.A., Marques, F., Cerqueira, J.J., Pinto, L., Sousa, N., et al. (2014). Astrocyte pathology in the prefrontal cortex impairs the cognitive function of rats. Mol. Psychiatry *19*, 834–841.

Liu, Y., Namba, T., Liu, J., Suzuki, R., Shioda, S., and Seki, T. (2010). Glial fibrillary acidic protein-expressing neural progenitors give rise to immature neurons via early intermediate progenitors expressing both glial fibrillary acidic protein and neuronal markers in the adult hippocampus. Neuroscience *166*, 241–251.

Maassen, J.A., Hart, L.M., Essen, E. Van, Heine, R.J., Nijpels, G., Roshan, S., Tafrechi, J., Raap, A.K., Janssen, G.M.C., and Lemkes, H.H.P.J. (2004). Mitochondrial diabetes. Diabetes *53*, 103–109.

Magistretti, P.J., Sorg, O., Naichen, Y., Pellerin, L., de Rham, S., and Martin, J.-L. (1994). Regulation of Astrocyte Energy Metabolism by Neurotransmitters. Kidney Blood Press. Res. *17*, 168–171.

Malenka, R.C., Carroll, R.C., Lissin, D. V., Zastrow, M. von, and Nicoll, R.A. (1999). Rapid redistribution of glutamate receptors contributes to long-term\ndepression in hippocampal cultures. Nat. Neurosci. *2*, 454–460.

Maragakis, N.J., and Rothstein, J.D. (2006). Mechanisms of Disease: astrocytes in neurodegenerative disease. Nat Clin Pr. Neurol *2*, 679–689.

Martin, S.J., Grimwood, P.D., and Morris, R.G.M. (2000). Synaptic plasticity and memory: An Evaluation of the Hypothesis. Annu. Rev. Neurosci. 649–711.

Masliah, E., and Terry, R. (1993). The Role of Synaptic Proteins in the Pathogenesis of Disorders of the Central Nervous System. Brain Pathol. *3*, 77–85.

Matyash, V., and Kettenmann, H. (2010). Heterogeneity in astrocyte morphology and physiology. Brain Res. Rev. *63*, 2–10.

Mayford, M., Siegelbaum, S.A., Kandel, E.R., Long-term, N.R., Lüscher, C., Malenka, R.C., Harris, K.M., Weinberg, R.J., Smart, T.G., Paoletti, P., et al. (2012). Synapses and Memory Storage. Cold Spring Harb Perspect Biol.

McAllister, M.S., Krizanac-Bengez, L., Macchia, F., Naftalin, R.J., Pedley, K.C., Mayberg, M.R., Marroni, M., Leaman, S., Stanness, K.A., and Janigro, D. (2001). Mechanisms of glucose transport at the blood-brain barrier: An in vitro study. Brain Res. *904*, 20–30.

McBean, G.J. (1994). Inhibition of the glutamate transporter and glial enzymes in rat striatum by the gliotoxin, ocaminoadipate. Br. J. Pharmacol. *113*, 536–540.

McGaugh, J.L. (1966). Time-dependent processes in memory storage. Science (80-.). *153*, 1351–1358.

McGaugh, J.L. (2000). Memory - A century of consolidation. Science (80-.). *287*, 248–251.

McHugh, S.B., Deacon, R.M.J., Rawlins, J.N.P., and Bannerman, D.M. (2004). Amygdala and Ventral Hippocampus Contribute Differentially to Mechanisms of Fear and

Anxiety. Behav. Neurosci. *118*, 63–78.

McKenna, M.C. (2013). Glutamate pays its own way in astrocytes. Front. Endocrinol. (Lausanne). *4*, 1–7.

McKenna, M.C., Dienel, G.A., Sonnewald, U., Waagepetersen, H.S., and Schousboe, A. (2012). Energy Metabolism of the Brain. Basic Neurochem. 200–231.

Meister, A. (1974). Glutamine Synthetase in mammals. In Academic Press, pp. 699–754.

Meister, a, and Tate, S.S. (1976). Glutathione and related gamma-glutamyl compounds: biosynthesis and utilization. Annu. Rev. Biochem. *45*, 559–604.

Meltzoff, A.N., Kuhl, P.K., Movellan, J.R., and Sejnowski, T.J. (2009). Foundations for a new science of learning. Science (80-.). *325*, 284–288.

Merrill, J.E. (1987). Macroglia: neural cells responsive to lymphokines and growth factors. Immunol. Today *8*, 146–150.

Miller, R.H., and Raff, M.C. (1984). Fibrous and Protoplasmic Astrocytes Are Biochemically and Developmentally Distinct'. J. Neurosci. *4*, 585–592.

Minagar, A., Shapshak, P., Fujimura, R., Ownby, R., Heyes, M., and Eisdorfer, C. (2002). The role of macrophage/microglia and astrocytes in the pathogenesis of three neurologic disorders: HIV-associated dementia, Alzheimer disease, and multiple sclerosis. J. Neurol. Sci. *202*, 13–23.

Minelli, a, Brecha, N.C., Karschin, C., DeBiasi, S., and Conti, F. (1995). GAT-1, a high-affinity GABA plasma membrane transporter, is localized to neurons and astroglia in the cerebral cortex. J. Neurosci. *15*, 7734–7746.

Minelli, a, DeBiasi, S., Brecha, N.C., Zuccarello, L. V, and Conti, F. (1996). GAT-3, a high-affinity GABA plasma membrane transporter, is localized to astrocytic processes, and it is not confined to the vicinity of GABAergic synapses in the cerebral cortex. J. Neurosci. *16*, 6255–6264.

Mitterauer, B.J. (2010). The syncytiopathy hypothesis of depression: Downregulation of glial connexins may protract synaptic information processing and cause memory impairment. Med. Hypotheses *74*, 497–502.

Miyamoto, E. (2006). Molecular Mechanism of Neuronal Plasticity: Induction and Maintenance of Long-Term Potentiation in the Hippocampus. J. Pharmacol. Sci. *100*, 433–442.

Molofsk, A. V., Krenick, R., Ullian, E., Tsai, H.H., Deneen, B., Richardson, W.D., Barres,

B.A., and Rowitch, D.H. (2012). Astrocytes and disease: A neurodevelopmental perspective. Genes Dev. *26*, 891–907.

Montgomery, J.M., and Madison, D. V. (2002). State-Dependent Heterogeneity in Synaptic Depression between Pyramidal Cell Pairs. Neuron *33*, 765–777.

Morris, R.G.M., Moser, E.I., Riedel, G., Martin, S.J., Sandin, J., Day, M., and O'Carroll, C. (2003). Elements of a neurobiological theory of the hippocampus: The role of activity-dependent synaptic plasticity in memory. Philos. Trans. R. Soc. B Biol. Sci. *358*, 773–786.

Moscovitch, M., Rosenbaum, R.S., Gilboa, A., Addis, D.R., Westmacott, R., Grady, C., McAndrews, M.P., Levine, B., Black, S., Winocur, G., et al. (2005). Functional neuroanatomy of remote episodic, semantic and spatial memory: A unified account based on multiple trace theory. J. Anat. *207*, 35–66.

Moser, M.B., and Moser, E.I. (1998). Functional differentiation in the hippocampus. Hippocampus *8*, 608–619.

Moser, M.B., Moser, E.I., Forrest, E., Andersen, P., and Morris, R.G. (1995). Spatial learning with a minislab in the dorsal hippocampus. Proc. Natl. Acad. Sci. *92*, 9697–9701.

Nader, K. (2003). Memory Traces unbound. Trends Neurosci. *26*, 65–72.

Nagele, R.G., Wegiel, J., Venkataraman, V., Imaki, H., Wang, K.C., and Wegiel, J. (2004). Contribution of glial cells to the development of amyloid plaques in Alzheimer's disease. Neurobiol. Aging *25*, 663–674.

Nagelhus, E.A., Horio, Y., Inanobe, A., Fujita, A., Haug, F.M., Nielsen, S., Kuhachi, Y., and Ottersen, O.P. (1999). Immunogold evidence suggests that coupling of K+ siphoning and water transport in rat retinal Muller cells is mediated by a coenrichment of Kir4.1 and AQP4 in specific membrane domains. Glia *26*, 47–54.

Nagy, J.I., and Rash, J.E. (2000). Connexins and gap junctions of astrocytes and oligodendrocytes in the CNS. Brain Res. Rev. *32*, 29–44.

Nagy, J.I., Patel, D., Ochalski, P.A.Y., and Stelmack, G.L. (1999). Connexin30 in rodent, cat and human brain: Selective expression in gray matter astrocytes, co-localization with connexin43 at gap junction and late developmental appearance. Neuroscience *88*, 447–468.

Nedergaard, M., Ransom, B., and Goldman, S.A. (2003). New roles for astrocytes :

Redefining the functional architecture of the brain. Trends Neurosci. *26*, 523–530.

Neves, G., Cooke, S.F., and Bliss, T.V.P. (2008). Synaptic plasticity, memory and the hippocampus: a neural network approach to causality. Nat. Rev. Neurosci. *9*, 65–75.

Nichols, N.R., Day, J.R., Laping, N.J., Johnson, S.A., and Finch, C.E. (1993). Gfap Messenger-Rna Increases with Age in Rat and Human Brain. Neurobiol. Aging *14*, 421–429.

Nilsson, L.H., and Hultman, E. (1973). Liver glycogen in man - the effect of total starvation or a carbohydrate-poor diet followed by carbohydrate refeeding. Scand. J. Clin. Lab. Invest. *32*, 325–330.

O'Keefe, J. (1990). A computational theory of the hippocampal cognitive map. Prog. Brain Res. *83*, 301–312.

Oberheim, N.A., Takano, T., Han, X., He, W., Lin, J.H.C., Wang, F., Xu, Q., Wyatt, J.D., Pilcher, W., Ojemann, J.G., et al. (2009). Uniquely Hominid Features of Adult Human Astrocytes. J. Neurosci. *29*, 3276–3287.

Olabarria, M., Noristani, H.N., Verkhratsky, A., and Rodríguez, J.J. (2011). Age-dependent decrease in glutamine synthetase expression in the hippocampal astroglia of the triple transgenic Alzheimer's disease mouse model: Mechanism for deficient glutamatergic transmission? Mol. Neurodegener. *6*, 1–9.

Olney, J.W., Ho, O.L., and Rhee, V. (1971). Cytotoxic effects of acidic and sulphur containing amino acids on the infant mouse central nervous system. Exp. Brain Res. *14*, 61–76.

Olney, J.W., de Gubareff, T., and Collins, J.F. (1980). Stereospecificity of the gliotoxic and anti-neurotoxic actions of alpha-aminoadipate. Neurosci. Lett. *19*, 277–282.

Orellana, J.A., and Stehberg, J. (2014). Hemichannels: New roles in astroglial function. Front. Physiol. *5 JUN*.

Orellana, J.A., Retamal, M.A., Moraga-Amaro, R., and Stehberg, J. (2016). Role of Astroglial Hemichannels and Pannexons in Memory and Neurodegenerative Diseases. Front. Integr. Neurosci. *10*, 1–9.

Orkand, R.K., Nicholls, J.G., and Kuffler, S.W. (1966). Effect of nerve impulses on the membrane potential of glial cells in the central nervous system of amphibia. J. Neurophysiol. *29*, 788–806.

Osborn, L.M., Kamphuis, W., Wadman, W.J., and Hol, E.M. (2016). Astrogliosis: An integral player in the pathogenesis of Alzheimer's disease. Prog. Neurobiol. *144*, 121–141.

Ota, Y., Zanetti, a T., and Hallock, R.M. (2013). The role of astrocytes in the regulation of synaptic plasticity and memory formation. Neural Plast *2013*, 185463.

Pagnussat, N., Almeida, A.S., Marques, D.M., Nunes, F., Chenet, G.C., Botton, P.H.S., Mioranzza, S., Loss, C.M., Cunha, R.A., and Porciúncula, L.O. (2015). Adenosine A2A receptors are necessary and sufficient to trigger memory impairment in adult mice. Br. J. Pharmacol. *172*, 3831–3845.

Parker, M.D., Bouyer, P., Daly, C.M., and Boron, W.F. (2008). Cloning and characterization of novel human SLC4A8 gene products encoding Na+-driven Cl-/HCO3(-) exchanger variants NDCBE-A, -C, and -D. Physiol. Genomics *34*, 265–276.

Parpura, V., Fisher, E.S., Lechleiter, J.D., Schousboe, A., Waagepetersen, H.S., Brunet, S., Baltan, S., and Verkhratsky, A. (2017). Glutamate and ATP at the Interface Between Signaling and Metabolism in Astroglia: Examples from Pathology. Neurochem. Res. *42*, 19–34.

Patel, A.J., and Ridgeway, T. (1993). Regulation of β-amyloid precursor protein isoform mRNAs by transforming growth factor-β1 and interleukin-1β in astrocytes. Mol. Brain Res. *19*, 251–256.

Paul, C.M., Magda, G., and Abel, S. (2009). Spatial memory: Theoretical basis and comparative review on experimental methods in rodents. Behav. Brain Res. *203*, 151–164.

Paxinos, G., and Franklin, K. (1997). The Mouse Brain in Stereotaxic Coordinates (Academic Press).

Pekny, M., and Nilsson, M. (2005). Astrocyte activation and reactive gliosis. Glia *50*, 427–434.

Pekny, M., and Pekna, M. (2014). Astrocyte Reactivity and Reactive Astrogliosis: Costs and Benefits. Physiol. Rev. *94*, 1077–1098.

Pellegri, G., Rossier, C., Magistretti, P.J., and Martin, J.L. (1996). Cloning, localization and induction of mouse brain glycogen synthase. Mol. Brain Res. *38*, 191–199.

Pellerin, L., and Magistretti, P.J. (2004). Neuroenergetics: Calling upon Astrocytes to

Satisfy Hungry Neurons. Neuroscientist *10*, 53–62.

Peña, L.A., Brecher, C.W., and Marshak, D.R. (1995). β-Amyloid regulates gene expression of glial trophic substance S100β in C6 glioma and primary astrocyte cultures. Control *34*, 118–126.

Perea, G., Navarrete, M., and Araque, A. (2009). Tripartite synapses: astrocytes process and control synaptic information. Trends Neurosci. *32*, 421–431.

Pereda, A.E. (2014). Electrical synapses and their functional interactions with chemical synapses. Nat. Rev. Neurosci. *15*, 250–263.

Pereira, M. (2017). Role of astrocytes in synaptic function and memory. Focus on adenosine A2A receptors. Master's thesis, Universidade de Coimbra.

Pereira, M.C., Amaral, I., Lopes, J.P., Lopes, C., Leitão, C., Cunha, R.A., and Agostinho, P. (2018). Pharmacological approaches to impinge astrocytic function: impact on mouse Hippocampal LTP (11th FENS Forum of Neuroscience in Berlin).

Pfeiffer-Guglielmi, B., Fleckenstein, B., Jung, G., and Hamprech, B. (2003). Immunocytochemical localization of glycogen phosphorylase isozymes in rat nervous tissues by using isozyme-specific antibodies. J. Neurochem. *85*, 73–81.

Planas, A.M., Justicia, C., and Soriano, M.A. (1998). Epidermal Growth Factor Receptor in Proliferating Reactive Glia Following Transient Focal Ischemia in the Rat Brain. Glia *129*, 120–129.

Popoli, M., Yan, Z., McEwen, B.S., and Sanacora, G. (2011). The stressed synapse: the impact of stress and glucocorticoids on glutamate transmission. Nat. Rev. Neurosci. *13*.

Le Prince, G., Delaere, P., Fages, C., Lefrançois, T., Touret, M., Salanon, M., and Tardy, M. (1995). Glutamine synthetase (GS) expression is reduced in senile dementia of the Alzheimer type. Neurochem. Res. *20*, 859–862.

Qi, L.Y., Xiu, M.H., Chen, D.C., Wang, F., Kosten, T.A., Kosten, T.R., and Zhang, X.Y. (2009). Increased serum S100B levels in chronic schizophrenic patients on long-term clozapine or typical antipsychotics. Neurosci. Lett. *462*, 113–117.

Rabchevsky, a G., Weinitz, J.M., Coulpier, M., Fages, C., Tinel, M., and Junier, M.P. (1998). A role for transforming growth factor alpha as an inducer of astrogliosis. J. Neurosci. *18*, 10541–10552.

Ramón y Cajal, S. (1913). Sobre un nuevo proceder de impregnacion de la neuroglia y

sus resultados en los centros nerviosos del hombre y animales. Trab. Lab. Invest. Biol. Univ. Madrid *11*.

Reddy, L. V., Koirala, S., Sugiura, Y., Herrera, A.A., and Ko, C.P. (2003). Glial cells maintain synaptic structure and function and promote development of the neuromuscular junction in vivo. Neuron *40*, 563–580.

Reichenbach, A., and Wolburg, H. (2005). Astrocytes and ependymal glia. Neuroglia *2*, 19–35.

Reichenbach, A., and Wolburg, H. (2009). Structural association of astrocytes with neurons and vasculature: Defining territorial boundaries. In Astrocytes in (Patho)Physiology of the Nervous System, P. Haydon, and V. Parpura, eds. (Boston: Springer).

Richmond, M.A., Yee, B.K., Pouzet, B., Veenman, L., Rawlins, J.N.P., Feldon, J., and Bannerman, D.M. (1999). Dissociation context and space whithin the Hippocampus: Effects Of Complete, Dorsal, and Ventral Excitotoxic Hippocampal lesions On Conditioned Freezing and Spatial Learning. Behav. Neurosci. *113*, 1189–1203.

Rodrigues, D.I., Gutierres, J., Pliássova, A., Oliveira, C.R., Cunha, R.A., and Agostinho, P. (2014). Synaptic and sub-synaptic localization of amyloid-β protein precursor in the rat hippocampus. J. Alzheimer's Dis. *40*, 981–992.

Rodríguez-Arellano, J.J., Parpura, V., Zorec, R., and Verkhratsky, A. (2016). Astrocytes in physiological aging and Alzheimer's disease. Neuroscience *323*, 170–182.

Rodriguez, J., Olabarria, M., Chvatal, A., and Verkhratsky, A. (2009). Astroglia in dementia and Alzheimer's disease. Cell Death … *16*, 378–385.

Rogawski, M.A., and Löscher, W. (2004). The neurobiology of antiepileptic drugs. Nat. Rev. Neurosci. *5*, 553–564.

Rosario Hernandez, M., Agapova, O.A., Yang, P., Salvador-Silva, M., Ricard, C.S., and Aoi, S. (2002). Differential gene expression in astrocytes from human normal and glaucomatous optic nerve head analyzed by cDNA microarray. Glia *38*, 45–64.

Rose, C.F., Verkhratsky, A., and Parpura, V. (2013). Astrocyte glutamine synthetase: pivotal in health and disease. Biochem. Soc. Trans. *41*, 1518–1524.

Roßner, S., Lange-Dohna, C., Zeitschel, U., and Perez-Polo, J.R. (2005). Alzheimer's disease β-secretase BACE1 is not a neuron-specific enzyme. J. Neurochem. *92*,

226–234.

Rothstein, J.D., Martin, L., Levey, A.I., Dykes-Hoberg, M., Jin, L., Wu, D., Nash, N., and Kuncl, R.W. (1994). Localization of neuronal and glial glutamate transporters. Neuron *13*, 713–725.

Rothstein, J.D., Dykes-Hoberg, M., Pardo, C.A., Bristol, L.A., Jin, L., Kuncl, R.W., Kanai, Y., Hediger, M.A., Wang, Y., Schielke, J.P., et al. (1996). Knockout of glutamate transporters reveals a major role for astroglial transport in excitotoxicity and clearance of glutamate. Neuron *16*, 675–686.

Rudy, C.C., Hunsberger, H.C., Weitzner, D.S., and Reed, M.N. (2015). The Role of the Tripartite Glutamatergic Synapse in the Pathophysiology of Alzheimer's Disease. Aging Dis. *6*, 131.

Rusakov, D.A., Bard, L., Stewart, M.G., and Henneberger, C. (2014). Diversity of astroglial functions alludes to subcellular specialisation. Trends Neurosci. *37*, 228–242.

Sastre, M., Dewachter, I., Rossner, S., Bogdanovic, N., Rosen, E., Borghgraef, P., Evert, B.O., Dumitrescu-Ozimek, L., Thal, D.R., Landreth, G., et al. (2006). Nonsteroidal anti-inflammatory drugs repress beta-secretase gene promoter activity by the activation of PPARgamma. Proc. Natl. Acad. Sci. U. S. A. *103*, 443–448.

Schacter, D.L., and Buckner, R.L. (1998). Priming and the Brain. Neuron *20*, 185–195.

Schmitt, B.M., Berger, U. V, Douglas, R.M., Bevensee, M.O., Hediger, M. a, Haddad, G.G., and Boron, W.F. (2000). Na/HCO3 cotransporters in rat brain: expression in glia, neurons, and choroid plexus. J. Neurosci. *20*, 6839–6848.

Schousboe, a., Thorbek, P., Hertz, L., and Krogsgaard-Larsen, P. (1979). Effects of Gaba Analogues of Restricted Conformation on Gaba Transport in Astrocytes and Brain Cortex Slices and on Gaba Receptor Binding. J. Neurochem. *33*, 181–189.

Scoville, W.B., and Milner, B. (2016). Loss of recent memory after bilateral hippocampal lesions: Memory and memories-looking back and looking forward. J. Neurol. Neurosurg. Psychiatry *87*, 230.

Seifert, G., Schilling, K., and Steinhäuser, C. (2006). Astrocyte dysfunction in neurological disorders: A molecular perspective. Nat. Rev. Neurosci. *7*, 194–206.

Sequeira, A., Mamdani, F., Ernst, C., Vawter, M.P., Bunney, W.E., Lebel, V., Rehal, S., Klempan, T., Gratton, A., Benkelfat, C., et al. (2009). Global brain gene expression analysis links Glutamatergic and GABAergic alterations to suicide and major

depression. PLoS One *4*, 21–23.

Silvers, J.M., Harrod, S.B., Mactutus, C.F., and Booze, R.M. (2007). Automation of novel object recognition task for use in adolescent rats. J. Neurosci. Methods *166*, 99–103.

Sofroniew, M. V., and Vinters, H. V. (2010). Astrocytes: Biology and pathology. Acta Neuropathol. *119*, 7–35.

Squire, L.R., and Davis, H.P. (1981). The pharmacology of memory: a neurobiological perspective. Ann. Rev. Pharmacol. Toxicol *21*, 323–356.

Squire, L.R., Kosslyn, S., Zola-Morgan, S., Haist, F., and Musen, G. (1992). Memory and the Hippocampus: A Synthesis From Findings With Rats, Monkeys, and Humans. Psychol. Rev. *99*, 195–231.

Stobart, J.L., and Anderson, C.M. (2013). Multifunctional role of astrocytes as gatekeepers of neuronal energy supply. Front. Cell. Neurosci. *7*, 1–21.

Suárez, I., Bodega, G., and Fernández, B. (2002). Glutamine synthetase in brain: Effect of ammonia. Neurochem. Int. *41*, 123–142.

Swanson, L.W., and Cowan, W.M. (1977). An Autoradiographic Study of the Organization of the Efferent Connections of the Hippocampal Formation in the Rat. J. Comp. Neur. *172*, 49–84.

Takada, M., and Hattori, T. (1986). Fine structural changes in the rat brain after local injections of gliotoxin, alpha-aminoadipic acid. Histol. Histopathol. *1*, 271–275.

Tavares, G., Martins, M., Correia, J.S., Sardinha, V.M., Guerra-Gomes, S., Das Neves, S.P., Marques, F., Sousa, N., and Oliveira, J.F. (2016). Employing an open-source tool to assess astrocyte tridimensional structure. Brain Struct. Funct. 1–11.

Terry, R.D., Masliah, E., Salmon, D.P., Butters, N., Deteresa, R., Hill, R., Hansen, L.A., and Katzman, R. (1991). Physical Basis of Cognitive Alterations in Alzheimer's Disease : Synapse loss is the Major Correlate of Cognitive Impairment. Ann. Neurol. *30*, 572–580.

Tian, G.F., Azmi, H., Takano, T., Xu, Q., Peng, W., Lin, J., Oberheim, N.A., Lou, N., Wang, X., Zielke, H.R., et al. (2005). An astrocytic basis of epilepsy. Nat. Med. *11*, 973–981.

Traystman, R.J. (1997). Regulation of cerebral blood flow by carbon dioxide. In Primer on Cerebrovascular Diseases, pp. 537–545.

Tulving, E. (1972). Episodic and semantic memory. Organ. Mem. *1*, 381–403.

Tulving, E. (1985). Memory and consciousness. Can. Psychol. Assoc. *26*, 1–12.

Vannucci, S.J., Maher, F., and Simpson, I.A. (1997). Glucose transporter proteins in brain: delivery of glucose to neurons and glia. Glia *21*, 2–21.

Verkhratsky, a, and Kettenmann, H. (1996). Calcium signalling in glial cells. Trends Neurosci. *19*, 346–352.

Verkhratsky, A., and Butt, A. (2013). General pathophysiology of neuroglia. Glial Physiol. Pathophysiol. Hoboken New Jersey 431–450.

Verkhratsky, A., and Parpura, V. (2014). The concept of neuroglia. In Introduction to Neuroglia, A. Verkhratsky, and V. Parpura, eds. (Colloquim series on neuroglia in biology and medicine: from physiology to disease - Morgan & Claypool Life Sciences), pp. 14–18.

Verkman, A.S. (2005). More than just water channels: unexpected cellular roles of aquaporins. J. Cell Sci. *118*, 3225–3232.

Verkman, A.S. (2009). Knock-out models reveal new aquaporin functions. Handb. Exp. Pharmacol. *190*, 359–381.

Villarreal, A., Aviles Reyes, R.X., Angelo, M.F., Reinesf, A.G., and Ramos, A.J. (2011). S100B alters neuronal survival and dendrite extension via RAGE-mediated NF-κB signaling. J. Neurochem. *117*, 321–332.

Virchow, R. (1856). Gesammelte Abbildung zur wissenschaftlichen Medizin.

Vogel-Ciernia, A., and Wood, M.A. (2015). Examining Object Location and Object Recognition Memory in Mice. Curr Protoc Neurosci *69*, 1–22.

Volterra, A., and Meldolesi, J. (2005). Astrocytes, from brain glue to communication elements: the revolution continues. Nat. Rev. Neurosci. *6*, 626–640.

Voutsinos-Porche, B., Bonvento, G., Tanaka, K., Steiner, P., Welker, E., Chatton, J.Y., Magistretti, P.J., and Pellerin, L. (2003). Glial glutamate transporters mediate a functional metabolic crosstalk between neurons and astrocytes in the mouse developing cortex. Neuron *37*, 275–286.

Walf, A.A., and Frye, C.A. (2007). The use of the elevated plus maze as an assay of anxiety-related behavior in rodents. Nat. Protoc. *2*, 322–328.

Walz, W. (2000). Role of astrocytes in the clearance of excess extracellular potassium. Neurochem. Int. *36*, 291–300.

Walz, W., and Hertz, L. (1984). Intense furosemide-sensitive potassium accumulation in astrocytes in the presence of pathologically high extracellular potassium levels. J. Cereb. Blood Flow Metab. *4*, 301–304.

Walz, W., and Wuttke, W.A. (1999). Independent mechanisms of potassium clearance by astrocytes in gliotic tissue. J. Neurosci. Res. *56*, 595–603.

Wang, D.D., and Bordey, A. (2008). The astrocyte odyssey. Prog. Neurobiol. *86*, 342–367.

Warburton, E.C., and Brown, M.W. (2015). Neural circuitry for rat recognition memory. Behav. Brain Res. *285*, 131–139.

Webster, M.J., O'Grady, J., Kleinman, J.E., and Weickert, C.S. (2005). Glial fibrillary acidic protein mRNA levels in the cingulate cortex of individuals with depression, bipolar disorder and schizophrenia. Neuroscience *133*, 453–461.

Wilder, P.T., Rustandi, R.R., Drohat, A.C., and Weber, D.J. (1998). S100B (ββ) inhibits the protein kinase C-dependent phosphorylation of a peptide derived from p53 in a Ca2+-dependent manner. Protein Sci. *7*, 794–798.

Willecke, K., Eiberger, J., Degen, J., Eckardt, D., Romualdi, A., Guldenagel, M., Deutsch, U., Sohl, G., Güldenagel, M., Deutsch, U., et al. (2002). Structural and functional diversity of connexin genes in the mouse and human genome. Biol.Chem. *383*, 725–737.

Winter, C.G., Saotome, Y., Levison, S.W., and Hirsh, D. (1995). A role for ciliary neurotrophic factor as an inducer of reactive gliosis, the glial response to central nervous system injury. Proc. Natl. Acad. Sci. U. S. A. *92*, 5865–5869.

Winters, B.D., Forwood, S.E., Cowell, R.A., Saksida, L.M., and Bussey, T.J. (2004). Double Dissociation between the Effects of Peri-Postrhinal Cortex and Hippocampal Lesions on Tests of Object Recognition and Spatial Memory: Heterogeneity of Function within the Temporal Lobe. J. Neurosci. *24*, 5901–5908.

Witter, M.P., Canto, C.B., Couey, J.J., Koganezawa, N., and O'Reilly, K.C. (2014). Architecture of spatial circuits in the hippocampal region. Philos. Trans. R. Soc. B Biol. Sci. *369*, 11–13.

Woolsey, T.A., Hanaway, J., and Gado, M.H. (2017). The brain atlas: a visual guide to the human central nervous system (John Wiley & Sons).

Wyss-Coray, T., Loike, J.D., Brionne, T.C., Lu, E., Anankov, R., Yan, F., Silverstein, S.C., and Husemann, J. (2003). Adult mouse astrocytes degrade amyloid-beta in vitro and in

situ. Nat. Med. *9*, 453–457.

Yankovskaya, V., Horsefield, R., Törnroth, S., Luna-Chavez, C., Miyoshi, H., Léger, C., Byrne, B., Cecchini, G., and Iwata, S. (2003). Architecture of succinate dehydrogenase and reactive oxygen species generation. Science (80-.). *299*, 700–704.

Zorec, R., Horvat, A., Vardjan, N., and Verkhratsky, A. (2015). Memory Formation Shaped by Astroglia. Front. Integr. Neurosci. *9*, 56.

Zorec, R., Parpura, V., Vardjan, N., and Verkhratsky, A. (2017). Astrocytic face of Alzheimer's disease. Behav. Brain Res. *322*, 250–257.